ADSORPTION OF ORGANIC ACIDS FROM DILUTE AQUEOUS SOLUTION ONTO ACTIVATED CARBON

by

Shie-Way Wang

ProQuest LLC.
789 East Eisenhower Parkway
P.O. Box 1346
Ann Arbor, MI 48106 – 1346

T-2293

A thesis submitted to the Faculty and the Board of Trustees of the Colorado School of Mines in partial fulfillment of the requirements for the degree of Doctor of Philosophy (Chemical and Petroleum-Refining Engineering).

Golden, Colorado

Date Jan. 10, 1980

Signed: Shie-Way Wang

Shie-Way Wang

Approved: Anthony L. Hines

Anthony L. Hines
Thesis Advisor

Golden, Colorado

Date Jan 22, 1980

P. F. Dickson
Head of Department

ABSTRACT

The radioisotope technique was used to study the removal of organic acid contaminants from dilute aqueous solutions onto activated carbon. Five single-solute systems (acetic acid, propionic acid, n-butyric acid, n-hexanoic acid and n-heptanoic acid) were studied at three different temperatures, 278, 298 and 313 K. Three bi-solute acid mixtures (A. acetic and propionic acids, B. acetic and butanoic acids, and C. propionic and butanoic acids) were studied at two different temperatures 278 and 298 K.

The purposes of this study are two-fold. First, experimental isotherms of single-solute systems were obtained at three different temperatures in the very dilute concentration region (less than 1% by weight). These data are very important in the prediction of bi-solute equilibrium data. Secondly, a Polanyi-based competitive adsorption potential theory was developed in this study and used to predict the bi-solute equilibrium uptakes.

The calculated values were compared with both experimental data and equilibrium uptakes as predicted by ideal adsorbed solution theory. The average errors between the values calculated by the competitive adsorption

potential theory and experimental data ranges from 4% to 14%. It was found in this study that the competitive adsorption potential theory gives slightly better results than those calculated by ideal adsorbed solution theory.

TABLE OF CONTENTS

LIST OF FIGURES

LIST OF TABLES

LIST OF SYMBOLS

a = activity

$\mathcal{A}$ = surface area per unit weight of solid

A = Hemholtz free energy

C = Concentration

f = fugacity

$\overline{G}$ = Molar Gibbs free energy

N_i^a = surface excess of component i

q_i = uptake of component i

R = gas content

T = absolute temperature

$\overline{V}_i$ = partial molar volume of component i

x_i = mole fraction of component i in the bulk liquid phase at equilibrium

Z_i = solvent free, mole fraction of solute i in the adsorbed phase

Greek letters

σ = surface tension

ε = adsorption potential

γ_i = activity coefficient of the i'^{th} component in the bulk liquid phase

γ_i' = activity coefficient of the i'^{th} component in the adsorbed phase

μ = chemical potential

ϕ_i^o = free energy of immersion of adsorbent in liquid solution

Greek letters, continued

ϕ_i^o = free energy of immersion of adsorbent in pure i'^{th} liquid

Subscript and Superscript

2 = acetic acid

3 = propionic acid

4 = n-butanoic acid

B = bulk liquid phase

i = i'^{th} component

0 = adsorption for single-solute systems

T = total uptake of the solutes

' = adsorbed phase

ϕ = adsorbed phase

ACKNOWLEDGEMENTS

The author would like to take this opportunity to give his sincere thanks to Dr. Anthony L. Hines, thesis advisor, for his continuous encouragement and support during the course of this work and for the many valuable lessons learned under his tutorship which made this work possible. Many informative discussions with Dr. Ching H. Wu are also gratefully acknowledged.

The author also thanks the U.S. Department of Energy, Laramie Energy Technology Center for the grant (contract number E(29-2)-3790) which supported my research for the past two years.

Additionally, the author thanks Drs. Michael S. Graboski, Arthur J. Kidnay, E. Dendy Sloan, Beatrice E. Willard, Ching H. Wu and Victor J. Yesavage for their service on his Ph. D. committee.

Finally, the author would like to give a special thanks to his parents and his wife for their unfailing support and encouragement during the pursuit of this goal.

I. Introduction

Due to the growing concern for potential carcinogenic, mutagenic and teratogenic compounds found in drinking water and the associated impact of developing alternate energy sources, the removal of biologically resistant organic contaminants from water has become more important in recent years (1, 2). The organic contaminants found in by-product water of synthetic fuel processes are mainly aliphatic organic acids, and phenol and its derivatives as will be shown later.

The adsorption of organic acids from aqueous solution has been studied primarily by chromatographic or spectroscopic techniques over moderate and higher concentration ranges. The adsorption data of aliphatic acids from dilute aqueous solution (less than 1% by weight) are not readily available in the literature.

This work presents the adsorption data of single-acid solutions and bi-acid solutions by using radioactive tracer techniques. Five carboxylic acids were studied at three different temperatures over five decades in low concentration range. The data obtained are important for developing theoretical adsorption models to predict competitive adsorption equilibrium data and for the design of fixed bed adsorption towers.

In studying competitive adsorption of organic acid from dilute aqueous solution, three acid mixtures were studied at two different temperatures over three decades in concentrations. In all these studies, activated carbon was used as the substrate because of its high capacity in removing organic contaminants from aqueous solution.

II. Literature Review

A. Experimental Works

Numerous pertinent studies of adsorption using carbon have been reported in the literature by different investigators (3-14). The monograph by Kipling (15) provides an excellent review on the adsorption at the liquid-solid interface for research done prior to 1965. Among those works mentioned above, the adsorption of organic acids from aqueous solution has been carefully studied by Linner and Gortner (3), Hansen and co-workers (5-9), and Smith and Hurley (4).

Linner and Gortner (3) studied the adsorption onto decolorizing carbon of thirty-one organic acids, differing in most cases in chemical configuration. The experiments were conducted at essentially room temperature which varied from 22°C to 30°C; the equilibrium concentrations were determined by titrimetric methods. Hansen and co-workers studied the homologous normal aliphatic acids from acetic acid to heptanoic acid at 25°C on three non-porous carbons, Spheron-6, Graphon, and Acheson Graphite (DAG-1). The results were analyzed interferometrically. Smith and Hurley studied the adsorption of acetic, capric, palmitic, and stearic acids onto six different carbon blacks at 25°C. Concentrations were determined volumetrically, using methanolic sodium hydroxide and phenalphathalein as an indicator.

All of their experimental work was devoted to single-solute systems only.

It has been found that few efforts have been directed toward using activated carbon as the adsorbing media. The main reason for not using activated carbon is to avoid the steric effect and the surface heterogeneity due to the microporous structure of activated carbon.

Since 1970, granular and powdered activated carbon have been widely used to remove organic contaminants from water. Also researchers have extended their experimental studies to multi-solute systems. Manes and co-workers (16-22) studied the adsorption of acrylamide, benzamide, benzoic acid, coumarin, glucose, methionine, phthalide, p-nitrophenol, thiourea, urea and valine at 25°C and the final concentrations were determined by U.V. spectrophotometry. Parkash (23) studied the adsorption of homologous aliphatic acids, from formic acid to n-caproic acid on four activated carbons at 25°C over a concentration range 0.02M to 0.20M. Radke and Prausnitz (24) reported the adsorption data for dilute aqueous solutions containing acetone and propionitrile, p-chlorophenol and p-cresol at 25°C using activated carbon as the adsorbent. The equilibrium concentrations were measured by a gas chromatograph with a flame ionization detector. The bi-solute mixture

of p-nitrophenol and phenol was thoroughly studied by Fritz and Schluender (25) at 20°C and the concentrations were determined by U.V. spectrophotometry.

In addition to these new experimental data, four competitive adsorption models have been proposed by different investigators. All these models require only that the single-solute adsorption isotherms be known.

B. Previous Theoretical Models

In the waste water retreatment problem, a competitive adsorption model based solely on single-solute isotherms is essential in determining the bed life of an adsorbent. Several models based on fundamental thermodynamic principles have been developed to predict the uptake of each solute from multi-solute mixtures.

Butler and Ockrent (27) proposed a competitive Langmuir model that found limited success because of thermodynamic inconsistency as indicated by Jain and Snoeyink (28). Radke and Prausnitz (24) developed the thermodynamic formulation for adsorption of multi-solute mixtures from dilute aqueous solutions by direct extension of the method proposed by Myers and Prausnitz (29). A simplified model based on the same concepts as the approach of Radke and Prausnitz has recently been proposed by Digiano, et al. (30).

The application of the above model is limited primarily

to the dilute concentration range. To overcome this shortcoming, Minka and Myers (31) proposed a method to predict the surface excess over the entire composition range in terms of the system variables. These are: the energy of immersion of the adsorbent, the capacity of the adsorbent at saturation, and the activity coefficients in the bulk and adsorbed phases. Using the Polanyi adsorption potential theory as a basis, Manes and co-workers (16-22) extended gas phase adsorption theory to the liquid phase. The modified potential theory has been used to predict the adsorption of organic liquids and solids from trace to saturated concentrations for partially miscible bi-solute and tri-solute aqueous mixtures.

The following part gives the summary of the main equations and assumptions for each model. For more detailed derivations, the listed references are recommended.

1. Ideal Adsorbed Solution Theory (IAS Model)

(a) Method of Radke and Prausnitz (24)

As shown by Gibbs (32), the solution-solid interface region can be considered as a separate two-dimensional phase. If the solid is assumed to be inert and to possess a specific surface area identical for all adsorbates, then the differential Helmhotz energy of the adsorbed phase, designated by superscript a is given by

$$dA^a = -S^a dT + \sigma d\mathcal{A} + \sum_i^n \mu_i^a dn_i^a + \mu_s^a dn_s^a \qquad (1)$$

where n_i^a and n_s^a are the surface excesses of solute i and solvent s respectively. By Euler's theorem, Equation (1) can be integrated to give

$$A^a = \sigma\mathcal{A} + \sum_i^n \mu_i^a n_i^a + \mu_s^a n_s^a \qquad (2)$$

where subscript i represents the solute and subscript s represents the solvent. The surface tension is indicated by σ and $\mathcal{A}$ stands for the surface area of the solid. By differentiation of Equation (2) and combining with Equation (1) leads to Gibbs isothermal adsorption equation.

$$-\mathcal{A}d\sigma = \sum_{i=1}^n n_i^a d\mu_i^a + n_s^a d\mu_s^a \quad \text{(constant T)} \qquad (3)$$

At equilibrium, the chemical potentials of the adsorbed and liquid phases are identical. Hence the isothermal Gibbs-Duhem equation can be written as

$$\sum_i C_i d\mu_i^a + C_s d\mu_s^a = 0 \qquad (4)$$

where C_i and C_s are the bulk liquid concentrations of solute i and solvent s in moles per unit volume.

Substitution of Equation (4) into Equation (3) gives the desired result which is valid over the entire solute concentration range.

$$-\mathcal{A}d\sigma = \mathcal{A}d\pi = \sum_i n_i^m d\mu_i^a \qquad (5)$$

where the summation is over the solute species only. The spreading pressure π is defined as the difference between the surface tension of the pure solvent-solid interface and that of the solution-solid interface at the same temperature, i.e.

$$\pi = \sigma_{\text{pure solvent-solid}} - \sigma_{\text{solution-solid}} \tag{6}$$

The quantity n_i^m is the invariant adsorption of solute i defined by

$$n_i^m = n_i^a - \frac{C_i}{C_s} n_s^a \tag{7}$$

Radke and Prausnitz (24) indicate that moles of solute and solvent adsorbed, n_i^a and n_s^a are defined as Gibbs surface excess quantities, relative to the dividing surface which makes the adsorption of the solid equal to zero. This is obviously a mistake. If the Gibbs dividing surface is chosen so that the adsorption of solid is zero, then there is no adsorbed phase at all.

Radke and Prausnitz show that for dilute solutions n_i^m can be approximated by measuring the solute concentration decrease ΔC_i caused by contacting a solution of known concentration and known volume V with a known mass of adsorbent. Thus

$$n_i^m = V \Delta C_i \tag{8}$$

Because of the approximate nature of Equation (8), its application is restricted to dilute solutions. Since only the invariant adsorption of solute species appear in Equation (5), Radke and Prausnitz suggest that the adsorbed phase can be treated as though it were solvent free.

Following the work of Innes and Rowley (33), the adsorbed-phase fugacity f_i^a is defined as

$$d\mu_i^a = RT\, d\ln f_i^a \tag{9}$$

and

$$\lim_{\pi \to 0} \frac{f_i^a}{z_i \pi} = 1 \tag{10}$$

where the adsorbed-phase mole fraction is defined by

$$z_i = \frac{n_i^m}{\sum_i n_i^m} = \frac{n_i^m}{n_T^m} \tag{11}$$

The adsorbed-phase fugacity is two-dimensional and has the same units as the spreading pressure π.

When solute species adsorb simultaneously from dilute solution at constant T and π, Radke and Prausnitz propose that the adsorbed phase forms an ideal solution, i.e.

$$f_i^a(T, \pi, z_i) = z_i f_i^{ao}(T, \pi) \tag{12}$$

where f_i^{ao} is the fugacity that single solute i exerts when it adsorbs singly from dilute solution at the same

temperature and spreading pressure as that of the mixture. The superscript "o" denotes single-solute adsorption.

Equation (5) can be rewritten as

$$\frac{A}{n_T^m} = \sum_i z_i \left(\frac{\partial \mu_i^a}{\partial \pi}\right)_{T, z_i} \tag{13}$$

For an ideal adsorbed phase, Equations (5), (9), and (12) give

$$\left(\frac{\partial \mu_i^a}{\partial \pi}\right)_{T, z_i} = \left(\frac{\partial \mu_i^{ao}}{\partial \pi}\right)_T = \frac{A}{n_i^{mo}} \tag{14}$$

Substituting Equation (14) into Equation (13) gives

$$\frac{1}{n_T^m} = \sum_i \frac{z_i}{n_i^{mo}} \tag{15}$$

Equation (15) provides one of two relationships of the ideal adsorbed solution theory for calculating multi-solute equilibria.

At equilibrium conditions, the chemical potential of solute i in the adsorbed phase is equal to that of the liquid phase

$$\mu_i^a = \mu_i^l \tag{16}$$

The chemical potential of the adsorbed phase depends on

temperature, spreading pressure and composition as measured by the mole fraction Z_i. Integrating Equation (9) together with the ideality assumption of Equation (12) gives

$$\mu_i^a(T, \pi, z_i) = \mu_i^{ao}(T, \pi) + RT \ln z_i \tag{17}$$

For single-solute adsorption the intensive variables T and π fix the concentration C_1^o in the dilute liquid phase. Thus, for μ_i^{ao} in Equation (17) we substitute

$$\mu_i^{ao} = \mu_i^{lo}[T, C_i^o(\pi)] = \mu_i^{l*} + RT \ln C_i^o(\pi) \tag{18}$$

where superscript * denotes the ideal dilute-solution (Henry's law) standard state of the liquid phase. No activity coefficient is required in Equation (18) when the liquid solution is dilute. The concentration $C_i^o(\pi)$ refers to solute i when the solute adsorbs singly from solution at the same temperature and spreading pressure as that of the mixture. In a dilute liquid mixture at constant temperature μ_i^l is a function only of C_i. Therefore, the right side of equation (16) becomes

$$\mu_i^l(T, C_i) = \mu_i^{l*}(T) + RT \ln C_i \tag{19}$$

Again, no activity coefficient is needed in Equation (19) when attention is restricted to dilute solutions. Equations (15) through (21) lead to the second relationship of ideal

adsorbed solution theory for calculating multi-solute equilibria.

$$C_i = C_i^\circ(\pi) \cdot z_i \tag{20}$$

In order to use Equation (15) and (20) spreading pressures must be known for the various singly-adsorbing solutes in the mixture. These spreading pressures can be evaluated from Equation (5) by

$$\pi(C_i^\circ) = \frac{RT}{A}\int_0^{C_i^\circ} \frac{n_i^{mo}(C_i^\circ)}{C_i^\circ} dC_i^\circ \tag{21}$$

Experimental single-solute isotherms are used to construct a curve of n_i^{mo}/C_i^{o} as a function of C_i^{o} and the area under this curve determines π.

Calculation of Multi-Solute Equilibria

The following procedure illustrates the calculation of competitive adsorption of bi-solute equilibrium data.

1. Experimental isotherm data are integrated according to Equation (21) giving the spreading pressure for each single solute as a function of concentration.

$$\pi_1 = f_1(C_1^\circ) \tag{22}$$

$$\pi_2 = f_2(C_2^\circ) \tag{23}$$

2. The equilibrium relationship is written as Equations (24) and (25) from Equation (20).

$$C_1 = C_1^{\circ} \cdot Z_1 \tag{24}$$

$$C_2 = C_2^{\circ} \cdot (1 - Z_1) \tag{25}$$

3. Since single-solute concentrations C_i° are defined at the same spreading pressure as that of the mixture,

$$\Pi_1 = \Pi_2 = \Pi_{mixture} \tag{26}$$

4. For given values of C_1 and C_2, Equations (22) through (26) determine the five unknowns: π_1, π_2, Z_1, C_1° and C_2°.

5. Total adsorption can now be calculated using single-solute isotherm data and Equation (15). The individual uptake can be obtained from the following:

$$n_1^m = n_T^m \cdot Z_1 \tag{27}$$

$$n_2^m = n_T^m \cdot (1 - Z_1) \tag{28}$$

b. Method of Digiano et al. (30). (A Simplified IAS Model)

The application of the ideal adsorbed solution theory depends on the ease with which the spreading pressure, as shown in Equation (21) can be evaluated. In order to overcome this difficulty, Digiano et al. (30) suggest that if the individual single-solute isotherms can be expressed

by some simple form, Equation (21) can be integrated explicitly. Then the ideal adsorbed solution theory can be extended easily to an N-component system without calculating spreading pressures. For example, if two different solutes have identical isotherms over the entire concentration range then the same relationship between π and C_i^o holds for these two solutes. It follows that for any given spreading pressure and temperature

$$C_1^o = C_2^o \tag{29}$$

From Equation (24) and (25), the ratio of the solutes adsorbed, $\frac{q_1}{q_2}$ in the mixture can be related to the corresponding ratio of the solute concentration C_1/C_2 in the mixture, i.e.

$$\frac{z_1}{z_2} = \frac{g_T \cdot z_1}{g_T \cdot z_2} = \frac{g_1}{g_2} = \frac{C_1}{C_2} \tag{30}$$

where q_1, q_2 represent the uptake of solutes 1 and 2 respectively and q_T denotes the uptake of all solutes. Combining Equations (24) and (25) gives

$$C_1^o = C_1 + C_2 \tag{31}$$

If a Freundlich isotherm is applied to a given concentration range, then

$$q_i^\circ = k(C_i^\circ)^n \tag{32}$$

where k and n are parameters from a curve fit of the equilibrium data. Thus, the total loading q_T is given by

$$q_T = q_1^\circ \tag{33}$$

The individual uptake can be calculated by combining Equations (30), (32) and (33) to yield

$$q_1 = k C_1 (C_1 + C_2)^{n-1} \tag{34}$$

$$q_2 = k C_2 (C_1 + C_2)^{n-1} \tag{35}$$

Digiano et al. (30) also show that the same procedures can be applied to the case where the experimental isotherms can be fitted by the Langmuir equation. However, the approach proposed by Digiano et al. is not an improvement on Radke's method. It is a special case of the IAS model. If the experimental single-solute isotherms can be fitted with simple equations then the IAS model can easily be programmed.

2. Method of Minka and Myers (31)

For multicomponent adsorption, two basic assumptions were postulated by Minka and Myers in deriving an equation for surface excess in terms of variables obtained from binary-solution data. The first assumption is that the

original liquid solution, consisting of n^o moles, may be divided into two phases after the establishment of equilibrium. These are an adsorbed phase containing n' moles and a bulk phase containing n moles. Thus

$$n^\circ = n + n' \tag{36}$$

The second assumption is that n' may be estimated for microporous adsorbents as shown

$$\frac{1}{n'} = \sum_i \frac{x_i'}{m_i} \tag{37}$$

where m_i is the capacity of the pores for the pure i^{th} liquid, given by the amount adsorbed from the vapor of that liquid at saturation. The superscript "prime" indicates the adsorbed phase and x_i' is the mole fraction of i in the adsorbed phase at equilibrium. Based on the assumptions in Equations (36) and (37), Minka and Myers developed the following equations to predict the surface excess for the adsorption from ternary liquid mixtures.

$$n_i^e = \frac{\sum_{j>i} x_i x_j (1 - K_{ij})}{\sum_{j=1}^{3} \frac{x_j K_{ij}}{m_j}} \tag{38}$$

$$K_{ij} = \frac{\gamma_i' \gamma_j}{\gamma_j' \gamma_i} \exp\left[\frac{(\phi - \phi_j^\circ)}{m_j RT} - \frac{(\phi - \phi_i^\circ)}{m_i RT}\right] \tag{39}$$

$$\frac{\phi-\phi_i^o}{RT} = \int_{\chi_i=1}^{\chi_i} \frac{\sum_{j\neq i}^{3} \chi_j (1-K_{ij})\left(\frac{d\ln\gamma_i}{d\chi_i} - \frac{1}{1-\chi_i}\right)d\chi_i}{\sum_{j=1}^{3} \frac{\chi_i K_{ij}}{m_i}} \qquad (40)$$

where ϕ_i^o is the free energy of immersion of the adsorbent in the pure liquid and ϕ is the free energy of immersion in the mixture.

Properties needed for calculating the surface excess in Equation (38) are: differences of free energies of immersion in the pure liquids $\left[\frac{(\phi-\phi_i^o)}{RT}\right]$, the capacities of the adsorbent $[m_i]$, activity coefficients in the bulk liquid $[\gamma_i(X_i)]$, and activity coefficients in the adsorbed phase $[\gamma_i'(X_i')]$. All these properties are obtained from single solute adsorption data. Activity coefficients in the liquid phase are obtained using the relationship developed by Chao (35) for the ternary system - benzene, ethyl acetate and cyclohexane. The difference of free energy of immersion is obtained by integration of Equation (41) as developed by Larinov and Myers (35).

$$\frac{\phi-\phi_i^o}{RT} = -\int_{\chi_i=1}^{\chi_i} \frac{n_i^e}{\chi_i \chi_j \gamma_i} d(\gamma_i \chi_i) \qquad (41)$$

However, the derivation of Equation (41) is questionable. [See Equations (5) to (7) in Reference (35)]. The ratio of the activity coefficients in the adsorbed phase is also

obtained by

$$\ln \frac{\gamma_j'}{\gamma_i'} = \ln \frac{\gamma_j}{\gamma_i} + \ln S - \frac{\phi - \phi_i}{m_i RT} + \frac{\phi - \phi_j^\circ}{m_j RT} \qquad (42)$$

where S is given by

$$S = \frac{x_j (x_i + \frac{n_i^e}{m_j})}{x_i (x_j - \frac{n_i^e}{m_i})} \qquad (43)$$

Therefore, for given values of x_i and x_j, (the mole fraction of component i and j in the liquid phase at equilibrium) the surface excess can be calculated from Equations (38) through (43).

It is clear from Equation (39) that only the experimental data for binary mixtures are needed to predict the surface excess for a ternary mixture. The application of Minka and Myers' approach is limited by the difficulties in the integration of Equation (40). Three sets of binary data, (the 1,2 system; the 1,3 system and the 2,3 system) must be known in order to predict the surface excesses of a ternary mixture. In addition, m_i in Equation (38) must be determined from saturated vapor phase adsorption data. Unfortunately, most of the organic contaminants

found in waste water have low vapor pressures which makes this determination difficult. Thus, the method of Minka and Myers may be of limited usefulness.

3. Polanyi-based Adsorption Potential Theory

Polanyi potential theory was originally proposed to deal with gas-phase adsorption (36). It was then extended by Polanyi (37) to account for the adsorption of solid solutes of limited solubility from solution. He proposed that adsorption or precipitation from the liquid phase is comparable to the liquification of gas. If C_s and C are the saturated and equilibrium concentrations of the solute and ε_s is the adsorption potential obtained from vapor phase data, then the potential for the liquid state is

$$\mathcal{E}_s = RT \ln \frac{C_s}{C} \tag{44}$$

In a later paper, Polanyi (38) corrected this equation to account for the energy required for the displacement of adsorbed solvent from the adsorption space when a solid is adsorbed. The criterion for adsorption becomes

$$\mathcal{E}_{sl} = \mathcal{E}_s - \frac{\mathcal{E}_l V_s}{V_l} \tag{45}$$

where ε_{s1} is the adsorption potential for the solute adsorbing from the solvent, ε_1 and ε_s are the gas phase adsorp-

tion potential of the solvent and solute and V_s and V_1 are the molar volumes of solute and solvent respectively.

a. The Hansen-Fackler Modification of the Potential Theory (39).

Hansen and Fackler modified the Polanyi theory to deal with the adsorption of binary liquid mixtures over the entire composition range. The idea is that the adsorption space is invariant, i.e. the adsorption of one component must be accompanied by the desorption of an equal volume of the other.

Based on the above assumption, Hansen and Fackler derived an Equation to predict the amount of component i adsorbed.

$$\frac{V\Delta C_i}{m} = \int_0^{\phi'} \left[\frac{x_{i\phi}}{V_\phi} - \frac{x_{iB}}{V_B} \right] d\phi' \qquad (46)$$

where V and ΔC_i refer to the volume of the bulk solution and the change in its concentration due to adsorption. The variable ϕ' represents the volume element in the adsorbed phase and $X_{i\phi}$ and X_{iB} are the mole fractions of component i in the adsorbed phase and bulk phase respectively. V_ϕ and V_B are the volumes per mole of mixture in the adsorbed phase and in the bulk respectively.

b. The Manes-Hofer Correlation of Liquid Phase Adsorption Data (17).

Manes and Hofer applied the Polanyi theory to the adsorption of solids from a number of different solvents. This work is important in that it provides an experimental test of the Polanyi theory with a large number of solvents. They rewrote Equation (45) as

$$\frac{\mathcal{E}_{s\ell}}{V_s} = \frac{\mathcal{E}_s}{V_s} - \frac{\mathcal{E}_\ell}{V_\ell} \tag{47}$$

or in shorter notation

$$\alpha_{s\ell} = \alpha_s - \alpha_\ell \tag{48}$$

where each α corresponds to an ε/V. If the characteristic curves for the solute and solvent are assumed to have the same functional form except for a multiplier in the abscissa, then adsorption isotherms can be predicted according to Equation (48) for any compound for which the scale factor can be found. Figure 1 illustrates the relation of $\alpha_{s1}=\alpha_s-\alpha_1$.

If the adsorbent has been characterized by some reference substance (for example n-Heptane), then the ratio of the α's in Equation (48) to α_h, which is the reference substance n-heptane, gives the abscissa scale factor, i.e.

$$\frac{\alpha_{s\ell}}{\alpha_h} = \frac{\alpha_s - \alpha_\ell}{\alpha_h} \tag{49}$$

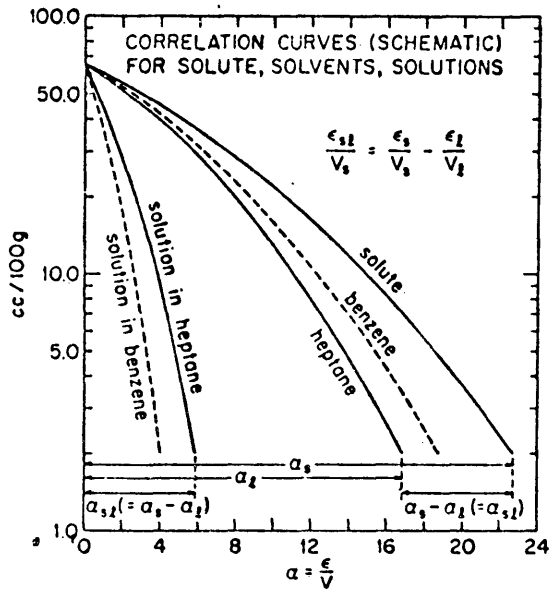

Figure 1. Schematic plot of the volume of adsorbate adsorbed (cm^3) per unit weight of carbon (100 g) *vs.* the adsorption potential per unit volume of the solvent (l), the solute (s), and the solute from solution (sl) illustrating the relation $\alpha_{sl} = \alpha_s - \alpha_l$. (17).

or more compactly

$$\gamma_{sl} = \gamma_s - \gamma_l \tag{50}$$

where $\gamma_i = \frac{\alpha_i}{\alpha_h}$

However, most solutes of interest are not volatile and one cannot determine α_s or γ_s independently from vapor phase studies.

If Equation (50) is to be useful, the estimation of γ_{sl} should not depend on gas-phase adsorption measurements. Manes and Hofer proposed that an approximation of γ_{sl} could be obtained from the polarizability per unit volume of solute and solvent using the relationship

$$\gamma_{sl} = \frac{P_s' - P_i'}{P_h'} \tag{51}$$

where P_i' is the polarizability per unit volume of various compounds. However, the polarizability per unit volume is proportional to the refractive index through the Lorentz-Lorentz Equation

$$P_i' = \frac{[R]}{V} = \frac{n_i^2 - 1}{n_i^2 + 2} \tag{52}$$

where [R] is the molar refraction and n is the refractive index. Manes and Hofer estimated the γ factors for liquids from their refractive indices and for solids from a table of bond refractivities. They were successful in correlating the low adsorbent loading for the adsorption of Sudan III (benzene-azo-p-benzene-azo-β-naphthal) and Butter Yellow (p-dimethylamino-azobenzene) from various solvents. However, when Equation (49) was used to correlate the same set of experimental data, the agreement was not good. Manes and Hofer suggested that steric hindrance was responsible for the discrepancy. The effect of steric hindrance was further studied by Chiou and Manes (40) for the adsorption of planer and octahedral complex solutes on activated carbon and on carbon black.

c. Adsorption of Partially Miscible Liquids from Water, Wohleber and Manes (18, 19).

Wohleber and Manes treated partially miscible liquids in essentially the same fashion as the Manes-Hofer treatment of solids, except for the empirical scale factor for water, γ=0.28. The correlation for liquids was better than for solids from solvent. All the correlations were limited to single-solute systems.

d. Application of the Polanyi-Based Adsorption Potential Theory to Predict the Competitive Adsorption of Solid Solutes from Aqueous Solution, Rosene and Manes (20-22).

In a series of recent articles, Rosene and Manes (20-22) presented experimental data and extended the Polanyi treatment to competitive adsorption of solid solutes from aqueous solutions. They proposed that the adsorption potential ε of the solutes can be approximated by

$$\mathcal{E} \doteq RT \ln \frac{C_s}{C} \tag{53}$$

where C_s is the saturated concentration of the solute and C is the equilibrium concentration of the solute in the bulk phase.

Rosene and Manes were successful in applying their model to predict the competitive adsorption of binary solid

solutes and ternary solid solutes from aqueous solutions onto activated carbon. Their approach is very similar to the model developed in this work. A detailed derivation is given in the theoretical section of this text.

The major disadvantage of their method is that it can not be applied to the case where the solutes are completely soluble in the solvent. Also, when applying this method an adjusted adsorbate volume factor must be used. Although Rosene and Manes gave some explanations about the physical meaning of the adjusted adsorbate volume factor, this adjusted adsorbate volume factor appears to be only a correction factor to fit the experimental data. Also their derivations are not thermodynamically rigorous.

The purpose of the present work is to overcome these shortcomings mentioned above so that the adsorption potential theory can be applied to predict competitive adsorption from liquid mixtures.

III. New Competitive Adsorption Potential Theory

Since the method of Rosene and Manes (20-22) is not thermodynamically sound and also their method can not be used to predict competitive adsorption data for completely water-soluble solutes. A new competitive adsorption potential theory is developed below. The main idea is that we assume the total adsorbed volume space can be determined from the more strongly adsorbed component as though it were adsorbed singly from aqueous solution. The individual adsorbed volume spaces can be determined from basic thermodynamics. However, the sum of the individual adsorbed volume spaces must be equal to the total adsorbed volume space. Then the uptake of each component can be obtained by dividing the individual adsorbed volume space by its corresponding molar volume.

If a mixture of solutes is in equilibrium with an adsorbent, the chemical potential of solute i in the adsorbed phase is equal to that in the bulk liquid phase

$$\mu_{i\phi} = \mu_{iB} \tag{54}$$

where the subscripts ϕ and B indicate the adsorbed phase and the bulk phase respectively. The chemical potentials for the two phases are

$$\mu_{i\phi} = \mu_{i\phi}^{\circ} + RT \ln a_{i\phi} \tag{55}$$

$$\mu_{iB} = \mu_{iB}^{\circ} + RT \ln a_{iB} \tag{56}$$

in which a_i is the activity of solute i.

Following the work of Hansen and Fackler (39), the adsorption potential of single solute i from aqueous solution is

$$\mu_{i\phi}^{\circ} - \mu_{iB}^{\circ} = -\mathcal{E}_i \tag{57}$$

Thus,

$$\mathcal{E}_i = RT \ln \frac{a_{i\phi}}{a_{iB}} \tag{58}$$

The standard state of the liquid phase is chosen to be the infinitely dilute solution at the mixture temperature. The activity is expressed as

$$a_{iB} = x_{iB} \gamma_{iB} \tag{59}$$

where x_{iB} and γ_{iB} are the mole fraction and activity coefficient of solute i in the bulk liquid phase respectively. In very dilute solutions, γ_{iB} can be assumed to be equal to 1.0.

$$\therefore \quad a_{iB} = x_{iB} \tag{60}$$

Assuming that the adsorbed phase forms an ideal

solution

$$f_{i\phi} = x_{i\phi} f_{i\phi}^{o} \tag{61}$$

in which $f_{i\phi}^{o}$ is the fugacity of single solute i when it adsorbs singly from dilute solution at the same temperature and total solute concentration as that of the mixture and $x_{i\phi}$ is the solvent free mole fraction of solute i in the adsorbed phase. A similar treatment, in which the adsorbed phase was treated as though it were solvent free, was also used by Radke and Prausnitz (24).

$$a_{i\phi} = \frac{f_{i\phi}}{f_{i\phi}^{o}} = x_{i\phi} \tag{62}$$

Using this approach, Equation (58) becomes

$$\varepsilon_i = RT \ln \frac{x_{i\phi}}{x_{iB}} \tag{63}$$

Paralleling the treatment of Hansen and Fackler (39), Rosene and Manes (20-22), let $\Delta\phi'$ be an infinitesimal volume increment enclosed between two equipotential surfaces ϕ and $\phi + \Delta\phi$. At equilibrium, for infinitesimal mass transfer between the liquid in $\Delta\phi'$ and the bulk solution, the change in $\Delta\phi'$ can be considered as invariant. Thus

$$d(\Delta\phi') = \bar{V}_i dn_i + \bar{V}_j dn_j = 0 \tag{64}$$

where $\overline{V}_i$ and $\overline{V}_j$ are the partial molar volumes of solutes i and j respectively. In the above treatment, the adsorption of water is neglected because of its very low adsorption potential per unit volume as shown in Figures (2) and (3) by Wohleber and Manes (18). Thus equation (64) becomes

$$dn_j = - \frac{\overline{V}_i}{\overline{V}_j} dn_i \tag{65}$$

The adsorption of any solute occurs whenever the following criteria is satisfied

$$\varepsilon_i \geq RT \ln \frac{x_{i\phi}}{x_{iB}} \tag{66}$$

The equality holds when equilibrium is reached. The driving force, on a per mole basis, for adsorption of single solute i is thus

$$-\Delta\overline{G}_i = \varepsilon_i - RT \ln \frac{x_{i\phi}}{x_{iB}} \tag{67}$$

The condition $\Delta G \leq 0$ is the criterion for any solute to be adsorbed in a given element of adsorption space. In a bi-solute system, the displacement of the j^{th} solute by the i^{th} solute will occur in a given element of adsorption space when

$$d(\Delta G) = \Delta\overline{G}_i dn_i + \Delta\overline{G}_j dn_j \leq 0 \tag{68}$$

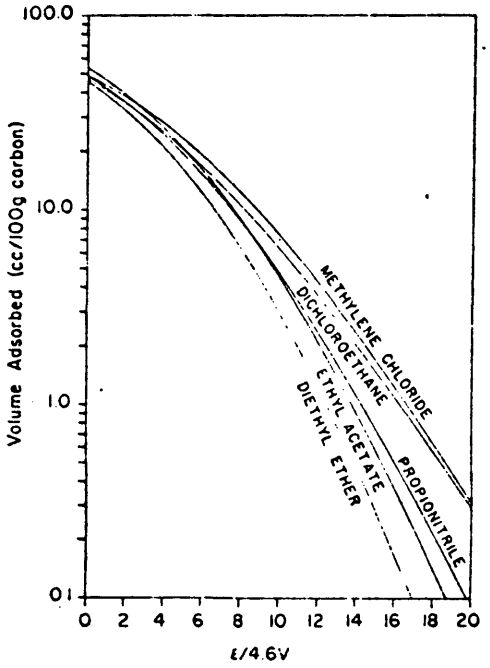

Figure 2. Volume of 1,2-dichloroethane, diethyl ether, ethyl acetate, methylene chloride, and propionitrile plotted as a function of adsorption potential. (18)

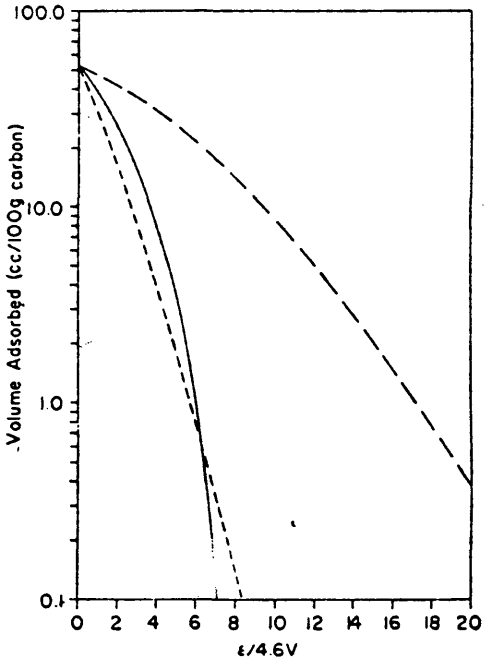

Figure 3. Correlation curves for water: ——, calculated from adsorption isotherm; - - - -, calculated from $\gamma_1 = 0.28$; — — —, calculated from refractive index. (18)

Substituting equations (65) and (67) into equation (68) gives

$$\frac{1}{\overline{V}_1}\frac{d(\Delta G)}{dn_i} = -\frac{\varepsilon_i}{\overline{V}_i} + \frac{RT}{\overline{V}_i}\ln\frac{x_{i\phi}}{x_{iB}} + \frac{\varepsilon_j}{\overline{V}_j} - \frac{RT}{\overline{V}_j}\ln\frac{x_{j\phi}}{x_{jB}} \leq 0 \quad (69)$$

Since $x_{i\phi} + x_{j\phi} = 1.0$, Equation (69) can be rearranged to give

$$\frac{\varepsilon_i}{\overline{V}_i} - \frac{RT}{\overline{V}_i}\ln\frac{x_{i\phi}}{x_{iB}} \leq \frac{\varepsilon_j}{\overline{V}_j} - \frac{RT}{\overline{V}_j}\ln\frac{x_{j\phi}}{x_{jB}} \quad (70)$$

The equality holds when equilibrium is reached. Equation (70) can thus be solved to yield values for $x_{i\phi}$ and $x_{j\phi}$. The calculational procedure is similar to that for the prediction of competitive adsorption of partially miscible solutes as presented by Rosene and Manes (20-22). The complete procedure is illustrated as follows:

1. Plot the adsorbed volume V_{ads} versus $\frac{\varepsilon}{\overline{V}}$ for each single solute from its corresponding adsorption isotherm (see curve j in Figure 4). $V_{i\ ads}$ is defined as the product of the molar volume of solute i and the moles of solute i adsorbed. ε_i is equal to $RT\ln\frac{x_{i\phi}}{x_{iB}}$. The adsorption potential of the solute i in the solvent $x_{i\phi}$ is assumed to be equal to 1 because of the very low adsorption potential of water.
2. For a given set of (x_{iB}, x_{jB}) try an assumed

value of $x_{i\phi}$ and use this value to calculate $\frac{RT}{\overline{V}_i} \ln \frac{x_{i\phi}}{x_{iB}}$.

3. Shift curve i to the left by an amount equal to $\frac{RT}{\overline{V}_i} \ln \frac{x_{i\phi}}{x_{iB}}$ (see curve i' in Figure 4).

4. The adsorption of component j will occur whenever

$$\frac{RT}{\overline{V}_j} \ln \frac{x_{j\phi}}{x_{jB}} = \frac{\varepsilon_j}{\overline{V}_j} - \frac{\varepsilon_i}{\overline{V}_i} + \frac{RT}{\overline{V}_i} \ln \frac{x_{i\phi}}{x_{iB}} \qquad (71)$$

The dashed line in Figure (4) shows the right hand side of Equation (71).

5. Enter $\frac{RT}{\overline{V}_j} \ln \frac{x_{j\phi}}{x_{jB}}$ on the abscissa of Figure (4) and find its corresponding ordinate C on the dashed line. This ordinate gives the volume of component j adsorbed. The volume of component i adsorbed is represented by the distance (B-C). If C>B, then the surface excess of component i is a negative value equal to B-C. This is contrary to the explanation of Rosene and Manes (20-22) who indicated that component i would be excluded. The fact that the surface excess is negative for component i does not mean that it is not adsorbed. It means only that the percent of

solute in the adsorbed phase is less than its value in the bulk phase. This results from the strong adsorption of the solvent molecules relative to the solute molecules.

6. Check to determine if the assumed x_j value is equal to that given by

$$x_{j\phi} = \frac{\frac{C}{\bar{V}_j}}{\frac{C}{\bar{V}_j} + \frac{(B-C)}{\bar{V}_i}} \qquad (72)$$

If the value calculated by Equation (72) is not equal to the assumed value, steps 2 through 6 should be repeated until the assumed and calculated values are equal.

A sample calculation is shown in Appendix B.

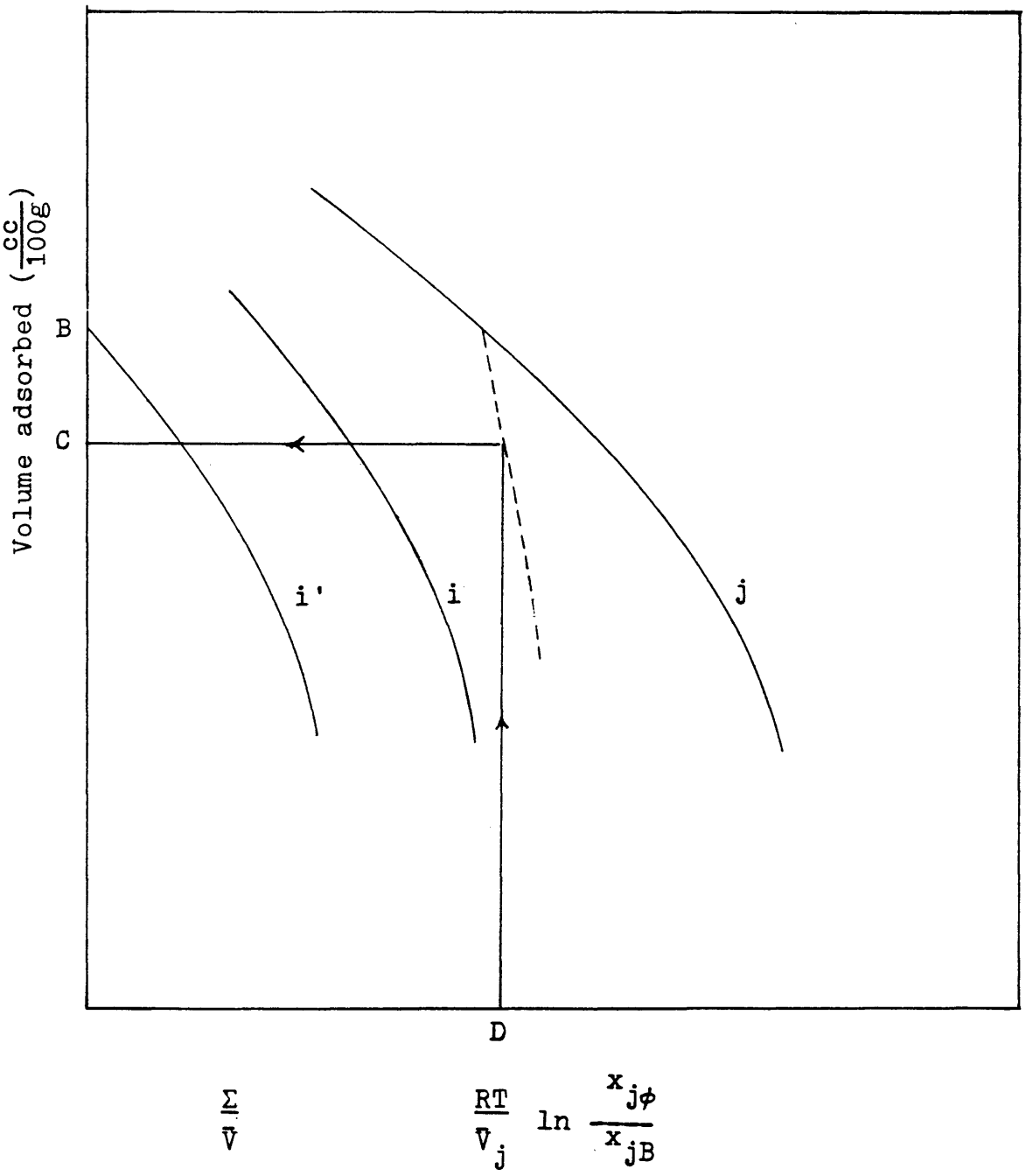

Figure 4 Schematic diagram of competitive adsorption potential theory

IV. Experimental Section

A. Adsorbent

Activated carbon was chosen as the adsorbent because of its high capacity for removing organic contaminants from aqueous solutions. The lignite based activated carbon was obtained from Darco Co., Denver, Co. A 20x40 mesh material with a total surface area of 667 m^2/g (determined by N_2-BET Method) was used. According to the report from the manufacturer, the activated carbon was washed by a strong acid to leach out undesirable inorganics such as calcium, magnesium, iron and aluminum. This was followed by water washing until the water extract reached a pH of 6. Table 1 shows the physical properties of the activated carbon used in this work.

The structure of microporous activated carbon consists of graphite-like layers stacked parallel to each other in packets of some 3 to 30 layers. In graphite, the resulting layers are stacked with a separation of about 3.35Å in the sequence of ABAB as shown in Figure 5. In microporous carbon, the interlayer distance is larger than in graphite - i.e. about 3.6Å. The stacking sequence is greatly perturbed with the result that many graphite layer planes are tilted with respect to one another.

Table 1. Physical Properties of DARCO (20x40) * Activated Carbon

Properties (Typical Values)	
Moisture content (max., as packed)	12%
Water-solubles (determined by 4 leachings with boiling water)	1%
pH of water extract	6.0
Bulk density (by vibrating feed method)	
g/ml	0.39
lbs/ft^3	24.5
Total surface area, m^2/g (by nitrogen adsorption)	700
Total pore volume, ml/g	1.0
Mean pore radius, Angstroms	29
Void space as loaded in plant column	50%
Regeneration loss per complete adsorption and regeneration cycle (by weight)	5%
Storage space needed (ft.^{3}/ton, approx.)	100

* Report from Darco Co., Denver, Colo.

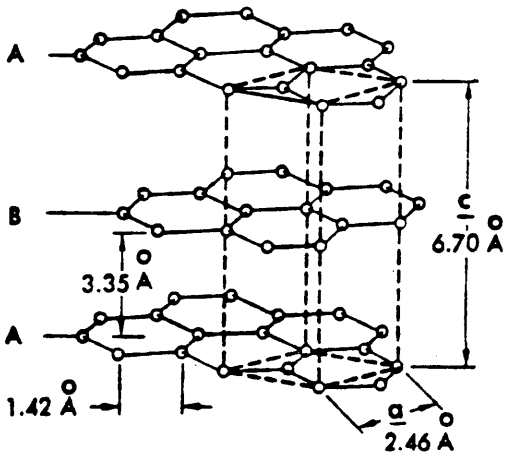

Fig. 5. Crystallographic structure - graphite

(taken from C. L. Mantell, "Carbon and Graphite Handbook", John Wiley, 1968).

Because of the structure of microporous carbon, the "free valence electrons" at the edges of the graphite layer planes are very reactive. These highly reactive free valence electrons can form compounds with any suitable foreign atoms (impurities) present in the carbon. Therefore, functional group or surface compounds can be expected to occur almost exclusively at the layer edges. Foreign atoms or molecules can only be weakly adsorbed on the basal faces by means of the graphite π electrons.

B. Adsorbate

Acetic, propionic, n-butanoic, n-hexanoic and n-heptanoic acids were chosen as adsorbates because these acids are the main organic contaminants found in by-product waters from certain synthetic fuel processes. Table 2 shows typical

ORNL DWG. 76-5074

Table 2. Organic Compounds Determined in By-Product Waters from Fossil Fuel Conversion Processes

Peak	Compound	Concentration (μg/ml)		
		Oil Shale Retorting	Synthane Coal Gasification	COED Coal Liquefaction
1	acetic acid	600	620	600
2	propanoic acid	210	60	90
3	n-butanoic acid	130	20	40
4	acetamide	230	—	—
5	n-pentanoic acid	200	10	30
6	propionamide	50	—	—
7	n-hexanoic acid	250	20	30
8	butyramide	10	—	—
9	phenol	10	2100	2100
10	n-heptanoic acid	260	—	—
11	o-cresol	30	670	650
12	m & p-cresols	20	1800	1800
13	n-octanoic acid	250	—	—
14	2,6-dimethylphenol	—	40	30
15	o-ethylphenol	—	30	30
16	2,5-dimethylphenol	—	250	220
17	3,5-dimethylphenol	—	230	240
18	2,3-dimethylphenol	—	30	30
19	n-nonanoic acid	100	—	—
20	3,4-dimethylphenol	—	100	900
21	n-decanoic acid	50	—	—
22	α-naphthol	—	10	—
23	β-naphthol	—	30	—

values for organic compounds found in by-product waters from fossil fuel conversion processes.

All organic acids were obtained from J. T. Baker Chemical Company with purities 99^{+}% as determined by a gas chromatograph. The operating condition of the chromatographic analysis is shown in Table 3.

Table 3. Operating Conditions for Purity Analysis

Column	10'x 1/8", 10% SP-1200 & 1% H_3PO_4 or Gas Chrom Q
Flow Rate	30 cc/min Helium
Initial Temperature	120°C
Final Temperature	180°C
Program Rate	2°/min
Flame Ionization	

Radioactive acetic acid, propionic acid and n-butanoic acid were obtained from Radiochemical Center, Amersham, England, whereas n-hexanoic acid and n-heptanoic acid were obtained from ICN Chemicals & Radioisotopes Inc.

C. Apparatus

The major experimental apparatus used in this study was a Beckman Instrument Co. Liquid Scintillation Counter, model LS-9000. A Blue-M refrigerator shakerbath was used for equilibrium. A complete procedure for carrying out this

study is given in the following section.

D. Procedures

The activated carbon used in this work was further cleaned by washing with double distilled water until no floculation was seen. Then the washed activated carbon was heated at 428 K for 9 hours. The same procedures were repeated twice before taking adsorption data. The concentrations of acetic, propionic, and n-butanoic acids varied from 1 to 10,000 ppm. The concentration of n-hexanoic acid varied from 100 to 2500 ppm, and the concentration of n-heptanoic acid varied from 100 to 2000 ppm. For bi-acid systems, the total acid concentrations varied from 1000 ppm to 5000 ppm.

The radioanalytical approach used in these adsorption experiments involved the addition of a small mass (less than 1 μg) of high specific activity radioactive solute to each of the stock solutions of solute made up at varying concentrations. This imparted a uniform and high solute specific activity to each of the stock solutions with negligible change to the final solute concentration. This method provides an equally sensitive and accurate radioanalysis for determining solute concentrations at both high and low levels. The net result is that the overall statistical variance and accuracy of the results obtained

are the same over the entire concentration range.

After preparing the radioactive solutions, samples of 5 mL were taken before and after equilibration with the activated carbon. The radioactivity was counted after mixing 1 mL (out of 5 mL) of each sample with 12 mL of Dimulume-30, Packard Instrument Co. Ninety-five milliliters of each sample solution was shaken with 0.5 g of activated carbon in a shaker bath set at either 278, 298, or 313 K, for 48 h to reach equilibrium.

Forty-eight hours was found to be adequate time for equilibrium as determined from kinetic studies as shown in Tables 4, 5 and Figures 6, 7.

Samples were placed in the liquid scintillation counter and dark adapted for at least 30 min prior to counting. Counting was performed in a wide open ^{14}C window and continued until a 2σ count rate error of 2% or less was achieved. Random coincidnece monitoring was used to ensure that the contribution of counting events not due to radioactivity disintegrations, e.g. chemiluminescence, was less than 0.2%. The counting efficiency was determined for each sample and was used to compute the absolute activity as disintegrations per minute (DPM). Efficiency corrections were made by instrumental measurement of the Compton edge inflection point (a Beckman modification of the external

standardization method). The determination of the counting efficiency was made from a calibration curve obtained from a series of water quenched ^{14}C standards of hexadecane prepared in Dimilume-30. Final DPM values were corrected by subtraction of background count rate. The background count rate was found to be 60 cpm. Appendix A illustrates the calculational procedures and the procedures in preparing the calibration curve. For more detailed information references (41-43) are highly recommended.

All the radioisotopes used in this study were labeled by ^{14}C. Thus, in taking the bi-solute equilibrium data, each sample solution was duplicated and injected with the isotopes of one of its components. To obtain the final countings, the duplicated sample solutions were counted separately in a single channel ^{14}C window. An error analysis of the experimental measurements is given in Appendix C.

Table 4 Kinetic study for the adsorption of acetic acid from aqueous solution at 298 K (initial concentration 2500 ppm)

Counts (DPM)	Time (hours)
10164	0
9943	2
9833	4
9816	6
9725	10
9691	12
9547	22
9503	26
9517	30
9480	34
9483	46
9502	59.5
9490	72.5

Table 5 Kinetic study for the adsorption of n-heptanoic acid from aqueous solution at 298 K (initial concentration 1 ppm)

DPM	Time (hours)
10907	0
3011	4
1274	7
242	11
100	23.25
82	27
87	31
78	36
79	48.25
78	54
80	60

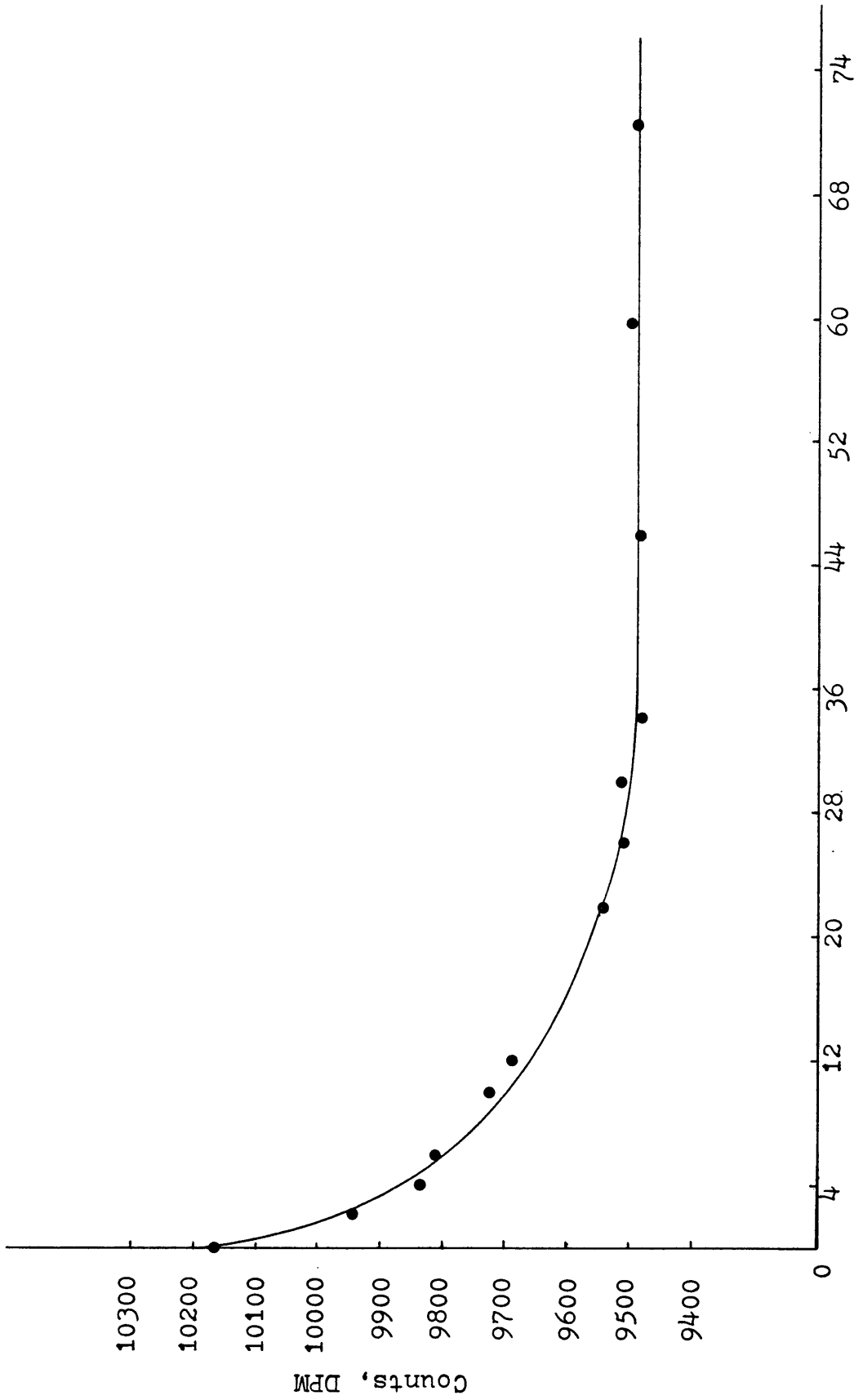

Figure 6 Equilibration test for the adsorption of acetic acid from aqueous solution at 298 K (initial concentration, 2500 ppm.)

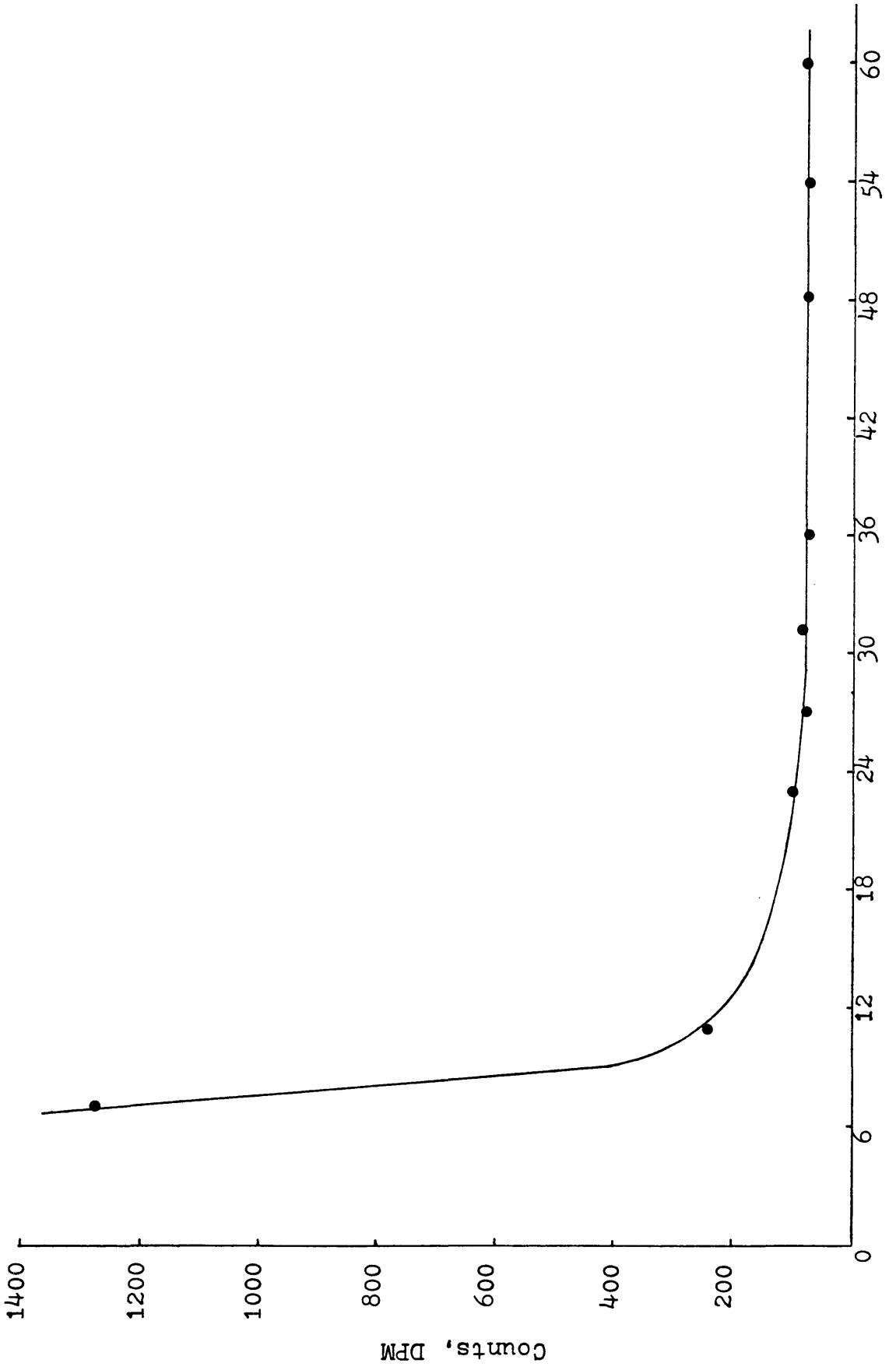

Figure 7 Equilibration test for the adsorption of n-heptanoic acid from aqueous solution at 298 K (initial concentration, 1 ppm.)

V. Results

The experimental data of single-acid systems are presented in Tables 6 through 10 and Figures 8 through 10. The adsorption isotherms were fitted with a three-parameter empirical equation proposed by Radke and Prausnitz (44)

$$\frac{1}{q} = \frac{1}{a C_f} + \frac{1}{b C_f^{\beta}} \qquad (73)$$

where q is the uptake of the solute by solid, m mole/g, C_f is the final equilibrium concentration of the solute in the bulk phase, m mole/l, and β is constrained to be less than 1.0. The data were fitted to within 1% by using the parameters given in Table 11. Tables 12 through 17 and Figures 11 and 12 give the adsorbate volume, Vads, versus $\frac{T}{\bar{V}_i} \log \frac{1}{x_{iB}}$ for the acids adsorbed singly from aqueous at 278K and 298K respectively.

The results of the individual adsorption of bi-solute organic acids, total amount of uptake and the average errors are presented in Tables 18 through 23. The average errors shown in the tables are taken to be the absolute errors compared with the experimental data. The predicted uptakes as found by the method proposed in this study are compared with experimental values and with values predicted by the method of Radke and Prausnitz (24). In all of the

calculations, the partial molar volumes of solutes are assumed to be equal to their molar volumes at the specified system temperatures. A sample calculation is given in Appendix B to illustrate the calculational procedures.

Figures 13 through 24 show predicted results for different mixtures at the specified system temperatures. Solid lines are the interpolated single solute isotherms, dotted lines are calculated from the potential theory as modified in this study herein and the dash lines represent values calculated by the method of Radke and Prausnitz (24). The experimental data are shown by the black points. Thirty-six experimental mixture points were measured over a two-decade range in solute concentration and adsorbent loading. However, only one point per calculated line is shown because of the difficulty in controlling the final equilibrium concentrations especially for completely miscible solutes. The experimental error of the bi-solute studies is estimated to be about 4%.

In applying the ideal adsorbed solution theory, the spreading pressures were calculated numerically and then fitted by a fourth order polynomial over the appropriate concentration range. The calculated spreading pressures were shown in Tables 24 and 25, and Figures 25 and 26. Tables 26 and 27 show the coefficients of the fourth order

polynomial used to fit the spreading pressures. A Newton-Raphson iterative method was used to solve Equations (22) through (26). The individual uptake was calculated by using Equations (15), (27) and (28).

Table 6. Adsorption Isotherm Data of Acetic Acid

278 K		298 K		313 K	
q, $\frac{\text{m.mole}}{\text{g}}$	C_f, $\frac{\text{mole}}{\text{l}}$	q, $\frac{\text{m.mole}}{\text{g}}$	C_f, $\frac{\text{mole}}{\text{l}}$	q, $\frac{\text{m.mole}}{\text{g}}$	C_f, $\frac{\text{mole}}{\text{l}}$
.60	7.46×10^{-2}	1.23	7.69×10^{-2}	1.06	7.78×10^{-2}
.14	3.61×10^{-2}	8.83×10^{-1}	3.70×10^{-2}	8.04×10^{-1}	3.74×10^{-2}
$.83 \times 10^{-1}$	1.33×10^{-2}	5.47×10^{-1}	1.41×10^{-2}	4.58×10^{-1}	1.43×10^{-2}
$.38 \times 10^{-1}$	5.98×10^{-3}	3.65×10^{-1}	6.52×10^{-3}	2.84×10^{-1}	6.84×10^{-3}
$.71 \times 10^{-1}$	2.74×10^{-3}	2.29×10^{-1}	2.96×10^{-3}	1.75×10^{-1}	3.25×10^{-3}
$.35 \times 10^{-1}$	9.56×10^{-4}	1.16×10^{-1}	1.06×10^{-3}	8.10×10^{-2}	1.24×10^{-3}
$.50 \times 10^{-2}$	4.40×10^{-4}	6.98×10^{-2}	5.04×10^{-4}	4.25×10^{-2}	5.10×10^{-4}
$.73 \times 10^{-2}$	7.58×10^{-5}	1.50×10^{-2}	7.77×10^{-5}	1.16×10^{-2}	1.06×10^{-4}
$.62 \times 10^{-3}$	6.01×10^{-6}	2.68×10^{-3}	9.00×10^{-6}	1.58×10^{-3}	8.34×10^{-6}

Table 7. Adsorption Isotherm Data of Propionic Acid

278 K		298 K		313 K	
q, $\frac{\text{m.mole}}{\text{g}}$	C_f, $\frac{\text{mole}}{\text{l}}$	q, $\frac{\text{m.mole}}{\text{g}}$	C_f, $\frac{\text{mole}}{\text{l}}$	q, $\frac{\text{m.mole}}{\text{g}}$	C_f, $\frac{\text{mole}}{\text{l}}$
.88	5.77×10^{-2}	1.30	2.71×10^{-2}	1.60	5.63×10^{-2}
55	2.71×10^{-2}	8.80×10^{-1}	8.79×10^{-3}	1.28	2.63×10^{-2}
00×10^{-1}	8.98×10^{-3}	5.72×10^{-1}	3.80×10^{-3}	8.03×10^{-1}	9.30×10^{-3}
40×10^{-1}	3.39×10^{-3}	3.55×10^{-1}	1.51×10^{-3}	4.95×10^{-1}	4.15×10^{-3}
94×10^{-1}	1.41×10^{-3}	1.70×10^{-2}	5.00×10^{-4}	3.10×10^{-1}	1.75×10^{-3}
80×10^{-1}	3.81×10^{-4}	8.95×10^{-2}	2.10×10^{-4}	1.56×10^{-1}	5.61×10^{-4}
46×10^{-2}	1.78×10^{-4}	2.02×10^{-2}	2.80×10^{-5}	8.50×10^{-2}	2.28×10^{-4}
07×10^{-2}	2.62×10^{-5}	---	---	2.00×10^{-2}	3.60×10^{-5}
57×10^{-3}	2.06×10^{-6}	---	---	2.40×10^{-3}	8.22×10^{-7}

Table 8. Adsorption Isotherm Data of Butyric Acid

278 K		298 K		313 K	
q, $\frac{\text{m.mole}}{\text{g}}$	C_f, $\frac{\text{mole}}{\text{l}}$	q, $\frac{\text{m.mole}}{\text{g}}$	C_f, $\frac{\text{mole}}{\text{l}}$	q, $\frac{\text{m.mole}}{\text{g}}$	C_f, $\frac{\text{mole}}{\text{l}}$
72	9.70×10^{-2}	2.43	1.00×10^{-1}	1.93	1.04×10^{-1}
05	4.66×10^{-2}	1.87	4.75×10^{-2}	1.65	4.80×10^{-2}
62	2.04×10^{-2}	1.42	2.12×10^{-2}	1.39	2.11×10^{-2}
11×10^{-1}	6.30×10^{-3}	9.24×10^{-1}	6.50×10^{-3}	8.45×10^{-1}	6.92×10^{-3}
04×10^{-1}	1.98×10^{-3}	6.57×10^{-1}	2.22×10^{-3}	5.96×10^{-1}	2.54×10^{-3}
30×10^{-1}	5.70×10^{-4}	4.08×10^{-1}	6.38×10^{-4}	3.77×10^{-1}	8.55×10^{-4}
95×10^{-1}	1.11×10^{-4}	1.98×10^{-1}	1.48×10^{-4}	1.84×10^{-1}	1.66×10^{-4}
03×10^{-1}	2.87×10^{-5}	1.00×10^{-1}	4.10×10^{-5}	9.72×10^{-2}	5.66×10^{-5}
---	---	3.11×10^{-2}	5.44×10^{-6}	2.09×10^{-2}	3.62×10^{-6}

Table 9. Adsorption Isotherm Data of Hexanoic Acid

278 K		298 K		313 K	
q, $\frac{m.mole}{g}$	C_f, $\frac{mole}{l}$	q, $\frac{m.mole}{g}$	C_f, $\frac{mole}{l}$	q, $\frac{m.mole}{g}$	C_f, $\frac{mole}{l}$
72	1.25×10^{-2}	1.66	1.28×10^{-2}	1.56	1.33×10^{-2}
30	2.32×10^{-3}	1.20	2.30×10^{-3}	1.08	2.90×10^{-3}
66×10^{-1}	2.80×10^{-4}	7.19×10^{-1}	3.72×10^{-4}	7.04×10^{-1}	6.05×10^{-4}
90×10^{-1}	3.87×10^{-5}	4.00×10^{-1}	6.45×10^{-5}	3.92×10^{-1}	8.87×10^{-5}
---	---	1.62×10^{-1}	7.16×10^{-6}	1.62×10^{-1}	1.02×10^{-5}

Table 10. Adsorption Isotherm Data of Heptanoic Acid

278 K		298 K		313 K	
q, $\frac{m.mole}{g}$	C_f, $\frac{mole}{l}$	q, $\frac{m.mole}{g}$	C_f, $\frac{mole}{l}$	q, $\frac{m.mole}{g}$	C_f, $\frac{mole}{l}$
.76	6.13×10^{-3}	1.60	6.96×10^{-3}	1.47	7.10×10^{-3}
.31	1.31×10^{-3}	1.19	1.73×10^{-3}	1.09	1.97×10^{-3}
$.97 \times 10^{-1}$	1.76×10^{-4}	6.90×10^{-1}	2.13×10^{-4}	6.30×10^{-1}	2.49×10^{-4}
$.10 \times 10^{-1}$	2.65×10^{-5}	3.60×10^{-1}	2.55×10^{-5}	3.40×10^{-1}	4.03×10^{-5}
---	---	---	---	1.41×10^{-1}	6.22×10^{-6}

Table 11. Parameters of Equation (73)

Aliphatic Acid	Temperature K	a	b	β
Acetic	278	0.2811	0.2743	0.4288
	298	0.2357	0.2181	0.4155
	313	0.1324	0.1706	0.4602
Propionic	278	0.8827	0.5202	0.3404
	298	0.8594	0.4024	0.3895
	313	0.7138	0.3377	0.4144
n-Butyric	278	9.0113	0.5620	0.3462
	298	6.7248	0.5010	0.3457
	313	3.0223	0.4921	0.3133
n-Hexanoic	278	72.0000	1.0265	0.2260
	298	52.4989	0.9349	0.2444
	313	43.4166	0.8185	0.2547
n-Heptanoic	278	111.3755	1.1626	0.2487
	298	70.0420	1.0411	0.2286
	313	46.7134	0.9278	0.2446

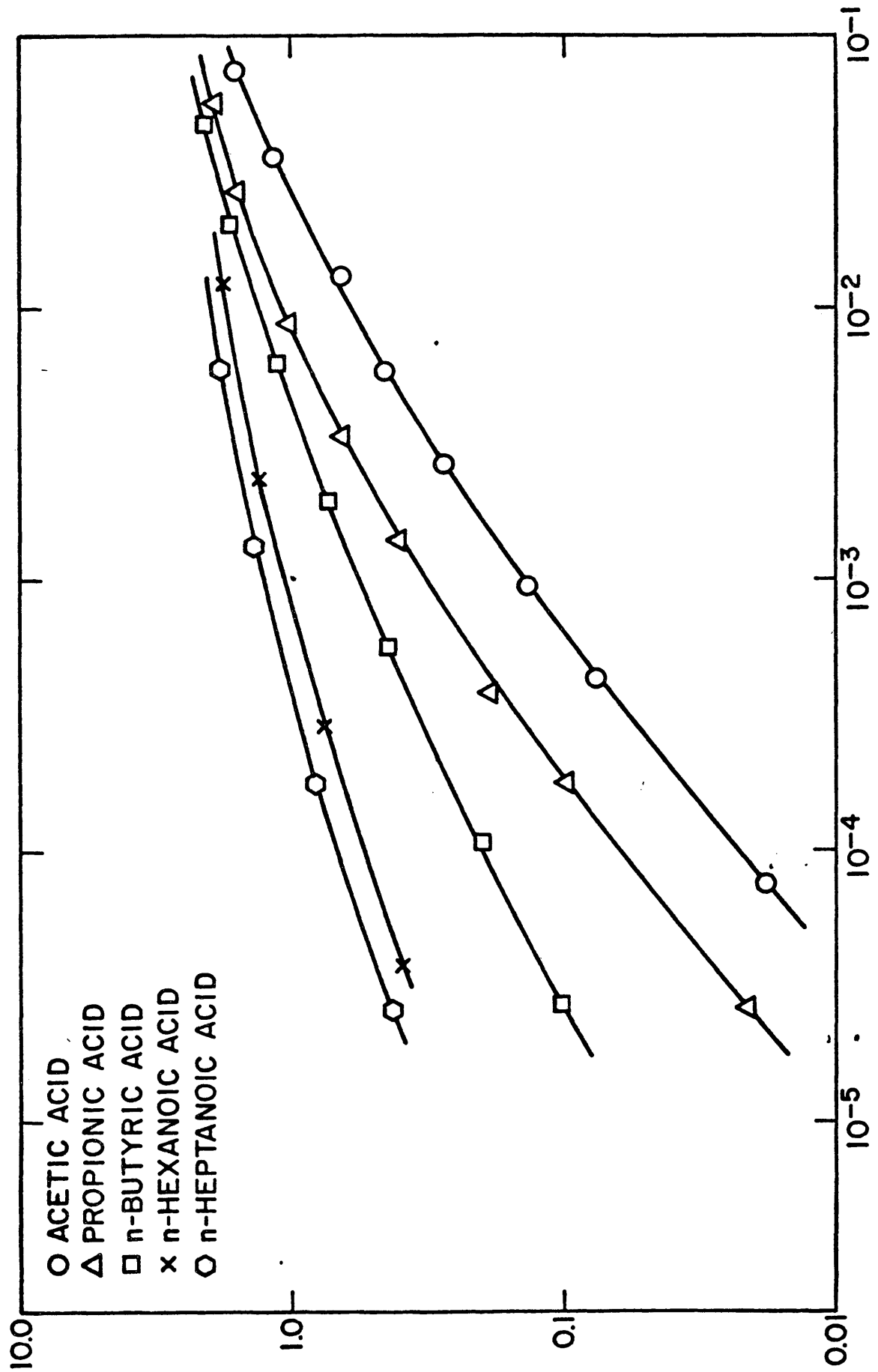

Figure 8. Adsorption isotherms at 278 K for single-solute systems

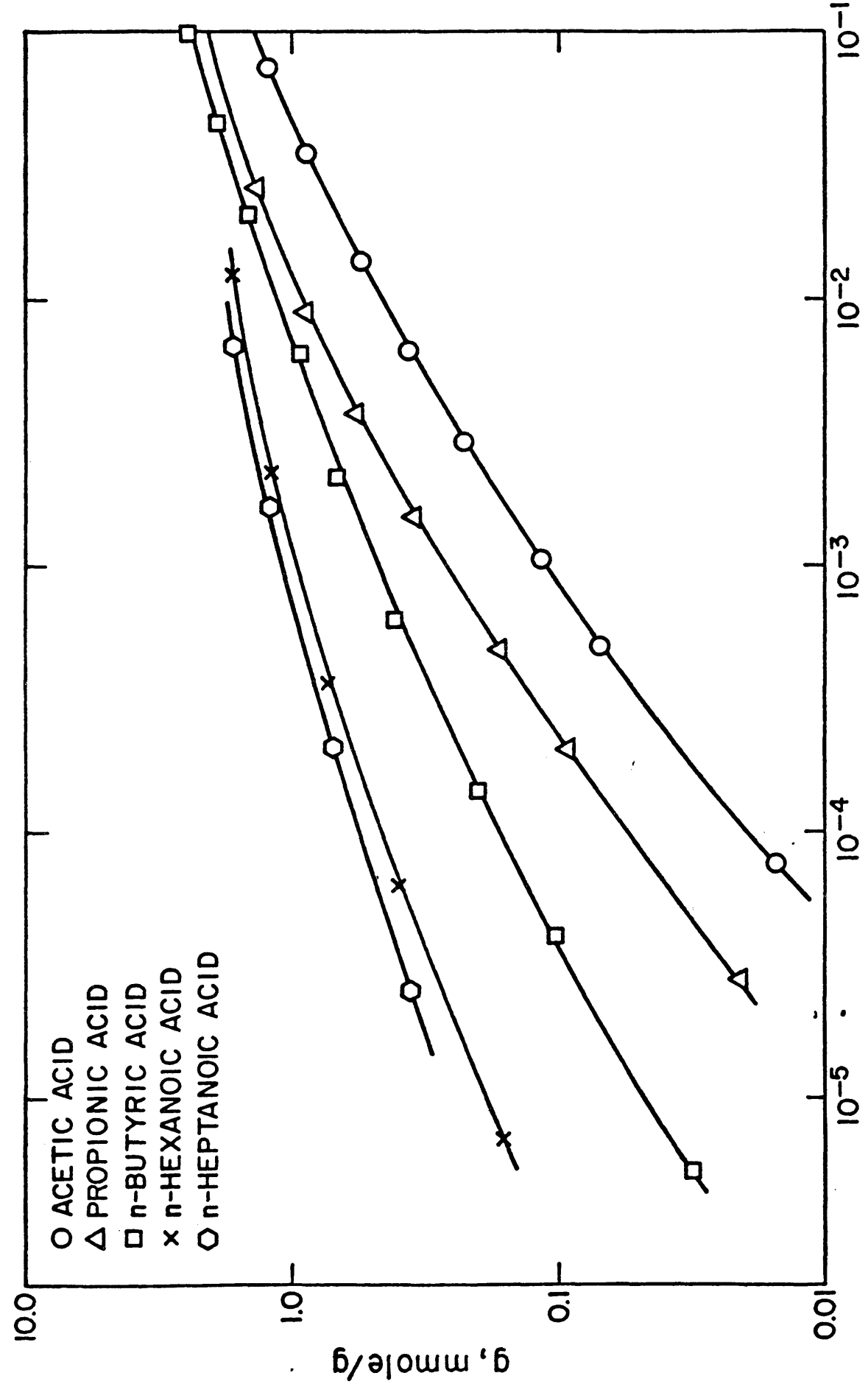

Figure 9. Adsorption isotherms at 298 K for single-solute systems

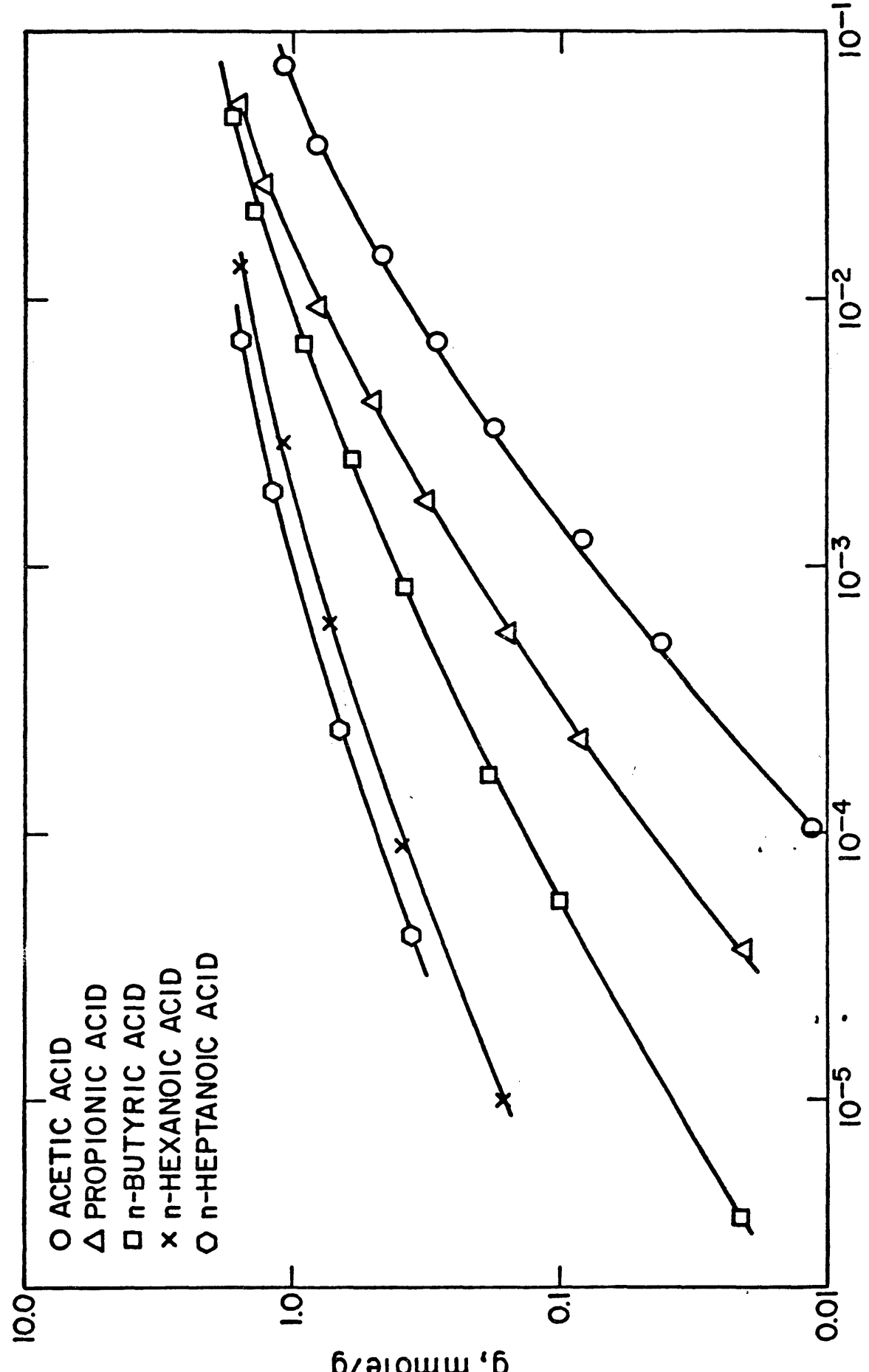

Figure 10. Adsorption isotherms at 313 K for single-solute systems

Table 12 Adsorption of acetic acids from aqueous solution at 278 K

Equilibrium Concentration	Weight Adsorbed	Volume Adsorbed	$\frac{\Sigma_2^*}{\bar{V}_2} = \frac{T}{\bar{V}_2} \log \frac{1}{X_{2B}}$
mole/l	m mole/g	ml/100g	
7.46×10^{-2}	1.60	9.16	14.04
3.61×10^{-2}	1.14	6.48	15.60
1.33×10^{-2}	6.83×10^{-1}	3,88	17.71
5.98×10^{-3}	4.38×10^{-1}	2.49	19.42
2.74×10^{-3}	2.71×10^{-1}	1.54	21.08
9.56×10^{-4}	1.35×10^{-1}	0.77	23.28
4.40×10^{-4}	7.50×10^{-2}	0.43	24.95
7.58×10^{-5}	1.73×10^{-3}	0.098	28.71
6.01×10^{-6}	1.62×10^{-3}		

$\bar{V}_2^+ = 56.83$ ml/mole

* The subscripts 2,3, and 4 refer to acetic acid, propionic acid and n-butanoic acid respectively

\+ from Perry's Handbook, 5th Ed.,McGraw Hill,(1973)

Table 13 Adsorption of propionic acid from aqueous solution at 278 K

Equilibrium Concentration	Weight Adsorbed	Volume Adsorbed	$\frac{\Sigma_3}{\bar{V}_3} = \frac{T}{\bar{V}_3} \log \frac{1}{X_{3B}}$
mole/l	m mole/g	ml/100g	
5.77×10^{-2}	1.88	13.75	11.32
2.71×10^{-2}	1.55	11.31	12.58
8.98×10^{-3}	1.00	7.35	14.40
3.39×10^{-3}	6.40×10^{-1}	4.68	16.00
1.41×10^{-3}	3.94×10^{-1}	2.88	17.49
3.81×10^{-4}	1.80×10^{-1}	1.32	19.62
1.78×10^{-4}	9.46×10^{-2}	0.69	20.87
2.62×10^{-5}	2.07×10^{-2}	0.18	24.06
2.06×10^{-6}	2.57×10^{-3}		

$$\bar{V}_3 = 73.5 \frac{ml}{mole}$$

Table 14 Adsorption of Butanoic acid from aqueous solution at 278 K

Equilibrium Concentration	Weight Adsorbed	Volume Adsorbed	$\frac{\Sigma_4}{\bar{V}_4} = \frac{T}{\bar{V}_4} \log \frac{1}{X_{4B}}$
mole/l	m mole/g	ml/100g	
9.7×10^{-2}	2.72	24.23	8.56
4.66×10^{-2}	2.05	18.36	9.56
2.04×10^{-2}	1.62	14.51	10.64
6.30×10^{-3}	1.11	9.90	12.22
1.98×10^{-3}	7.04×10^{-1}	6.30	13.80
5.70×10^{-4}	4.30×10^{-1}	3.85	15.49
1.11×10^{-4}	1.95×10^{-1}	1.74	17.70
2.87×10^{-5}	1.03×10^{-1}	0.92	19.52

$$\bar{V}_4 = 89.6 \frac{ml}{mole}$$

Table 15 Adsorption of acetic acid from aqueous solution at 298 K

Equilibrium Concentration	Weight Adsorbed	Volume Adsorbed	$\frac{\Sigma_2}{\bar{V}_2} = \frac{T}{\bar{V}_2} \log \frac{1}{X_{2B}}$
mole/l	m.mole/g	ml/100g	
7.69×10^{-2}	1.23	7.04	14.88
3.70×10^{-2}	8.83×10^{-1}	5.05	16.54
1.41×10^{-2}	5.47×10^{-1}	3.13	18.73
6.52×10^{-3}	3.65×10^{-1}	2.09	20.46
2.96×10^{-3}	2.29×10^{-1}	1.13	22.27
1.06×10^{-3}	1.16×10^{-1}	0.664	24.57
5.04×10^{-4}	6.98×10^{-2}	0.40	26.23
7.77×10^{-5}	1.50×10^{-2}	0.086	30.47
9.00×10^{-6}	2.68×10^{-3}		

$\bar{V}_2 = 57.24$ ml/mole

Table 16 Adsorption of propionic acid from aqueous solution at 298 K

Equilibrium Concentration	Weight Adsorped	Volume Adsorbed	$\frac{\Sigma_3}{\bar{V}_3} = \frac{T}{\bar{V}_3} \log \frac{1}{X_{3B}}$
mole/l	m mole/g	ml/100g	
2.71×10^{-2}	1.30	9.76	13.15
8.79×10^{-3}	8.80×10^{-1}	6.60	15.10
3.80×10^{-3}	5.72×10^{-1}	4.30	16.55
1.51×10^{-3}	3.55×10^{-1}	2.66	18.11
5.00×10^{-4}	1.70×10^{-1}	1.27	20.02
2.10×10^{-4}	8.95×10^{-2}	0.67	21.53
2.80×10^{-5}	2.02×10^{-2}	0.144	25.00

$$\bar{V}_3 = 75 \frac{\text{ml}}{\text{mole}}$$

Table 17 Adsorption of butanoic acid from aqueous solution at 298 K

Equilibrium Concentration	Weight Adsorbed	Volume Adsorbed	$\frac{\Sigma_4}{\bar{V}_4} = \frac{\Sigma_4}{\bar{V}_4} \log \frac{1}{X_{4B}}$
mole/l	m.mole/g	ml/100g	
1.00×10^{-1}	2.43	22.20	8.93
4.75×10^{-2}	1.87	17.08	10.00
2.12×10^{-2}	1.42	12.98	11.15
6.50×10^{-3}	9.24×10^{-1}	8.44	12.81
2.22×10^{-3}	6.57×10^{-1}	6.00	14.34
6.38×10^{-4}	4.08×10^{-1}	3.73	16.11
1.48×10^{-4}	1.98×10^{-1}	1.81	18.16
4.10×10^{-5}	1.00×10^{-1}	0.91	19.99
5.44×10^{-6}	3.11×10^{-2}		

$$\bar{V}_4 = 91.4 \frac{\text{ml}}{\text{mole}}$$

Table 18 Competitive adsorption data for the mixture of acetic acid and propionic acid at 298 K

	C_2^+	C_3	q_2^{exp}	q_2^*	q_2^{**}	q_3^{exp}	q_3^*	q_3^{**}	q_T^{exp}	q_T^*	q_T^{**}
	mole/l	mole/l	m mole / g	m mole / g	m mole / g	m mole / g	m mole / g	m mole / g	m mole / g	m mole / g	m mole / g
1	7.28×10^{-3}	4.52×10^{-3}	0.219	0.242	0.210	0.445	0.514	0.507	0.664	0.756	0.717
2	1.52×10^{-2}	4.69×10^{-3}	0.353	0.385	0.367	0.431	0.473	0.467	0.784	0.858	0.834
3	3.54×10^{-2}	1.45×10^{-2}	0.450	0.495	0.546	0.735	0.783	0.760	1.185	1.279	1.306
4	3.96×10^{-2}	2.34×10^{-2}	0.442	0.490	0.506	0.868	1.000	1.010	1.310	1.490	1.516
5	6.38×10^{-2}	1.51×10^{-2}	0.743	0.758	0.804	0.607	0.635	0.706	1.350	1.393	1.510
6	6.36×10^{-2}	2.30×10^{-2}	0.605	0.640	0.768	0.821	0.887	0.866	1.426	1.527	1.652
average error				8.1%	13.7%		9.9%	10.5%		9.2%	11.3%

* Radke & Prausnitz

** Potential Theory

\+ Subscript 2,3 and 4 refer to acetic acid, propionic acid and n-butanoic acid and n-butanoic acid respectively

Subscript T indicates total uptake of the solutes

Table 19 Competitive adsorption data for the mixture of acetic acid and n-butanoic acid at 298 K

	C_2	C_4	q_2^{exp}	q_2^{*}	q_2^{**}	q_4^{exp}	q_4^{*}	q_4^{**}	q_T^{exp}	q_T^{*}	q_T^{**}
	mole/l	mole/l	m mole/g	m mole/g	m mole/g	m mole/g	m mole/g	m mole/g	m mole/g	m mole/g	m mole/g
1	7.31×10^{-3}	2.50×10^{-3}	0.194	0.196	0.192	0.605	0.589	0.644	0.799	0.758	0.836
2	1.15×10^{-2}	1.98×10^{-3}	0.327	0.355	0.314	0.588	0.579	0.602	0.905	0.934	0.899
3	3.98×10^{-2}	6.93×10^{-3}	0.397	0.480	0.472	0.842	0.750	0.853	1.239	1.230	1.325
4	4.01×10^{-2}	1.19×10^{-2}	0.413	0.420	0.454	0.975	0.994	1.028	1.388	1.414	1.482
5	6.32×10^{-2}	1.66×10^{-2}	0.659	0.549	0.594	1.170	1.050	1.160	1.829	1.595	1.754
6	6.30×10^{-2}	7.09×10^{-3}	0.690	0.690	0.699	0.751	0.675	0.788	1.441	1.365	1.487
average error				8.7%	7.9%		6.2%	3.6%		4.2%	4.4%

Table 20 Competitive adsorption data for the mixture of propionic acid and n-butanoic acid at 298 K

	C_3	C_4	q_3^{exp}	q_3^*	q_3^{**}	q_4^{exp}	q_4^*	q_4^{**}	q_T^{exp}	q_T^*	q_T^{**}
	mole/l	mole/l	m mole / g	m mole / g	m mole / g	m mole / g	m mole / g	m mole / g	m mole / g	m mole / g	m mole / g
1	5.28×10^{-3}	3.02×10^{-2}	0.302	0.329	0.293	0.525	0.586	0.569	0.827	0.915	0.862
2	9.78×10^{-3}	3.13×10^{-3}	0.697	0.642	0.480	0.485	0.437	0.525	1.182	1.079	1.005
3	2.32×10^{-2}	7.94×10^{-2}	0.727	0.861	0.682	0.651	0.623	0.650	1.378	1.484	1.332
4	2.94×10^{-2}	1.29×10^{-2}	0.877	0.920	0.746	0.786	0.758	0.875	1.663	1.678	1.621
5	3.62×10^{-2}	3.75×10^{-3}	0.856	1.067	0.907	0.563	0.573	0.635	1.419	1.640	1.542
6	3.67×10^{-2}	1.83×10^{-2}	0.738	0.895	0.800	0.836	0.895	0.985	1.574	1.790	1.785
average error				14.4%	11.6%		6.4%	9.8%		9.6%	7.9%

Table 21 Competitive adsorption data for the mixture of acetic acid and propionic acid at 278 K

	C_2^+	C_3	q_2^{exp}	q_2^*	q_2^{**}	q_3^{exp}	q_3^*	q_3^{**}	q_T^{exp}	q_T^*	q_T^{**}
	mole/l	mole/l	m mole / g	m mole / g	m mole / g	m mole / g	m mole / g	m mole / g	m mole / g	m mole / g	m mole / g
1	7.05×10^{-3}	4.11×10^{-3}	0.244	0.280	0.264	0.513	0.578	0.554	0.753	0.858	0.808
2	1.46×10^{-2}	4.31×10^{-3}	0.423	0.518	0.475	0.464	0.482	0.449	0.887	1.000	0.924
3	3.00×10^{-2}	1.03×10^{-2}	0.626	0.669	0.615	0.652	0.724	0.707	1.278	1.393	1.323
4	3.78×10^{-2}	1.62×10^{-2}	0.737	0.684	0.704	0.787	0.886	0.843	1.524	1.570	1.547
5	4.56×10^{-2}	1.06×10^{-2}	0.841	0.902	0.827	0.584	0.650	0.639	1.425	1.552	1.446
6	4.67×10^{-2}	2.26×10^{-2}	0.682	0.742	0.752	0.881	0.984	0.952	1.563	1.726	1.704
average error				11.2%	6.4%		10.5%	7.1%		9.6%	4.6%

Table 22 Competitive adsorption data for the mixture of acetic acid and n-butanoic acid at 278 K

	C_2	C_3	q_2^{exp}	q_2^{*}	q_2^{**}	q_4^{exp}	q_4^{*}	q_4^{**}	q_T^{exp}	q_T^{*}	q_T^{**}
	mole/l	mole/l	m mole/g	m mole/g	m mole/g	m mole/g	m mole/g	m mole/g	m mole/g	m mole/g	m mole/g
1	7.29×10^{-3}	2.31×10^{-3}	0.214	0.219	0.245	0.640	0.674	0.578	0.854	0.893	0.823
2	1.49×10^{-2}	2.48×10^{-3}	0.373	0.447	0.405	0.608	0.593	0.569	0.981	1.070	0.974
3	3.83×10^{-2}	6.89×10^{-3}	0.633	0.665	0.669	0.850	0.836	0.804	1.483	1.496	1.473
4	3.93×10^{-2}	1.63×10^{-2}	0.465	0.512	0.528	1.220	1.220	1.194	1.685	1.732	1.722
5	6.25×10^{-2}	7.13×10^{-2}	0.792	0.855	0.880	0.804	0.670	0.781	1.595	1.525	1.661
6	6.28×10^{-2}	1.67×10^{-2}	0.727	0.726	0.757	1.150	1.144	1.105	1.877	1.870	1.862
average error				8.8%	9.6%		4.4%	5.1%		3.7%	2.0%

Table 23 Competitive adsorption data for the mixture of propionic acid and n-butanoic acid at 278 K

	C_3	C_4	q_3^{exp}	q_3^{*}	q_3^{**}	q_4^{exp}	q_4^{*}	q_4^{**}	q_T^{exp}	q_T^{*}	q_T^{**}
	mole/l	mole/l	m mole/g	m mole/g	m mole/g	m mole/g	m mole/g	m mole/g	m mole/g	m mole/g	m mole/g
1	5.12×10^{-3}	2.90×10^{-3}	0.321	0.374	0.367	0.539	0.665	0.569	0.860	1.039	0.936
2	9.70×10^{-3}	3.06×10^{-3}	0.724	0.738	0.571	0.498	0.474	0.491	1.220	1.212	1.062
3	2.30×10^{-3}	7.69×10^{-3}	0.765	0.851	0.816	0.708	0.799	0.670	1.473	1.650	1.486
4	2.92×10^{-2}	1.29×10^{-2}	0.917	1.000	0.816	0.793	0.836	0.881	1.710	1.836	1.697
5	3.48×10^{-2}	8.13×10^{-3}	1.165	1.226	1.116	0.615	0.557	0.640	1.780	1.783	1.756
6	3.58×10^{-2}	1.76×10^{-2}	0.886	1.000	0.870	0.980	0.979	1.004	1.866	1.979	1.874
average error				9.5%	9.9%		9.3%	5.0%		7.9%	4.7%

Table 24 Spreading pressures of acetic, propionic and butanoic acids at 278 K

Concentration ($m\frac{mole}{l}$)	π(acetic acid) (erg/cm^2)	π(propionic acid) erg/cm^2	π(butanoic acid) erg/cm^2
5	1.9765	4.4404	7.5402
10	3.1239	6.4918	9.9158
20	4.8218	9.2918	13.2658
30	6.1374	11.3206	15.6398
40	7.2467	12.9619	17.5412
50	8.2215	14.3622	19.1536
60	9.0998	15.5949	20.5676
70	9.9046	16.7033	21.8353
80	10.6509	17.7149	22.9899
90	11.3493	18.6487	24.0540
100	12.0075	19.5181	25.0435
110	12.6315	20.3334	25.9705
120	13.2258	21.1024	26.8440
130	13.7940	21.8312	27.6712
140	14.3391	22.5247	28.4580
150	14.8636	23.1869	29.2088
160	15.3648	23.8212	29.9277
170	15.8537	24.4304	30.6179
180	16.3271	25.0168	31.2820

Table 25 Spreading pressures of acetic, propionic and butanoic acids at 298 K

Concentration (m mole/l)	π(acetic acid) (erg/cm^2)	π(propionic acid) erg/cm^2	π(butanoic acid) erg/cm^2
5	1.7163	4.0360	7.0847
10	2.6853	5.9405	9.3610
20	4.1025	8.6106	12.5512
30	5.1902	10.5888	14.8129
40	6.1017	12.2214	16.6245
50	6.8992	13.6156	18.1608
60	7.6152	14.8616	19.5082
70	8.2695	15.9907	20.7161
80	8.8875	17.0281	21.8163
90	9.4399	17.9913	22.8302
100	9.9717	18.8931	23.7731
110	10.4749	19.7427	24.6563
120	10.9535	20.5475	25.4886
130	11.4105	21.3133	26.2768
140	11.8483	22.0448	27.0264
150	12.2691	22.7456	27.7418
160	12.6746	23.4191	28.4267
170	13.0662	24.0679	29.0843
180	13.4450	24.6942	29.9170

Table 26 Coefficients of the fourth order polynomial in curve fitting the spreading pressures at 278 K

$$\pi_i = AC_i + BC_i^2 + CC_i^3 + DC_i^4$$

π_i erg/cm^2 , C_i: m mole/l

For $C_i \leq 50.0$ m mole/l

	A	B	C	D
Acetic acid	0.42054E0	-0.13443E-1	0.26797E-3	-0.20315E-5
Pripionic acid	0.93539E0	-0.36006E-1	0.750748E-3	-0.57990E-5
n-butanoic acid	0.15106E1	-0.66078E-1	0.14353E-2	-0.11298E-4

For $C_i > 50$ m mole/l

	A	B	C	D
Acetic acid	0.30312E0	-0.39789E-2	0.29311E-4	-079259E-7
Propionic acid	0.60838E0	-0.93489E-2	0.71625E-4	-0.19708E-6

$E \pm n = 10^{\pm n}$

Table 27 Coefficients of the fourth order polynomial in curve fitting the spreading pressures at 298 K

$$\pi_i = AC_i + BC_i^2 + CC_i^3 + DC_i^4$$

π : $\frac{erg}{cm^2}$ C_i: m mole/l

For $C_i \leq 50.0$ m mole/l

	A	B	C	D
Acetic acid	0.36553E0	-0.12085E-1	0.24386E-3	-0.18639E-5
propionic acid	0.84723E0	-0.318362E-1	0.66248E-3	-0.51158E-5
n-butanoic acid	0.14238E1	-0.62062E-1	0.13467E-2	-0.10596E-4

For $C_i > 50.0$ m mole/l

	A	B	C	D
Acetic acid	0.25947E0	-0.34929E-2	0.25886E-4	-0.70188E-7
propionic acid	0.55890E0	-0.83273E-2	0.63496E-4	-0.17443E-6

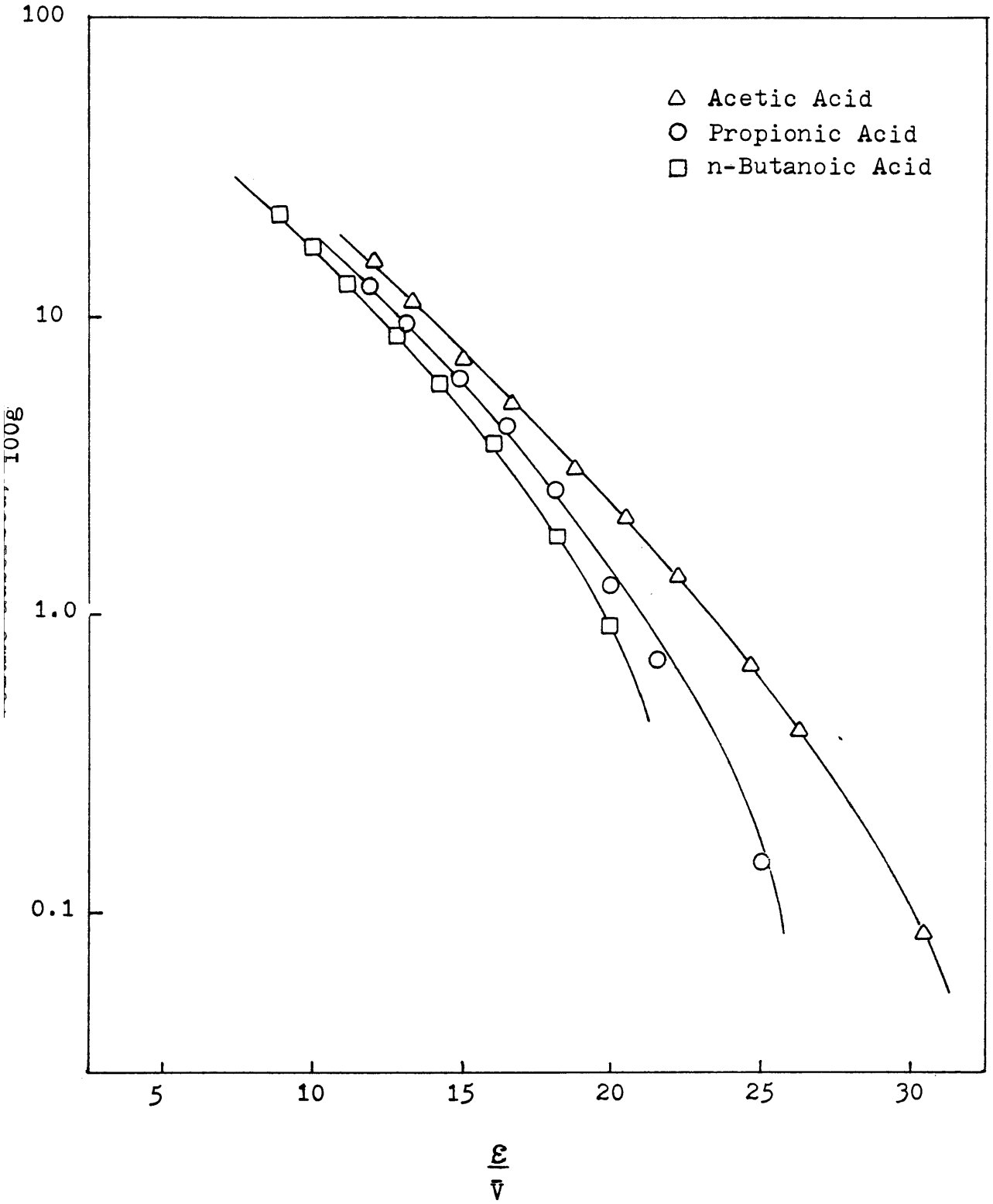

Figure 11 Volume adsorbed versus adsorption potentials of acetic, propionic and n-butanoic acids at 278 K

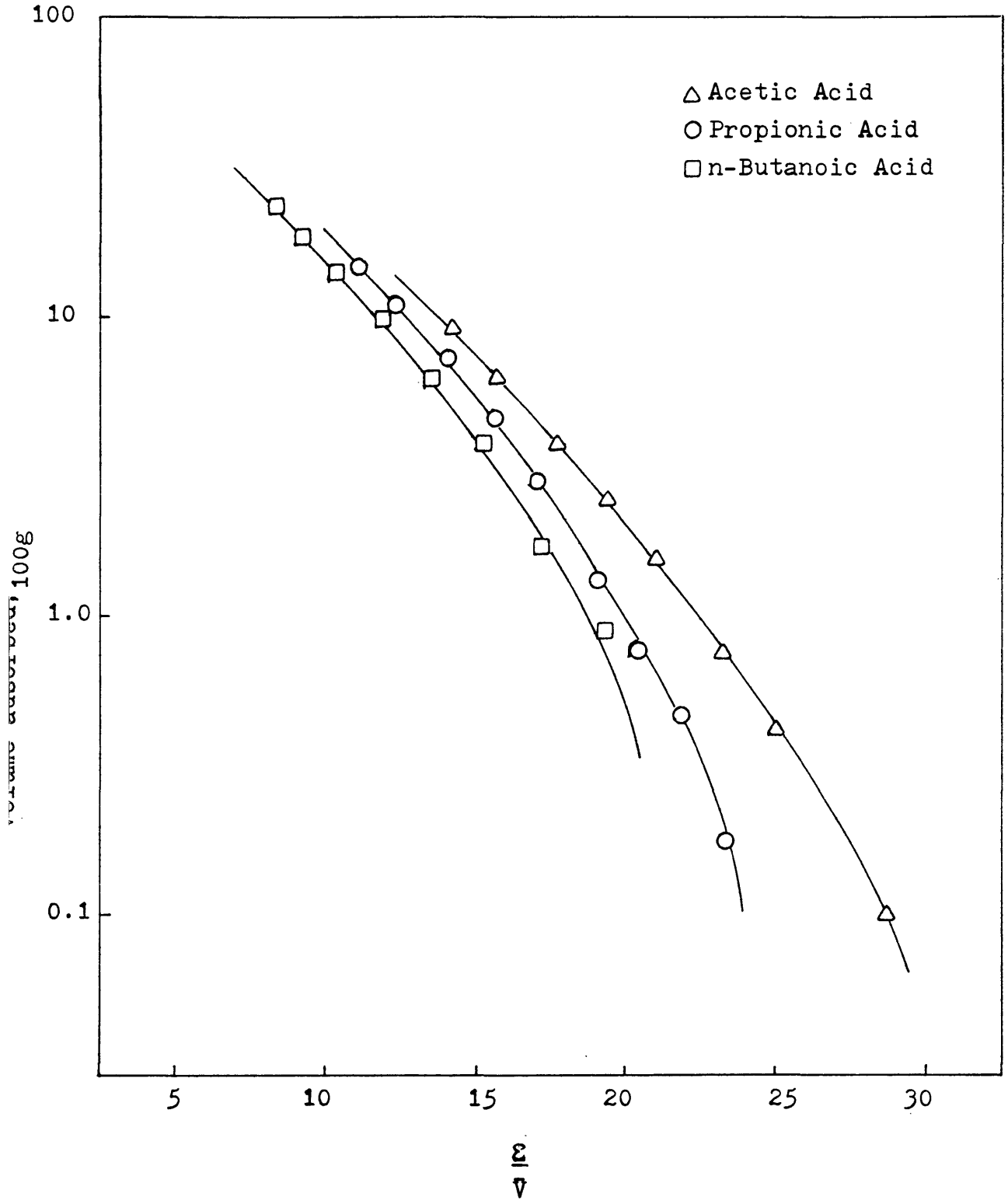

Figure 12 Volume adsorbed versus adsorption potentials of acetic, propionic and n-butanoic acids at 298 K

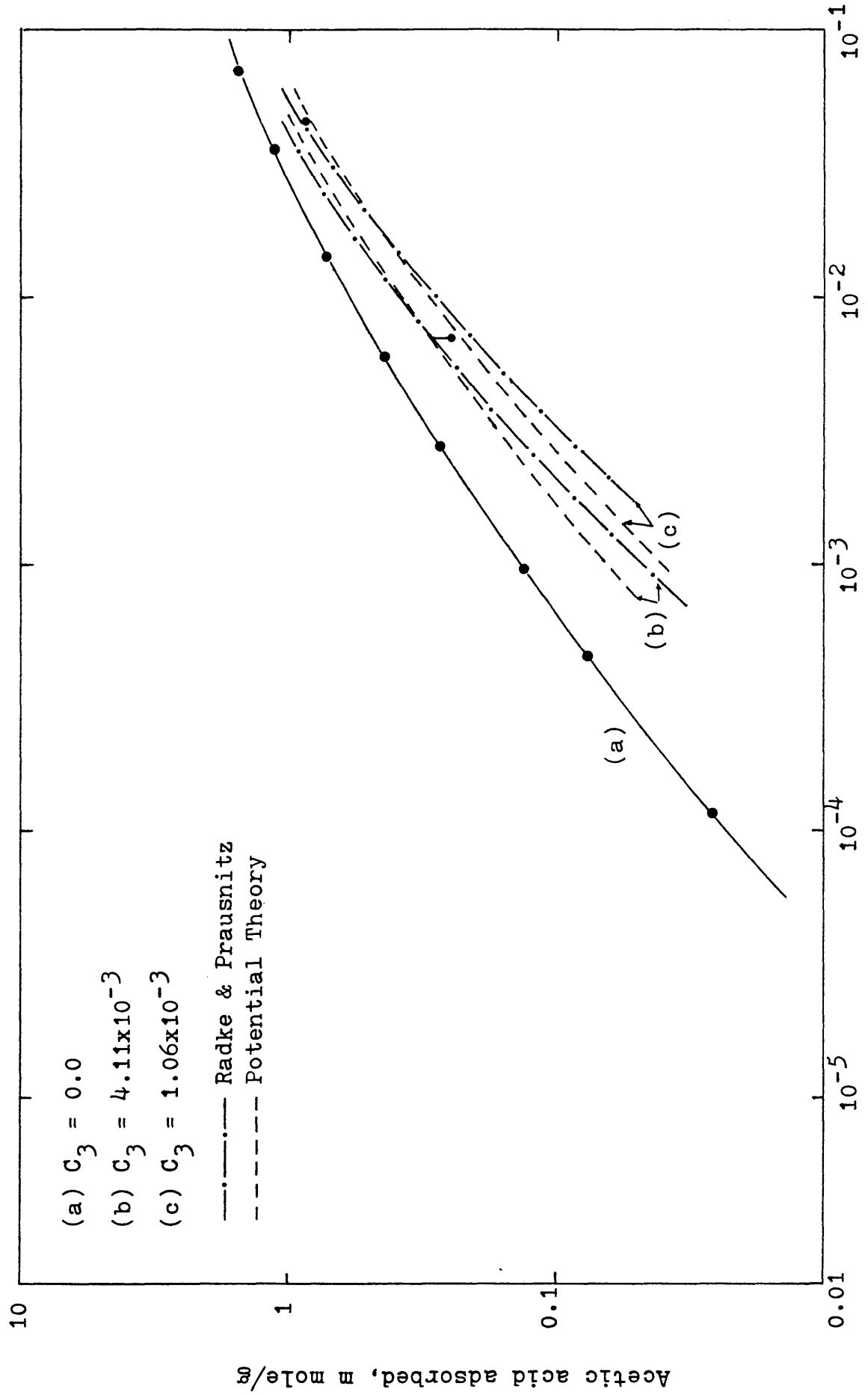

Figure 13 Adsorption of acetic acid in the presence of propionic acid at 278 K

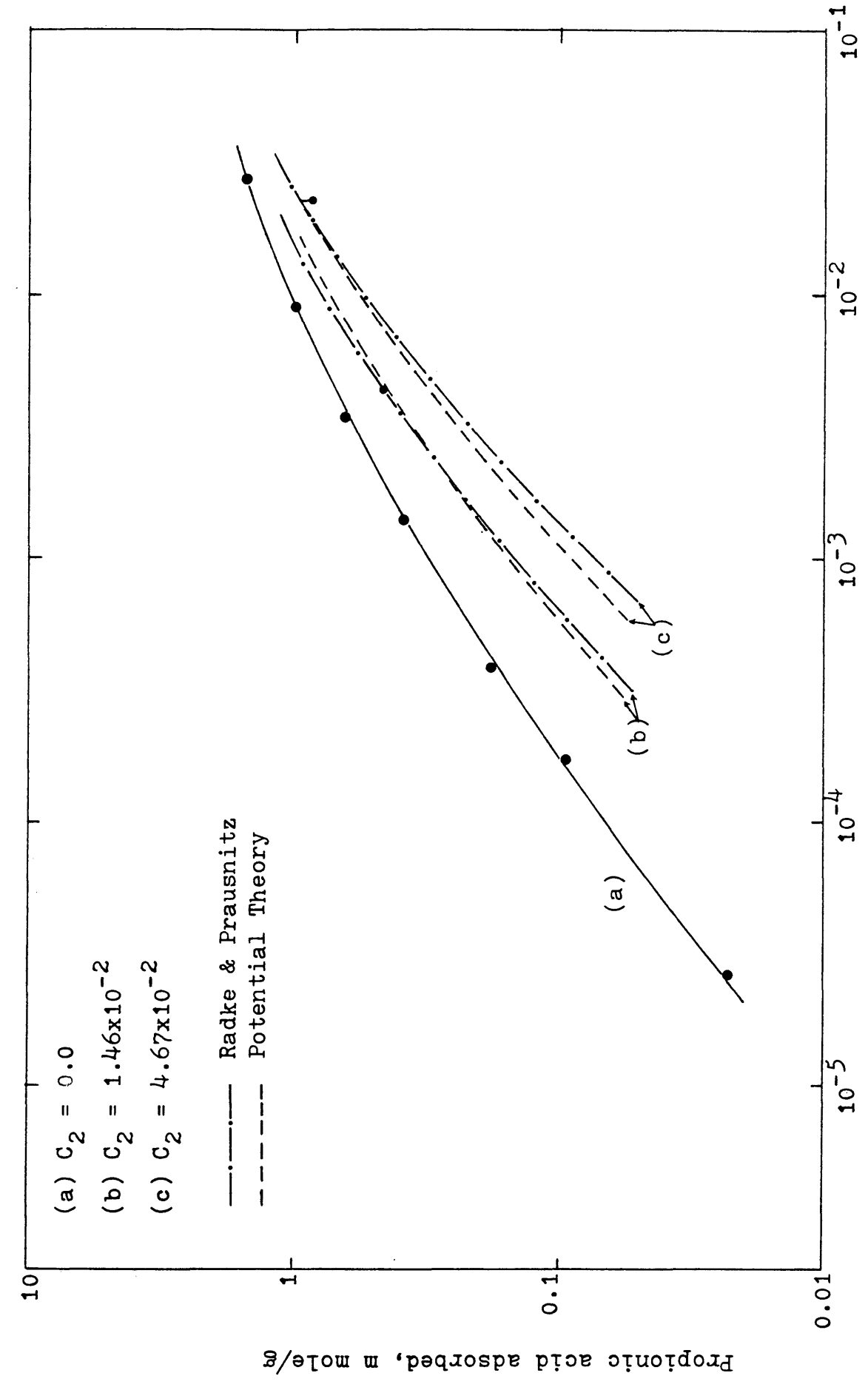

Figure 14 Adsorption of propionic acid in the presence of acetic acid at 278 K

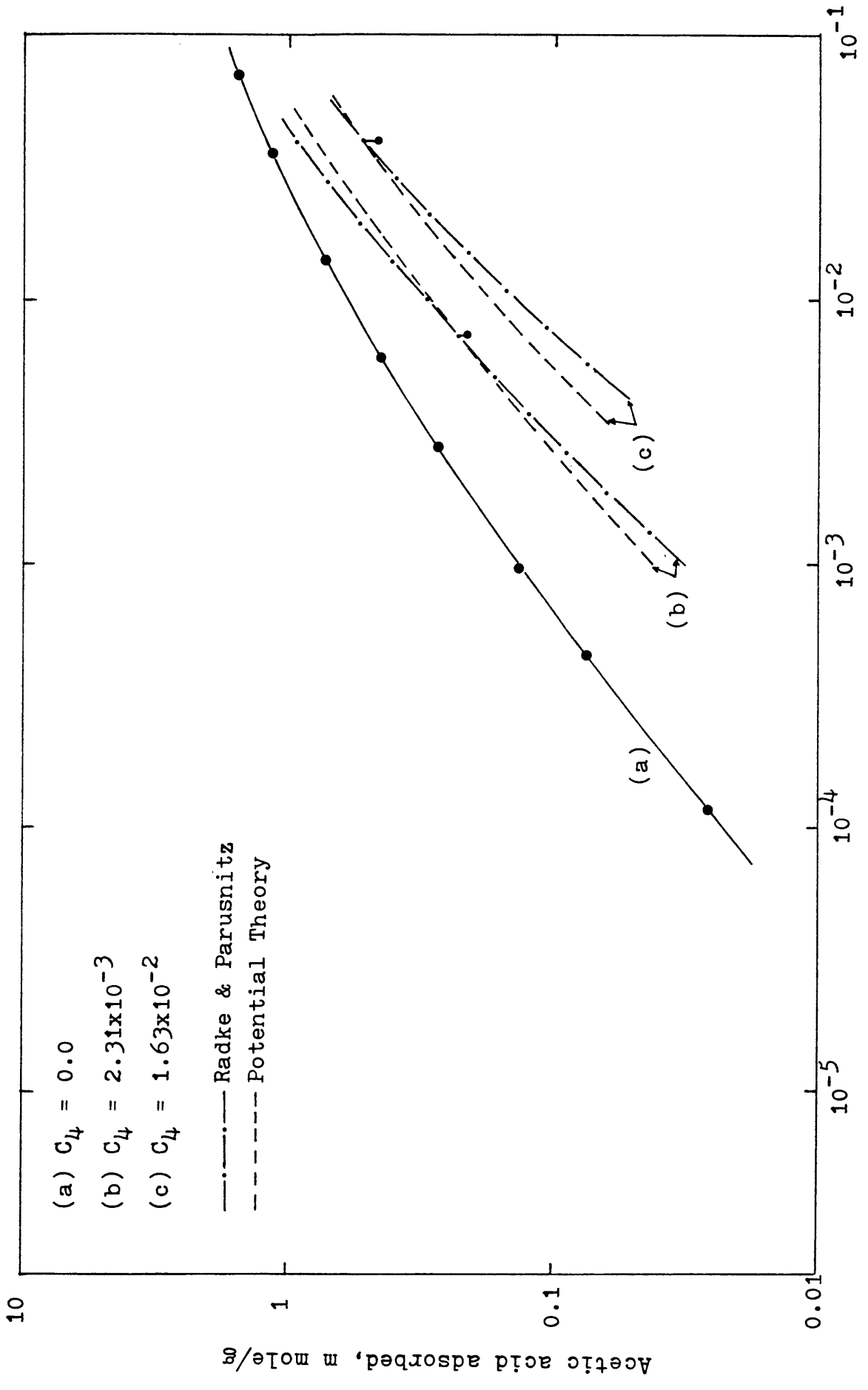

Figure 15 Adsorption of acetic acid in the presence of n-butanoic acid at 278 K

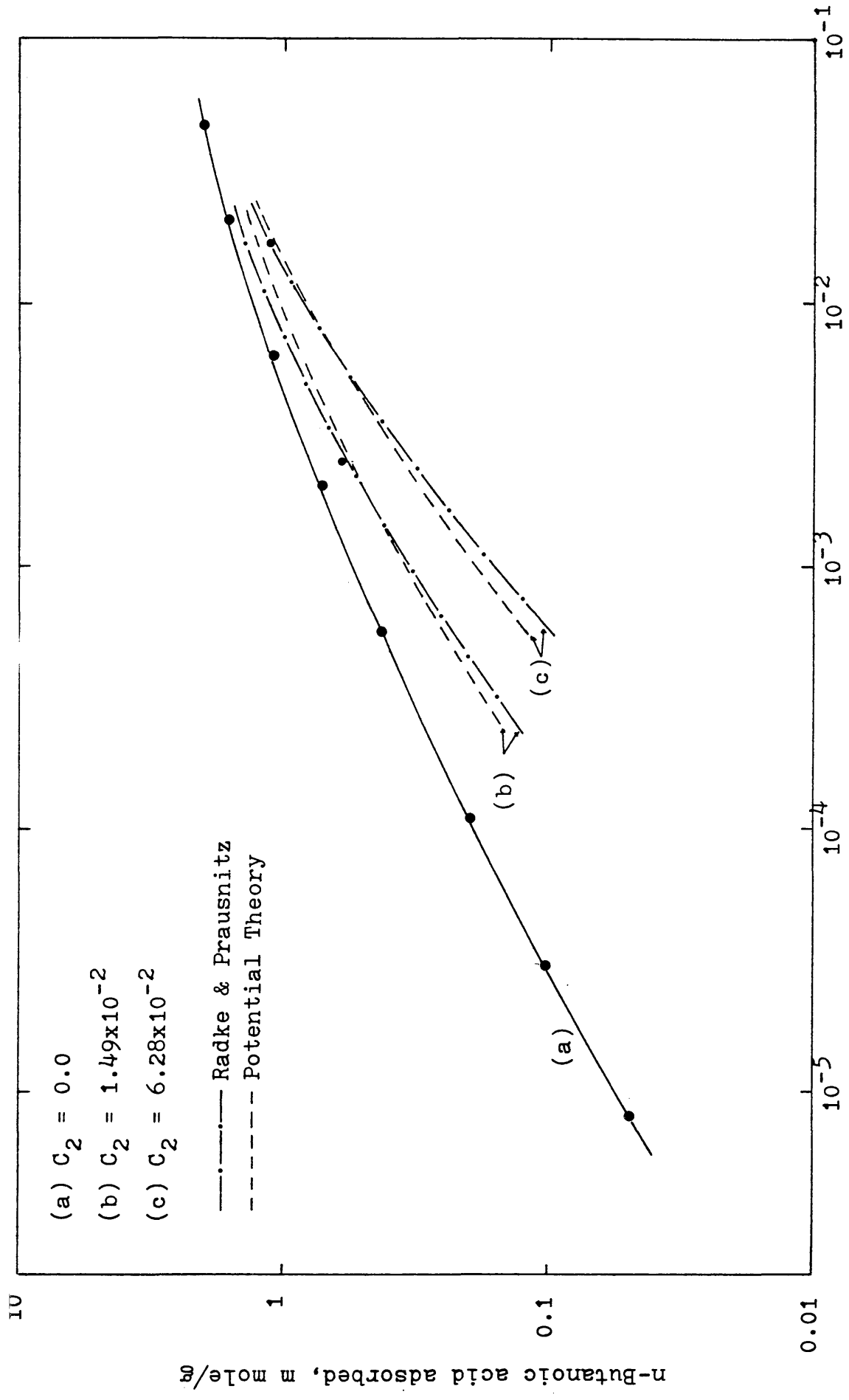

Figure 16 Adsorption of n-butanoic acid in the presence of acetic acid at 278 K

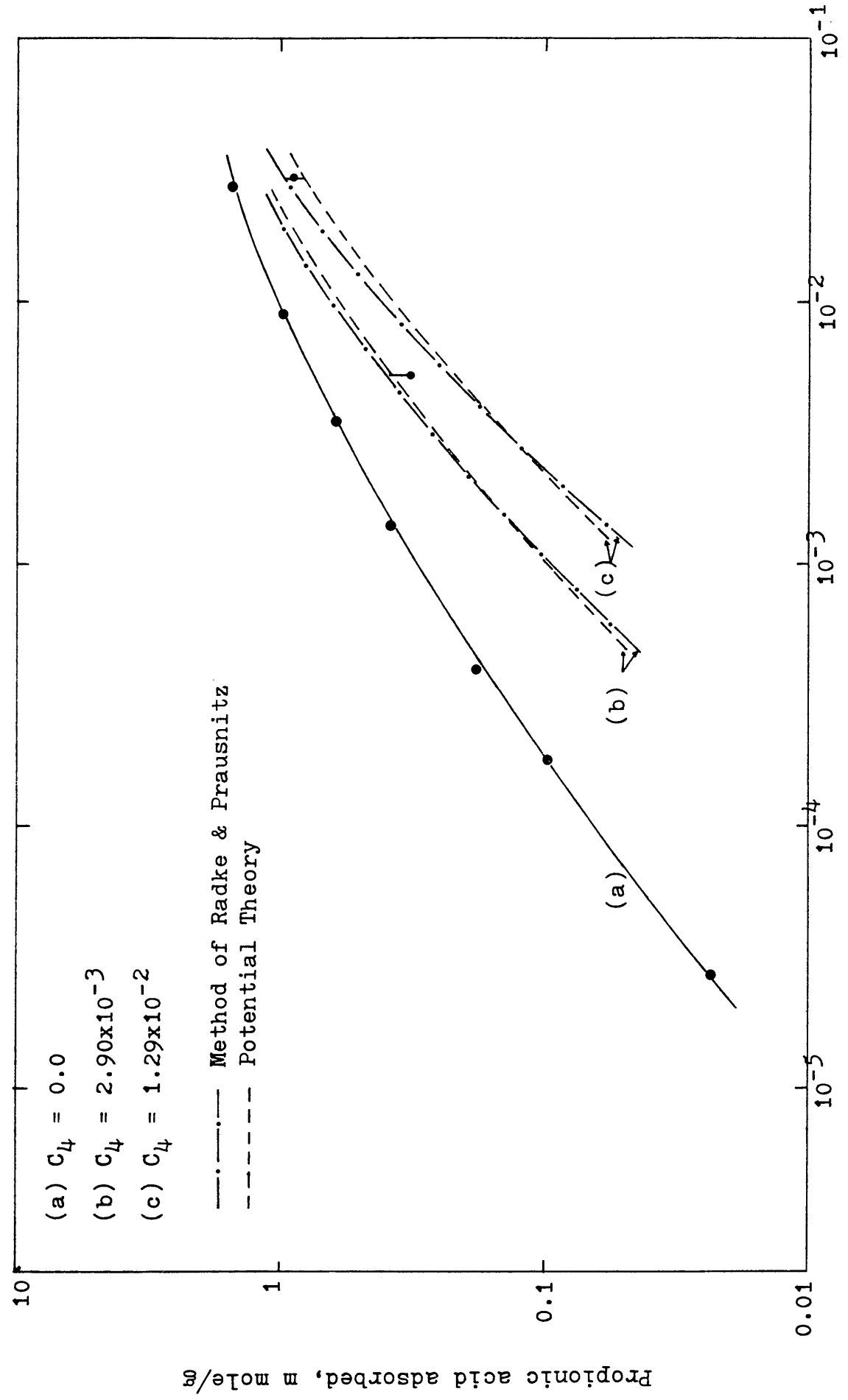

Figure 17 Adsorption of propionic acid in the presence of n-butanoic acid at 278 K

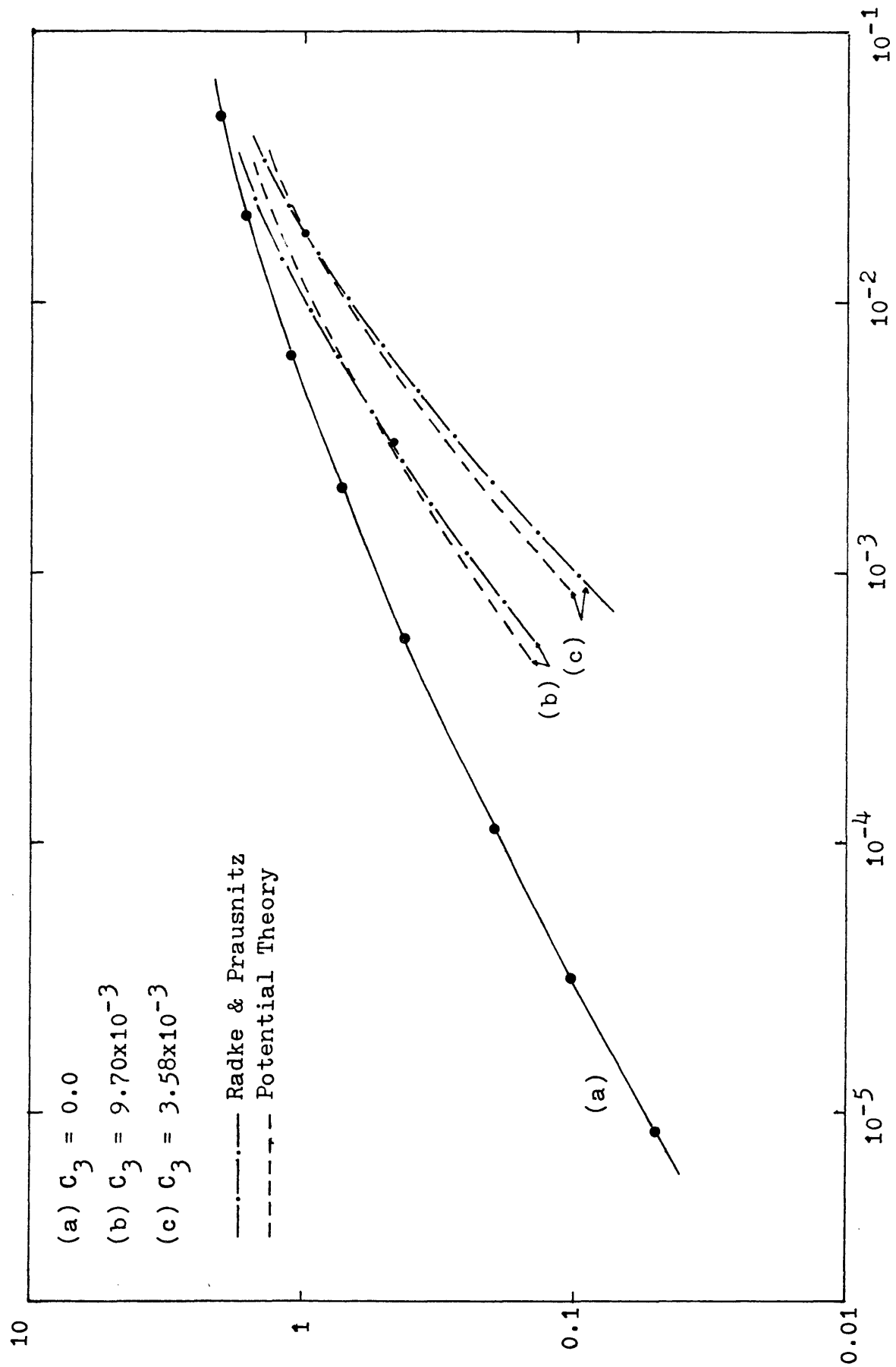

Figure 18 Adsorption of n-butanoic acid in the presence of propionic acid at 278 K

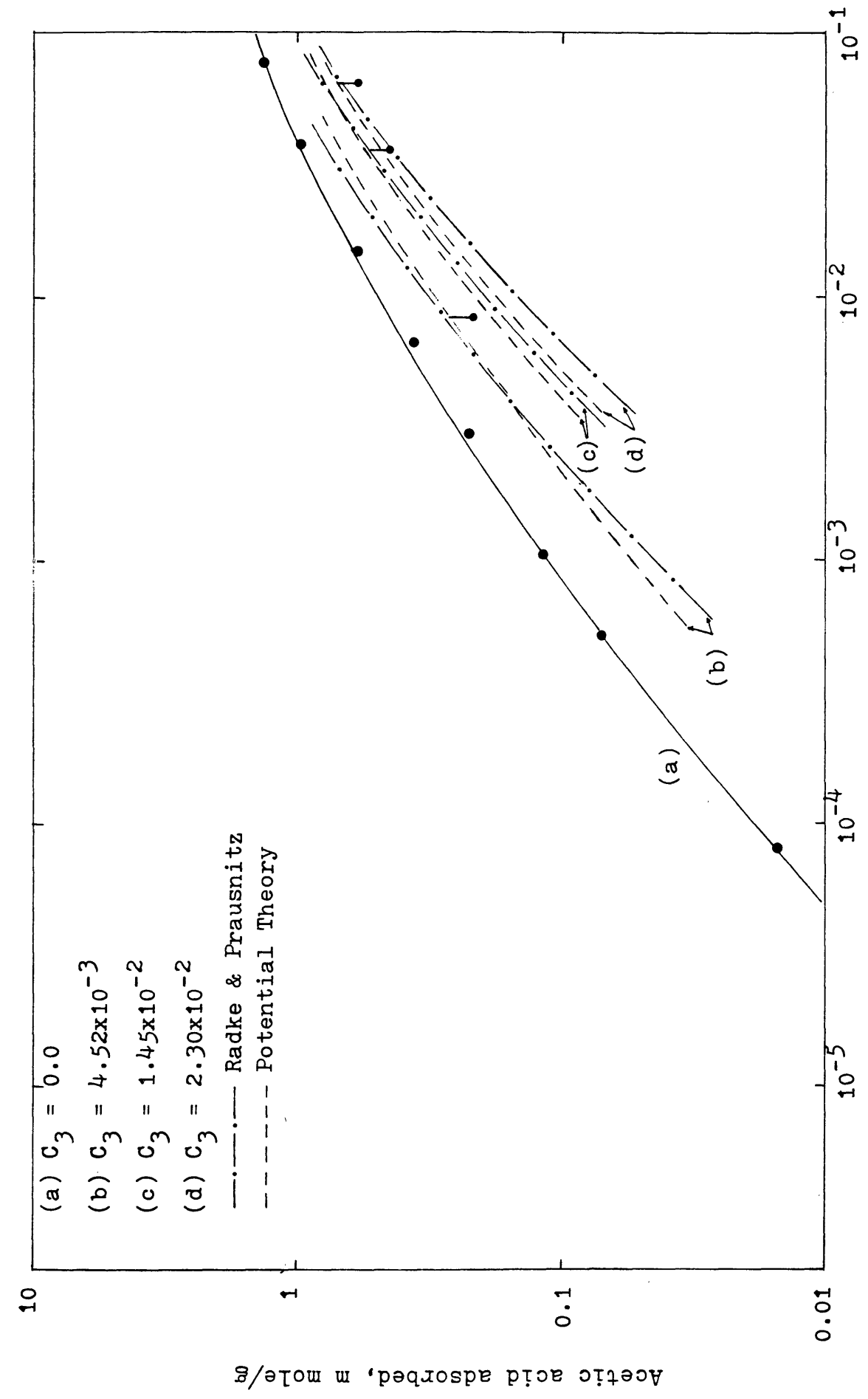

Figure 19 Adsorption of acetic acid in the presence of propionic acid at 298 K

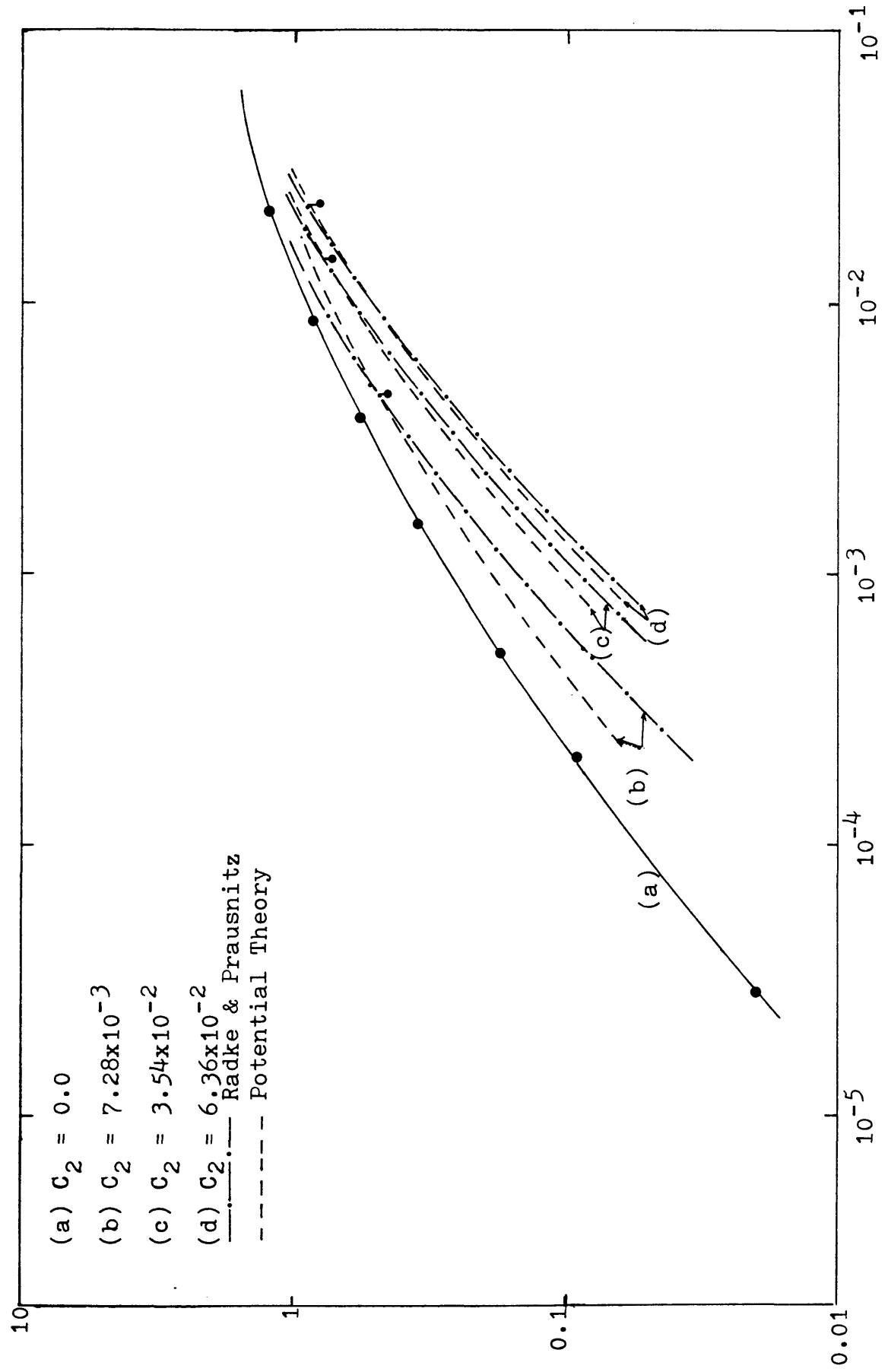

Figure 20 Adsorption of propionic acid in the presence of acetic acid at 298 K

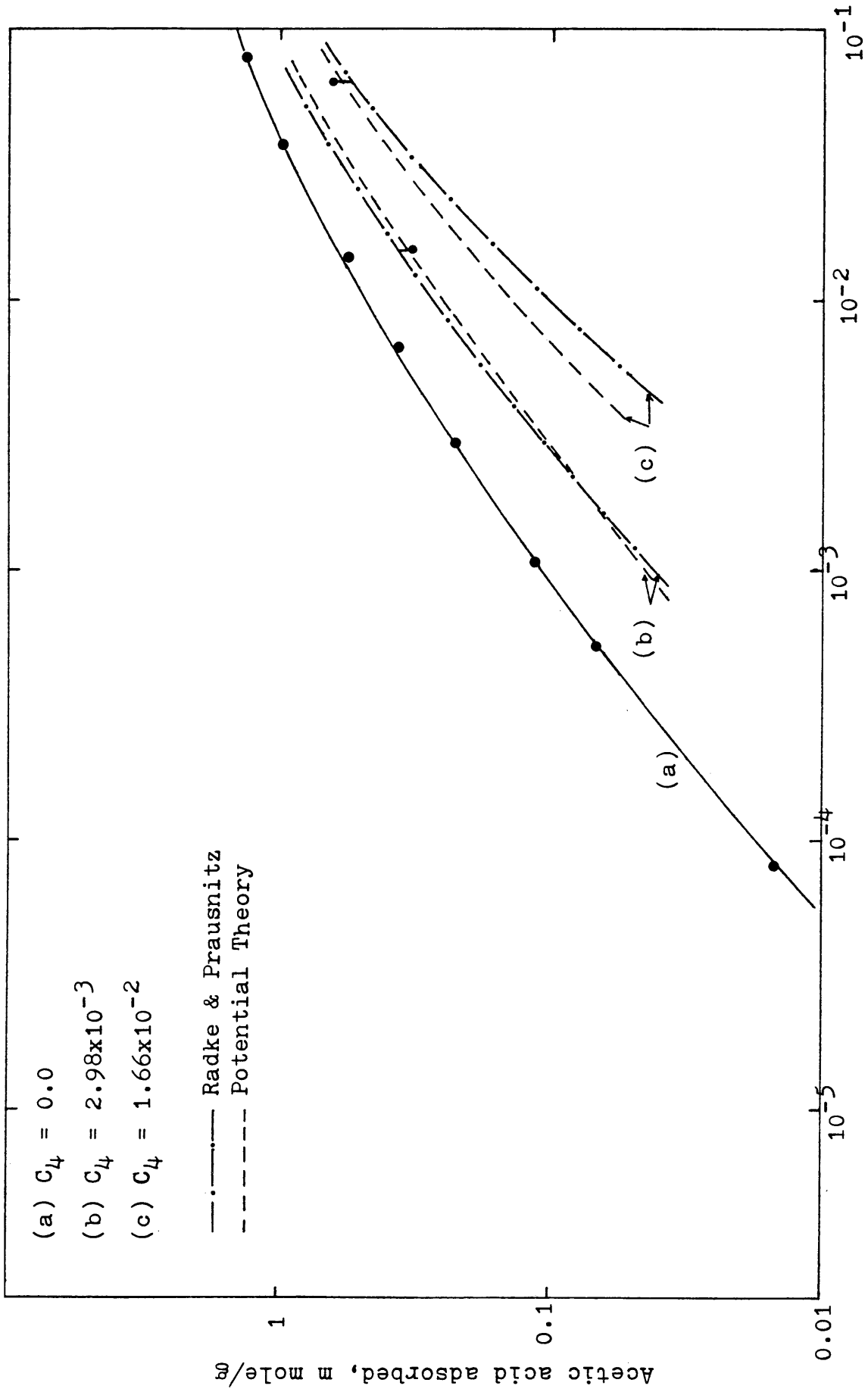

Figure 21 Adsorption of acetic acid in the presence of n-butanoic acid at 298 K

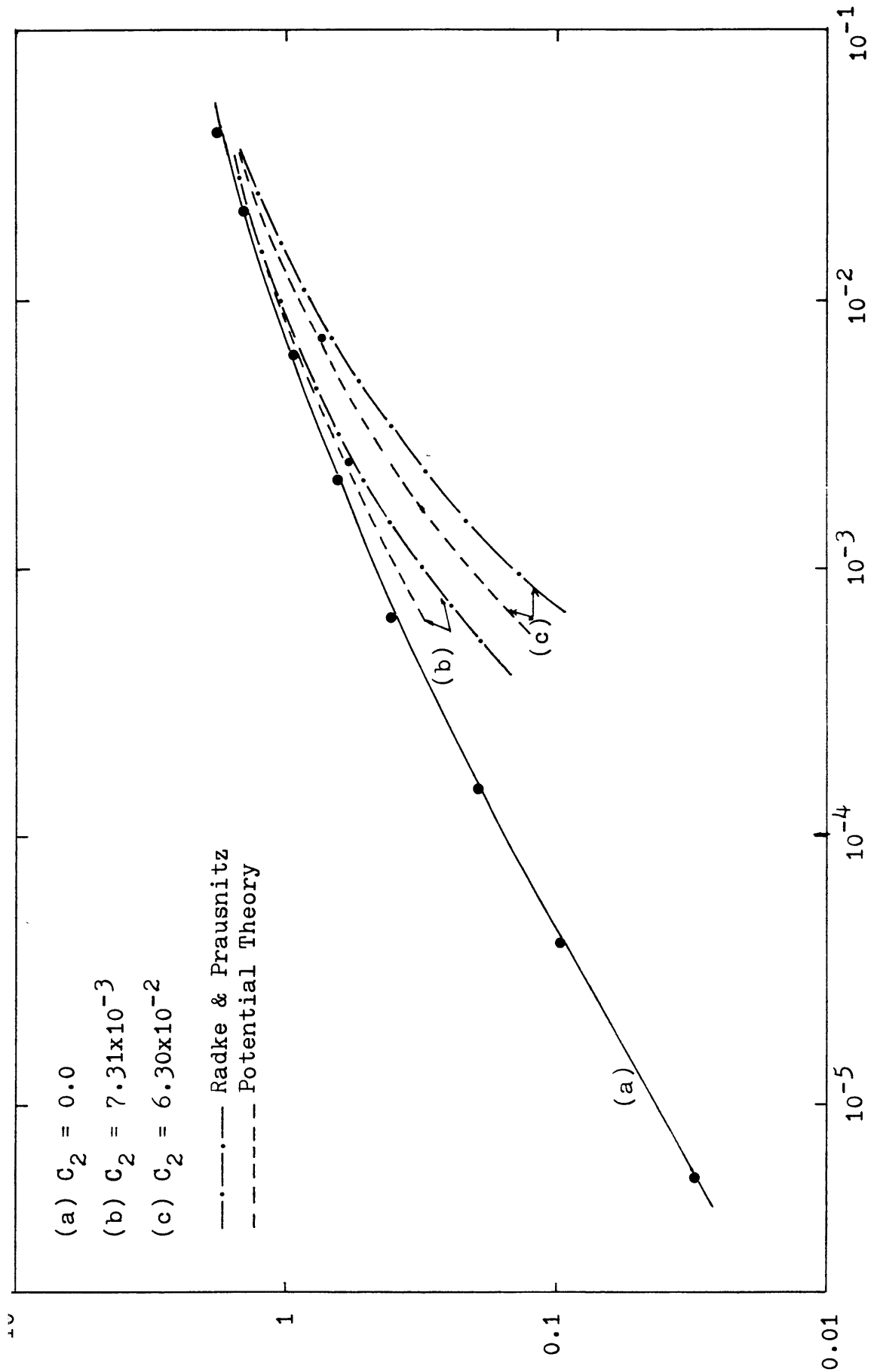

Figure 22 Adsorption of n-butanoic acid in the presence of acetic acid at 298 K

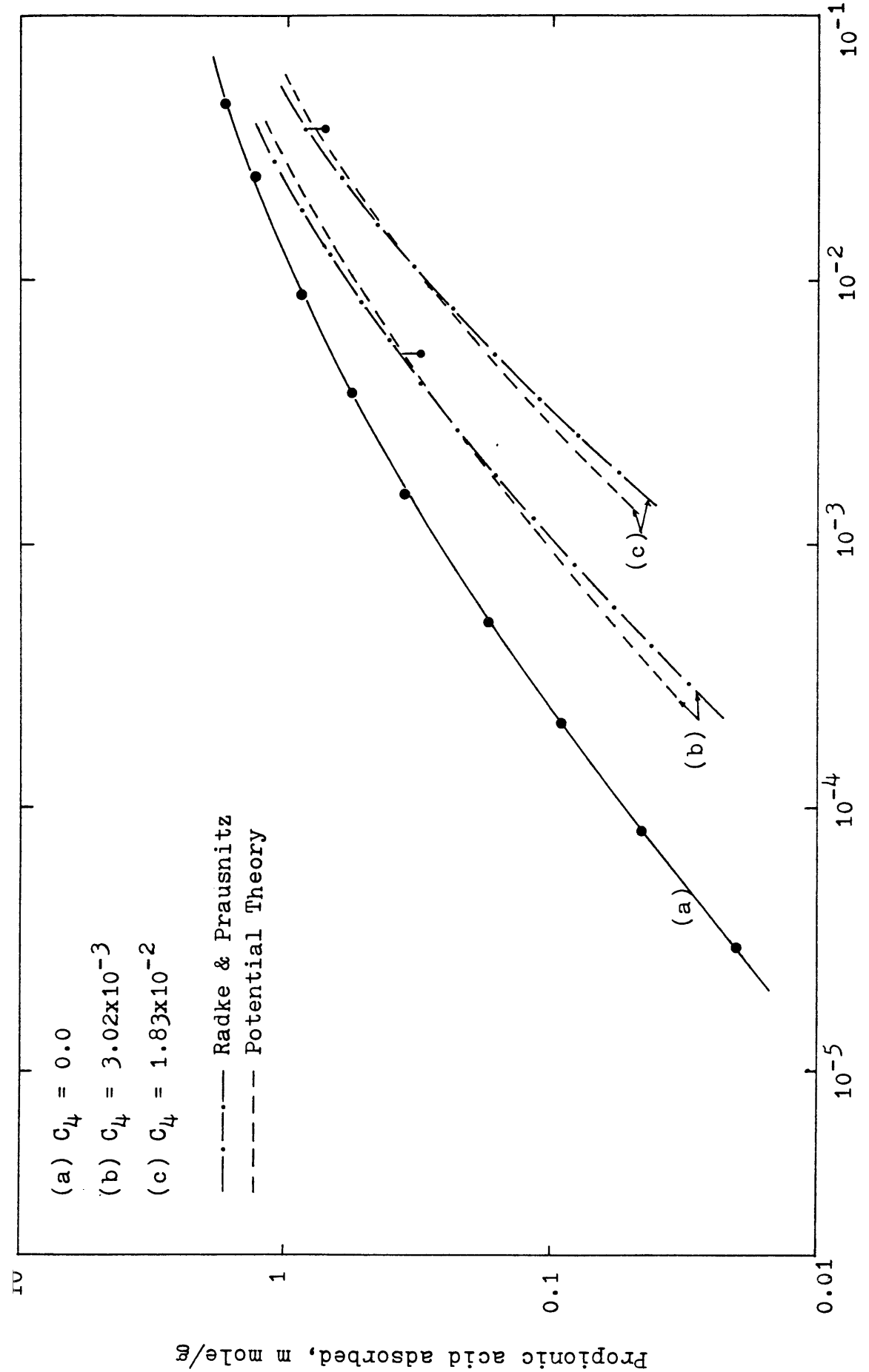

Figure 23 Adsorption of propionic acid in the presence of n-butanoic acid at 298 K

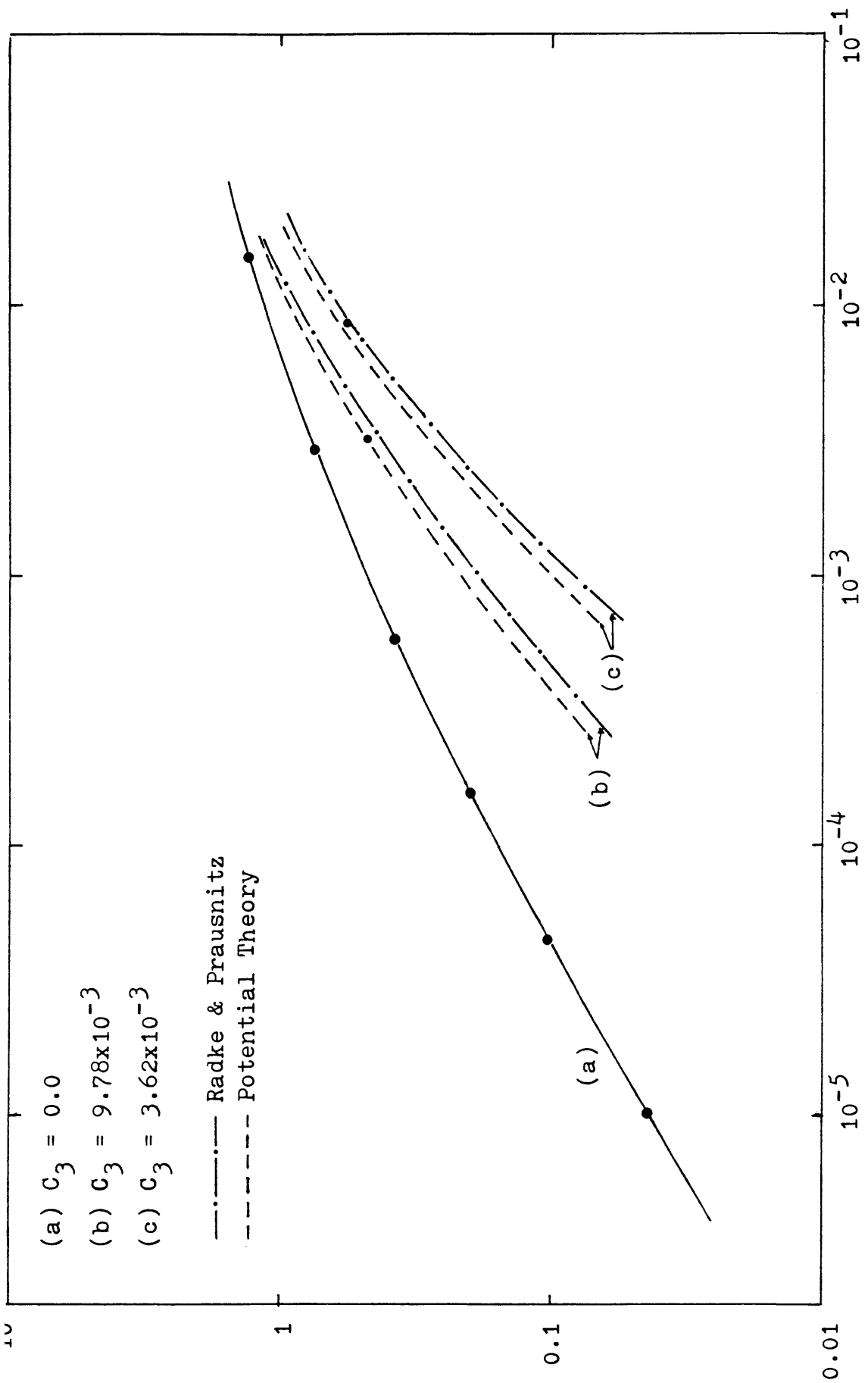

Figure 24 Adsorption of n-butanoic acid in the presence of propionic acid at 298 K

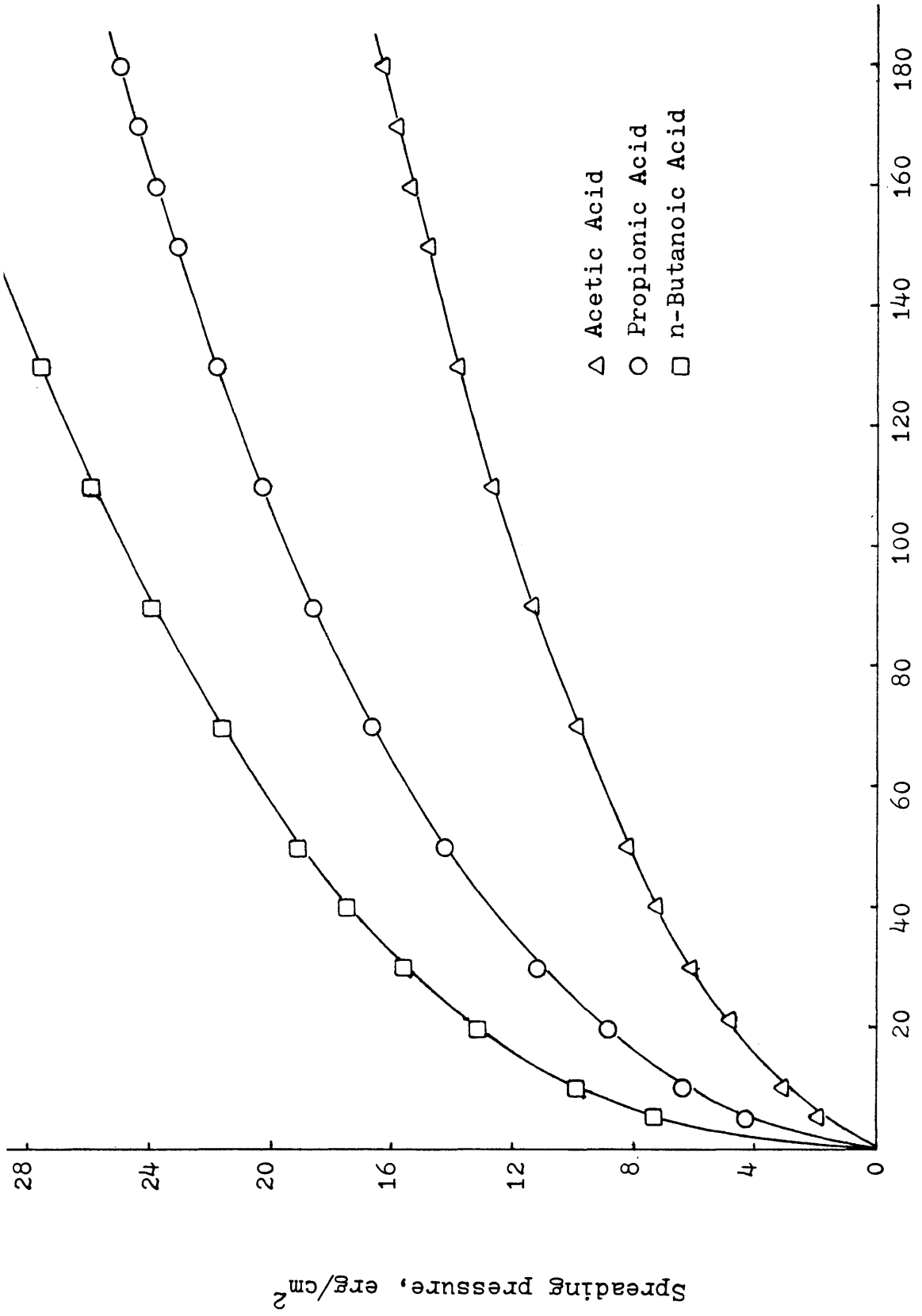

Figure 25 Spreading pressures of acetic, propionic and n-butanoic acids at 278 K

Figure 26 Spreading pressures of acetic, propionic and n-butanoic acids at 298 K

VI. Discussions

A direct comparison of this work was made with the study of Parkash (23) at 298 K. For an equilibrium concentration of 0.1 M, the uptake of the various acids in this study is about 37% greater than the uptake found by Parkash for the same adsorbent. The greater uptake found in this work can be attributed to the more extensive pretreatment prior to use. Parkash indicated that in his study all adsorbents were thoroughly refluxed with boiling distilled water and vacuum-dried at 70°C.

An examination of the adsorption data shows that the adsorption of lower aliphatic acids from aqueous solutions increases with increasing chain length. This result agrees with Traube's Rule: i.e., the addition of the CH_2 group to the aliphatic acid molecule reduces its solubility in water. In the dilute solution region, Equation (70) will give a straight line and the parameter "a" becomes the Henry constant. As shown in Table 11 the parameter "a" decreases with increasing temperature and with increasing molecular size. This result not only supports the Traube's Rule but also indicates that the adsorption of organic acids is an exothermic process as expected.

For competitive adsorption studies, the adsorption potential theory developed in this study has been tested at

two different temperatures, 278K and 298K and has been shown to give slightly better results than the method by Radke and Prausnitz (24). No attempt was made to compare this work with the simplified model as proposed by Digiano et al. (30) because of the difficulties in fitting the single-solute isotherms with simple equations such as the Langmuir or Freundlich type equations.

The average deviation between predicted and experimental loading ranges from 4.4% to 14.4% for uptake of the individual components and from 2% to 11% for the total uptake of both components. The average error between the predicted and experimental loading is greater than the 4% estimated experimental error. This could be the result of several factors including the pH effects and the non-ideal behavior of the adsorbed phase. The errors in using the ideal adsorbed solution model (24) are possibly due in part to the extrapolation error introduced when evaluating the spreading pressure in the very low concentration region. However, as shown in Tables 18 through 23, as well as in Figures 13 through 24, the errors do not appear to be systematic.

Figures 13 through 24 show that the potential theory generally predicts lower adsorption in the high concentration range and higher adsorption in the lower concentration range than the method of Radke and Prausnitz. The higher

adsorption in the lower concentration range is probably due to the effect of neglecting the adsorption potential of the solvent, which in this case is water. By the same argument the potential theory as presented here might be expected to predict higher adsorption uptakes even in moderate or high concentration ranges. As shown in Figures 13 through 24 this does not appear to be the case for all of the data. The disagreement again may be due to the pH effects, steric hinderance or chemisorption in the higher concentration range (44).

In contrast to the studies of Manes and co-workers, an adjusted adsorbate volume correction factor was not necessary in predicting bi-solute uptake. The reasons are twofold. First, the surface excess is zero when pure solute is used (7, 10, 31, 35). Secondly, it is not possible at the present time to give a meaningful adjusted volume correction factor because of many-body effects and the unknown structure of the adsorbed liquid phase (46). The lack of quantitative information on intermolecular potentials, to say nothing of the complexity of a multi-layer model of a dense-fluid adsorbate, is the main reason for not using the adjusted adsorbate volume factor.

Based on almost the same assumptions as that of the ideal adsorbed solution theory, the adsorption potential

theory provides a simple way to predict competitive adsorption equilibrium data for bi-solute systems. A major difference between the method of Radke and Prausnitz and the adsorption potential theory is that it is the pore volume and not the surface area that plays the major role in the model presented in this work.

It is indicated by Minka and Myers (31) that the surface area has no meaning for microporous adsorbents. This argument is also supported by the experimental data when amberlite XAD synthetic resins are used as adsorbents as shown in Tables 28 and 29. It is clear from the results in Tables 28 and 29 that the nature of the adsorbent surface, the pore size distribution, the extent of pretreatment of the adsorbent and the nature of solvents are more important than the surface area when predicting adsorption capacities.

Also the spreading pressure used by Radke and Prausnitz is not clear cut in the case of liquid phase adsorption. Unlike gas phase adsorption, there is no clear phase boundary between the adsorbed phase and the bulk phase. In the adsorption potential, the multilayer character of the adsorbed phase is explained by the decay of the potential energy between the adsorbate molecules and the adsorbent as their separation distance increases. The significance of this approach is that it is not necessary to postulate a specific

thickness for the adsorbed layer, since adsorption is considered as only a function of the adsorption potential at any distance from the adsorbing surface (15).

In the ideal adsorbed solution theory, the adsorbed phase is considered to be of zero thickness and the small pressure effect is neglected. In monolayer surface coverage or less, the concept of zero-thickness adsorbed phase may be a good approximation. However, it can not be applied to the case where multi-layer adsorption occurs. Radke and Prausnitz indicated that the adsorbed phase was determined according to the Gibbs dividing surface. The concept of Gibbs dividing surface was originally developed to deal with the vapor-liquid interface or immiscible liquid-liquid interface. To the author's knowledge, it is not appropriate to apply the Gibbs dividing surface to treat the adsorption at a liquid-solid interface because there is no shape density change in the liquid phase. A thorough discussion of this problem is given in references (15) and (47).

The application of the potential theory in this study is based on the assumptions that the bulk phase and adsorbed phase form ideal solutions. In addition, it was assumed that the amount of water adsorbed in the adsorption space near the surface can be neglected because of its low

adsorption potential as substantiated by Wohleber and Manes (18). Thus, the application of the potential theory as presented here is limited to predicting adsorption in dilute solutions or for systems where the adsorption potential of the solvent is so low compared to the solute that it can be neglected even at potential surfaces somewhat removed from the solid surface. Obviously, for adsorption in volume elements far from the surface, the solvent uptake cannot be neglected. However, it is important to note that if the adsorption potential of the pure solvent is known, its uptake in any adsorption space can be predicted. Thus, the potential theory can conceivably be extended to more concentrated solutions and to potential surfaces far removed from the solid surface.

For more concentrated solutions, the activity coefficients must be introduced for both the bulk liquid phase and the adsorbed phase. Unfortunately, adsorbed-phase activity coefficients can not be measured independently. Therefore, the proposed model can be more accurately utilized for dilute solutions.

Adsorbent[1]	Functionality	Helium Porosity (Vol. %)	Helium Porosity (cm^3/gram)	Mercury Porosity[2] (Vol. %)	Mercury Porosity[2] (cm^3/gram)	Area (m^2/gram)	Diameter[3] (A)	Density (grams/cm^3)
			Non-Polar					
XAD-2	Styrene-DVB	42.0	0.693	39.3	0.648	300	90	1.081
XAD-4	Styrene-DVB	51.3	0.998	50.2	0.976	784	50	1.085
			Intermediate Polarity					
XAD-7	Acrylic Ester	55.0	1.080	58.2	1.144	450	90	1.251
XAD-8	Acrylic Ester	52.4	0.822	51.9	0.787	140	235	1.259
			Polar					
XAD-9	Sulfoxide	44.9	0.609	40.2	0.545	69	366	1.268
XAD-11	Amide	41.4	0.616	-	-	69	352	1.209
XAD-12	Very Polar Nitrogen-Oxygen Group	45.1	0.787	50.4	0.880	22	1300	1.169
XE-284	Sulfonic Acid	47.2	0.657	39.1	0.544	571	44	1.437

1 Amberlite XAD-2, Amberlite XAD-4, Amberlite XAD-7, Amberlite XAD-12 and Amberlite XE-284 are available in Plant or Semi-Works quantities. Amberlite XAD-8, Amberlite XAD-9 and Amberlite XAD-11 are available in laboratory quantities.

2 Mercury porosities, usually quite comparable to helium porosities, sometimes deviate significantly, as for Amberlite XE-284. These differences may be due to (1) physical alteration of the polymer at the high pressures (50,000 lb./$in.^2$) used for mercury penetration, or (2) a change in the mercury contact angle on the surface of the highly polar adsorbents (thus invalidating the pressure-penetration relationship used to calculate porosity).

3 Average pore diameter is calculated from the following relationship:

$$\text{average pore diameter} = \frac{40{,}000}{\text{surface area} \cdot \text{skeletal density}} \cdot \frac{\text{porosity (helium)}}{1 - \text{porosity (helium)}}$$

-2293

Table 29. Equilibrium adsorption of carboxylic acids from toluene onto XAD resins at 25°C

Equilibrium Adsorption of Carboxylic Acids From Toluene at 25° C.

Adsorbent	Acetic Acid Wt. Ads. (mg/g)	Acetic Acid DW*	Oleic Acid Wt. Ads. (mg/g)	Oleic Acid DW*
XAD-4	68.7	3.85	23.3	3.51
XAD-8	71.7	5.90	33.0	4.95
XAD-11	152	9.77	46.0	8.62
XAD-12	371	37.2	79.0	34.0
XE-284, H^+	161	10.4	93.3	254

*DW = m. moles acid/gram dry resin / m. moles acid/ml. of solution

(taken from the manufacture's report by)
Rohm and Hass Company

VII. Conclusions

Adsorption of organic acid from dilute aqueous solutions onto activated carbon was studied at three different temperatures: 278K, 298K and 313K. Based on this information, a competitive adsorption potential theory was developed in this study to predict the bi-solute equilibrium data. The agreement between the calculated values and the experimental data is good. The success of the competitive adsorption potential theory indicates several important conclusions.

1. The adjusted adsorbate volume factor is not necessary when the surface loading is not high. This is in contrast to the approach of Rosene and Manes (20-22).

2. The derivation of the model presented in this work is thermodynamically rigorous. It can be extended to more concentrated solutions provided the activity coefficients of the adsorbed and the bulk liquid phases are known or can be calculated. However, the method of Rosene and Manes is not thermodynamically sound and can not be applied to more concentrated solutions.

3. The model presented in this work can also be applied to predict competitive binary gas phase adsorption equilibrium data because the adsorption potential of the solvent is neglected. The method of Rosene and Manes can not be extended in this manner.

4. It is not necessary to assume that the adsorbed phase is of zero thickness as proposed by Radke and Prausnitz (24). The idea of finite adsorbed volume space occupied by adsorbates describes the actual physical system more closely than the conventional Gibbs adsorption equation.

5. The model presented in this work provides a simpler way to predict bi-solute equilibrium data than does the ideal adsorbed solution theory. In order to use the IAS model, it is necessary to solve equations (22) through (26) simultaneously together with the curve fitting of the spreading pressures.

In applying the competitive adsorption potential theory, only equation (71) is necessary for the prediction of bi-solute equilibria.

6. The disadvantage of the model presented in this work is that it is difficult to extend the present model to predict tri-solute equilibria. This shortcoming may limit its practical usefulness in predicting multicomponent equilibria.

VIII. Recommendations

It is recommended that the competitive adsorption potential theory be tested in the very low concentration region. This can be done by properly choosing the solutes. The purpose of running experiments at very low concentrations is to differentiate the IAS model and the competitive adsorption potential theory.

The most difficult thing in the prediction of multisolute equilibria is to predict the total uptake of the solutes. It is recommended that the research work in the prediction of the total uptake be given a high priority.

In the waste water retreatment, the continuous flow process is of practical importance. It is recommended that liquid phase adsorption studies also be conducted in a packed-bed, continuous flow process.

Appendix A. Liquid Scintillation Counting Theory and Techniques.

The application of radioisotope technique in adsorption studies is based on the following assumption. It is assumed that the ratio of radioactive molecules to radioinactive molecules remains constant before and after the sample solution is equilibrated with activated carbon. Isotopes refers to atoms of the same chemical properties but different atomic mass. Two different isotopes of an element would have the same number of protons but a different number of neutrons.

Liquid scintillation depends on the critical interactions between the radioactive sample and the surrounding medium which is a liquid solution. This liquid scintillation solution is often called a "cocktail". In this report, the two terms are used interchangeably. In order to count the radioactivity of the samples, certain amount of cocktail (12 mL in this case) must be added to the samples. The function of adding cocktails is to amplify the production of Compton electrons during the scintillation process. The Compton electrons then excite other cocktail molecules which will soon return to their ground energy states by emitting photons. The amount of photons monitored by the photomultiplier tubes is a measure of the radiointensity of the radio-

active sample. However the production of Compton electrons is decreased by the amount of water present in the sample solutions. This is due to the lack of π electrons of the water molecules. Such effect is called "quenching".

Procedures for quench correction:

(1) Prepare samples and standards. Standards must be prepared which have the same chemical composition as the samples (buffer, salt, etc.) with the same type of quenching agent, e.g. water. The standards have the same type of isotope as the samples but their activites are known.

(2) Count standards using the same channel settings as the samples. Eight samples with different amounts of quenching agent are usually needed to prepare the quenching curve.

(3) Plot a counting efficiency curve of efficiency (y-axis) as a function of Horrock's number (H# in x-axis). The H# is a measure of the decrease in the light produced by the excited electron energy due to the quenching that is present in the sample.

$$\text{counting efficiency} = \frac{\text{observed counts per minute-background}}{\text{actual disintegration per minute}} \times 100\%$$

(4) Curvefit the counting efficiency by a fourth order polynomial.

$$\text{Efficiency} = AH + BH^2 + CH^3 + DH^4$$

(5) Determine sample activity as

$$DPM = \frac{CPM}{\text{counting efficiency}}$$

The quenching curve determined in this study when water is the quenching agent is

$$\text{Efficiency} = 88.6586H - 0.113705H^2 + 0.001827H^3 + 0.00000528H^4$$

Sample Calculation for Single Solute Uptake

Temperature 298K

Initial Counting and Concentration of acetic acid:

2500 ppm, 47676 CPM, H=75

Final Counting: 42394 CPM. H=74

Find the final equilibrium concentration and the amount of uptake when 0.5 g of activated charcoal is used?

Initial H = 75

Initial efficiency = $88.6586 \times 75 - 0.113705 \times 75^2 + 0.001827 \times 75^3 + 0.00000528 \times 75^4 = 89.13\%$

Initial DPM = $\frac{47676}{89.13\%} = 53490.0$

Final Counting Efficiency = $88.6586 \times 74 - 0.113705 \times 75^2 + 0.001827 \times 75^3 + 0.00000528 \times 75^4 = 89.21\%$

Final DPM = $\frac{42394}{89.21\%} = 47522.0$

Molecular weight of $CH_3COOH = 60.0$

Final solute concentration

$$= 2500 \text{ ppm} \times \frac{47522}{53490} \times \frac{1}{60 \text{g/mole}} \times 100 \text{ ml} \times 10.0$$

$$= 3.70 \times 10^{-2} \text{ mole/l} \quad \leftarrow\text{--------Ans}$$

the amount of uptake

$$= 2500 \text{ ppm} \times \left(1 - \frac{47522}{53490}\right) \frac{\times 0.95 \times 10^{3}}{(0.5 \times 60)}$$

$$= 8.83 \times 10^{-1} \text{ m mole/g} \quad \leftarrow\text{--------Ans}$$

Here, 10^3 is the conversion factor for changing moles to m moles and 0.95 is due to the fact that only 95 mL of the original sample solution is used in equilibration with 0.5 g of activated carbon.

The amount of radioactive organic acids injected per mL of radioactive stock solution is shown as follows:

A.	acetic acid	2.496×10^{-6} g/mL
B.	propionic acid	3.246×10^{-6} g/mL
C.	butanoic acid	9.167×10^{-6} g/mL
D.	hexanoic acid	2.900×10^{-5} g/mL
E.	heptanoic acid	4.750×10^{-5} g/mL

The amount of radioactive acids injected should be corrected when the initial solute concentration is less than 1 ppm. The amount of isotopes injected should not be confused with the radioactivity of the isotopes injected.

Appendix B. Sample Calculation for Competitive Adsorption

Problem: Predict the competitive adsorption equilibrium data for the mixture of acetic acid and priopionic acid at 25°C. The final equilibrium concentrations are

C_2 (acetic acid) 1.52×10^{-2} mole/l

C_3 (propionic acid) 4.69×10^{-3} mole/l

V_2 (molar volume of acetic acid) at 25°C = 57.24 ml/mole

V_3 (molar volume of propionic acid) at 25°C = 75.0 ml/mole

Calculation:

x_2 (mole fraction of acetic acid) in the bulk phase = 2.7462×10^{-4}

x_3 (mole fraction of propionic acid) in the bulk phase = 8.4428×10^{-5}

(Step 1) Plot the adsorbed volume Vads versus

$$\frac{E_i}{V_i} = \frac{RT}{V_i} \ln\left(\frac{1}{x_{iB}}\right)$$ for each solute from its

corresponding adsorption isotherm (see curves 2 and 3 in Figure 27).

(Step 2) Assume $x_{2\phi} = 0.4$, $x_{3\phi} = 0.6$

$$\frac{RT}{V_2} \ln\left(\frac{x_{2\phi}}{x_{2B}}\right) = 16.477$$

$$\frac{RT}{V_3} \ln \left(\frac{x_{3\phi}}{x_{3B}}\right) = 15.304$$

(Step 3) Shift curve 3 to the left by an amount equal to $\frac{RT}{V_3} \ln \left(\frac{x_{3\phi}}{x_{3B}}\right) = 15.304$

(see curve 3' in Figure 27)

(Step 4) the adsorption will occur whenever

$$\frac{RT}{V_2} \ln \frac{x_{2\phi}}{x_{2B}} = \frac{E_2}{V_2} - \frac{E_3}{V_3} + \frac{RT}{V_3} \ln \frac{x_{3\phi}}{x_{3B}} \qquad (68)$$

The dashed line in Figure 27 represents the right hand of Equation (68).

(Step 5) Enter $\frac{RT}{V_2} \ln \frac{x_{2\phi}}{x_{2B}} = 16.477$ on the abscissa of Figure 27 and find its corresponding ordinate C from the dashed line.

$$C = \frac{3.6 \text{ cc}}{100 \text{ g}}, \quad B = \frac{5.4 \text{ cc}}{100 \text{ g}}$$

q_2 = moles of acetic acid adsorbed

$$= \frac{3.6}{57.24}$$

$$= 0.629 \text{ m mole/g}$$

q_3 = moles of propionic acid adsorbed

$$= \frac{5.4 - 3.6}{75}$$

$$= 0.240 \text{ m mole/g}$$

(Step 6) Check

$$(x_{2\phi})_{calc.} = \frac{0.629}{0.629+0.24}$$

$$= 72.4\% \neq (x_{2\phi})_{assum.}$$

So, repeat steps 2 through 6.

Assume $x_{2\phi} = 0.445$

$$\frac{RT}{V_2} \ln \frac{x_{2\phi}}{x_{2B}} = 16.718$$

$$\frac{RT}{V_3} \ln \frac{x_{3\phi}}{x_{3B}} = 15.169$$

Then, construct Figure 28.

Enter $\frac{RT}{V_2} \ln \frac{x_{2\phi}}{x_{2B}} = 16.718$ on the abscissa of Figure 28.

$$B = 5.6; \quad C = 2.1$$

$$q_2 = \frac{2.1}{57.24} = 0.367 \frac{\text{m mole}}{\text{g}}$$

$$q_3 = \frac{5.6-2.1}{75} = 0.467 \frac{\text{m mole}}{\text{g}}$$

Check

$$(x_{2\phi})_{calc} = \frac{0.367}{0.367+0.467}$$

$$= 0.44 = (x_{2\phi})_{assum}$$

$$\therefore \quad q_2 = 0.367 \text{ m mole/g}$$

$$q_3 = 0.467 \text{ m mole/g.}$$

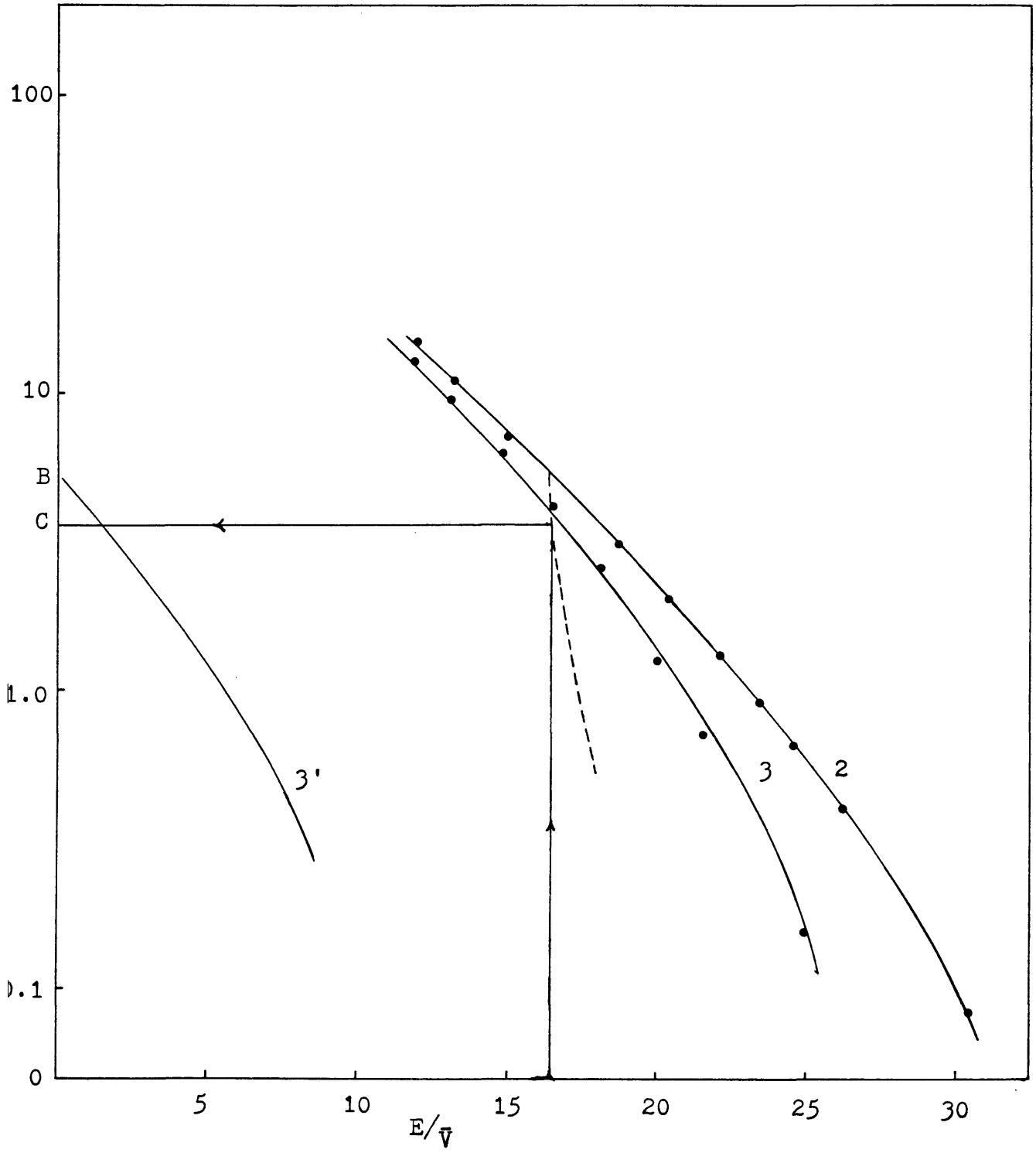

Figure 27 Schematic diagram for predicting competitive adsorption

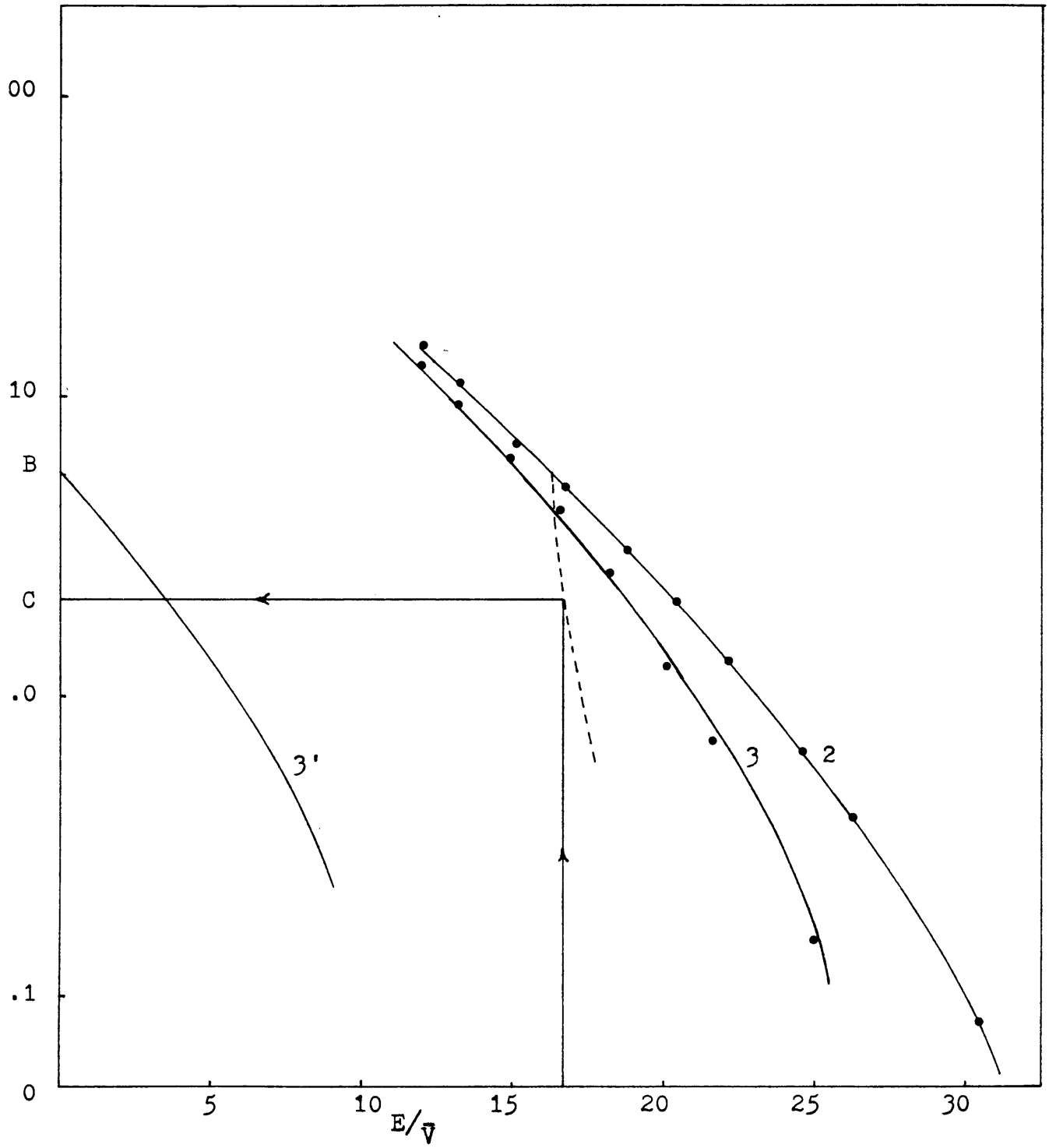

Figure 28 Schematic diagram for predicting competitive adsorption

Appendix C. Error Analysis

An estimate of the random errors associated with the measurement of the final liquid equilibrium concentration and the uptake can be made from an estimate of the errors involved in the individual parameters. Uncertainties in the measurement of experimental variables are given as follows:

Experimental variables	Uncertainty
weight of solute Wa	±0.00001g
weight of activated carbon W_c	±0.00001g
solution volume Vs	±1 ml
initial solute activity Dpm_i	±1%
final solute activity Dpm_f	±1%
temperature K(^oC)	±1K(^oC)

The final solute concentration was calculated by the use of equation (C-1).

$$C_f = \frac{Wa}{Vs} \times \frac{Dpm_f}{Dpm_i} \qquad (C\text{-}1)$$

where C_f is the final solute equilibrium concentration. Differentiating equation (C-1) gives

$$dC_f = \frac{dWa}{Vs} \times \frac{Dpm_f}{Dpm_i} + \frac{Wa}{Vs} \times \frac{dDpm_f}{Dpm_f} - \frac{Wa\,Dpm_f}{Vs^2 Dpm_i} \times dVs$$

$$- \frac{Wa\,Dpm_f\,d\,Dpm_i}{Vs(Dpm_i)^2} \qquad \text{(C-2)}$$

By representing the derivatives as difference values and dividing each term in equation (C-2) by equation (C-1) the following equation is obtained:

$$\frac{\Delta C_f}{C_f} = \frac{\Delta Wa}{Wa} + \frac{\Delta Vs}{Vs} + \frac{\Delta Dpm_f}{Dpm_f} + \frac{\Delta Dpm_i}{Dpm_i} \qquad \text{(C-3)}$$

The sign on each term has been chosen to yield the maximum error in C_f values. It is seen from equation (C-3) that the maximum error occurs at the smallest solute concentration. Two examples are shown below to demonstrate the analysis of experimental errors.

1) initial solute concentration = 1 ppm

$$\frac{\Delta Wa}{Wa} = \frac{0.00001\ g}{1\ ppm \times 100\ ml} = 0.1$$

where 100 ml is the solution volume used in the equilibration study.

$$\frac{\Delta C_f}{C_f} = 0.1 + \frac{1}{100} + 1\% + 1\%$$

$$= 13\%$$

2) initial solute concentration = 10 ppm

$$\frac{\Delta Wa}{Wa} = \frac{0.00001\ g}{10\ ppm \times 100\ ml} = 0.01$$

$$\frac{\Delta C_f}{C_f} = 0.01 + \frac{1}{100} + 1\% + 1\%$$

$$= 4\%$$

From these two examples, it is clear that the maximum error is about 13% when the initial solute concentration is 1 ppm. The error in the calculation of the final solute concentration is controlled by the first term of equation (C-3). When the initial solute concentration is 10 ppm or higher, the error in C_f decreases to 4% or even less. Since the amount of uptake is calculated from the difference between the initial and final solute concentrations, the error for the uptakes is the same as that of the final equilibrium concentration.

Therefore, the uncertainties in both the final solute concentration and uptake are estimated to be about 4% for the entire data reported in this study.

REFERENCES

1. Shuval, H. I., "Water Renovation and Reuse", H. I. Shuval Ed. Academic Press, New York, pp. 33-72 (1977).

2. "Preliminary Assessment of Suspected Carcinogenes in Drinking Water", Interim Report to Congress EPA, Office of Toxic Substances, Washington, D.C. December 1975.

3. Linner, E. R., Gortner, R. A., J. Phys. Chem. 39, 35 (1935).

4. Smith, H. A., Hurley, R. B., J. Phys. Colloid Chem. 53, 1409 (1949).

5. Hansen, R. S., Miller, F. A., J. Phys. Chem. 58 (3), 193 (1954).

6. Hansen, R. S., Hansen, R. B., J. Phys. Chem. 59, 496 (1954).

7. Hansen, R. S., Craig, R. P., J. Phys. Chem. 58, 211 (1954).

8. Hansen,R. S., Fu, Y., Bartell, F. E., J. Phys. Colloid Chem., 53, 769 (1949).

9. Graham, D., Hansen, R. S., J. Phys. Chem. 60 (8), 1153 (1956).

10. Blackburn, A., Kippling, J. J., Tester, D. A., J. Phys. Chem. 2373 (1957).

11. Joyce, R., Sukenik, V. A., Adv. Waste Water Treatment Res. U.S. Public Health Service, Cincinnati, Ohio, May 16, 1962.

12. Weber, W. J., Morris, J. C., J. Sanit. Eng. Div. Am. Soc. Civil Engrs. 89 (SA2), 31 (1963).

13. Weber, W. J., Morris, J. C., ibid. 90 (SA3), 19 (1964).

14. Zarifyanz, Y. A., Kiselev, V. F., Lezhev, N. N., Nikitina, O. V. Carbon 5, pp. 127-135 (1967).

15. Kipling, J. J., "Adsorption from Solutions of Non-Electrolytes" Academic Press (1965).

16. Hofer, L. J. E., Manes, M., Chem. Eng. Prog. 65,84 (1969).

17. Manes, M., Hofer, L. J. E., J. Phys. Chem. 73, 584 (1969).

18. Wohleber, C. A., Manes, M., J. Phys. Chem. 75, 61 (1971).

19. Wohleber, D. A., Manes M., J. Phys. Chem. 75, 3720 (1971).

20. Rosene, M. R., Manes, M., J. Phys. Chem. 80, 953 (1976).

21. Rosene, M. R., Ozcan, M., Manes, M., J. Phys. Chem. 80, 2586 (1976).

22. Rosene, M. R., Manes, M., J. Phys. Chem. 81, 1646 (1977).

23. Parkash, S. Carbon, 12, 37 (1974).

24. Radke, C. J., Prausnitz, J. M. AIChEJ. 18 761 (1972).

25. Fritz, W., Schluender, E-U, Chem. Eng. Sci. 29, 1279 (1974).

26. Fritz, W., Schluender, E-U, Chem. Eng. Sci. 29, 1279 (1974).

27. Butler, J. A. V., Ockrent, C. J., J. Phys. Chem. 34, 2841, (1930).

28. Jain, J. S., Snoeyink, V. L., J. Water Pollut. Control Fed. 45, pp. 2463-79 (1973).

29. Myers, A. L., Prausnitz, J. M., AIChE J., 11, 121 (1965).

30. Digiano, F. A., Baldauf, G., Frick, B., Sontheimer, H., Chem. Eng. Sci. 33, 1667-73 (1978).

31. Minka, C., Myers, A. L., AIChE J., 19 (3), 453 (1973).

32. Gibbs., J. W., "The Scientific Papers of J. Willard Gibbs" Vol. 1, p. 219, Dover, New York (1961).

33. Innes, W. B., Rowley, H. H., J. Phys. Chem. 46, 548 (1942).

34. Chao, K. C. "Vapor-Liquid Equilibrium in Ternary System: Ethyl Acetate-Benzene-Cyclohexane" Ph.D. thesis. Univ. Wisconsin, Madison (1956).

35. Larinov, O. G., Myers, A. L., Chem. Eng. Sci. 26, pp. 1025-1030 (1971).

36. Polanyi, M., Verhand. deut. phys. Ges., 16, 1012 (1914).

37. Polanyi, M., Verhand deut. phys. Ges., 16, 1012 (1914).

38. Polanyi, M. Z. Phys., 2, 111 (1920).

39. Hansen, R. S., Fackler, W. V. Jr., J. Phys. Chem., 57, 634 (1953).

40. Chiou, C. C. T., Manes, M., J. Phys. Chem., 75, 61 (1973).

41. Long, E. C., "Liquid Scintillation Counting Theory and Techniques" Bechman Inst. Corp. (1976).

42. Long, E. C. "Applications of Quench Morning by Comton Edge: The H#", Beckman Inst. Corp. (1977).

43. Morrocks, D. L. "The H Number Concept", Beckman Inst. Corp. (1977).

44. Radke, C. J., Prausnitz, J. M., Ind. Eng. Chem. Fundam., 11 (4), 445 (1972).

45. Coughlin, R. W., Ezra, F. S., Enviro. Sci. & Technol. 2(4), 291 (1968).

46. Radke, C. J., Prausnitz, J. M., J. Chem. Phys. 57 (2), 714 (1972).

47. Defay, R., Prigogine, I., Bellemans, A., Everett, D. H., "Surface Tension and Adsorption" John Wiley, New York (1966).

```
C      ***** POW2.FOR; DATA:OCT.18,1979 *****
C      ***** THIS PROGRAM IS TAKEN FROM JAMES L. KUESTER &
C      ***** JOE H. MIZE; "OPTIMIZATION TECHNIQUES",
C      ***** MCGRAW HILL,(1973)
C      ***** UNCONSTRAINED NONLINEAR MINIMIZATION
C      *******MAIN PROGRAM OF THE POWELL METHOD**********
       COMMON/LIST1/X(5),E(5),W(100)
       COMMON/LIST2/Q(15),C(15),T(15),Y(15),ERR(15)
       COMMON/LIST3/IN,IO
       IN=12
       IO=4
30     READ(IN,5)N,NDATA,IPRINT,MAXIT,ESCALE
5      FORMAT(4I,F)
C      ***** TEST OF IPRINT, IF IPRINT LESS THAN ZERO, STOP ****
       IF(IPRINT.LT.0) STOP
       READ(IN,6) (X(II),II=1,N)
6      FORMAT(5G)
       READ(IN,6)(E(JJ),JJ=1,N)
       READ(IN,10) (Q(I),C(I),I=1,NDATA)
10     FORMAT(2F)
       NW=N*(N+3)
       CALL POWELL (X,E,N,F,ESCALE,IPRINT,MAXIT,W,NW,NDATA,Q,C)
       WRITE(IO,1)
1      FORMAT(//,5X,'VALUES OF THE VARIABLES')
       WRITE(IO,2)X(1),X(2),X(3),X(4),X(5)
2      FORMAT(/,5X,'X(1)=',E,5X,'X(2)=',E,5X,'X(3)=',E,5X,'X(4)='
      1 ,E/5X,'X(5)=',E)
       WRITE(IO,3)F
3      FORMAT(//,5X,'OPTIMUM VALUE OF F=',E16.8)
       DO 100 I=1,NDATA
       Y(I)=X(1)*C(I)+X(2)*C(I)**2+X(3)*C(I)**3+X(4)*C(I)**4
       ERR(I)=(Q(I)-Y(I))/Q(I)*100.0
       WRITE(IO,20) Q(I),Y(I),ERR(I)
20     FORMAT(5X,'Q(I)=',E,5X,'Y(I)=',E,5X,'ERR(%)=',E)
100    CONTINUE
       GO TO 30
       STOP
       END
```

```
C     ***** END OF THE MAIN PROGRAM *****
      SUBROUTINE POWELL(X,E,N,F,ESCALE,IPRINT,MAXIT,W,NW,NDATA,Q,C)
      DIMENSION X(5),E(5),W(100)
      DIMENSION Q(15),C(15),T(15)
      COMMON/LIST3/IN,IO
      WRITE(IO,2)N,MAXIT,ESCALE,(E(I),I=1,N)
2     FORMAT(//,2X,'N=',I2,4X,'MAXIT=',I4,4X,'ESCALE=',F,//,2X,
     1 'ACCURACY REQUIRED FOR VARIABLES',/,3X,'E(1)=',
     2 F,3X,'E(2)=',F,3X,'E(3)=',F,3X,'E(4)=',F,3X,'E(5)=',F)
      DDMAG=0.1*ESCALE
      SCER=0.05*1.0/ESCALE
      JJ=N*N+N
      JJJ=JJ+1
      K=N+1
      NFCC=1
      IND=1
      INN=1
      DO 4 I=1,N
      W(I)=ESCALE
      DO 4 J=1,N
      W(K)=0.0
      IF(I-J) 4,3,4
3     W(K)=ABS(E(I))
4     K=K+1
      ITERC=1
      ISGRAD=2
      CALL RESTNT(N,X,F,NDATA,Q,C)
      FKEEP=ABS(F)+ABS(F)
5     ITONE=1
      FP=F
      SUM=0.0
      IXP=JJ
      DO 6 I=1,N
      IXP=IXP+1
      W(IXP)=X(I)
6     CONTINUE
      IDIRN=N+1
      ILINE=1
7     DMAX=W(ILINE)
      DACC=DMAX*SCER
      DMAG=AMIN1(DDMAG,0.1*DMAX)
      DMAG=AMAX1(DMAG,20.0*DACC)
      DDMAX=10.0*DMAG
      GO TO (70,70,71) ,ITONE
70    DL=0.0
      D=DMAG
      FPREV=F
      IS=5
      FA=F
      DA=DL
8     DD=D-DL
```

```
      DL=D
58    K=IDIRN
      DO 9 I=1,N
      X(I)=X(I)+DD*W(K)
      K=K+1
9     CONTINUE
      CALL RESTNT(N,X,F,NDATA,Q,C)
      NFCC=NFCC+1
      GO TO (10,11,12,13,14,96),IS
14    IF(F-FA) 15,16,24
16    IF(ABS(D)-DMAX) 17,17,18
17    D=D+D
      GOTO 8
18    WRITE(IO,19)
19    FORMAT(5X,'MAXIMUM CHANGE DOES NOT ALTER FUNCTION')
      GO TO 20
15    FB=F
      DB=D
      GO TO 21
24    FB=FA
      DB=DA
      FA=F
      DA=D
21    GO TO (83,23),ISGRAD
23    D=DB+DB-DA
      IS=1
      GO TO 8
83    D=0.5*(DA+DB-(FA-FB)/(DA-DB))
      IS=4
      IF((DA-D)*(D-DB)) 25,8,8
25    IS=1
      IF(ABS(D-DB)-DDMAX)8,8,26
26    D=DB+SIGN(DDMAX,DB-DA)
      IS=1
      DDMAX=DDMAX+DDMAX
      DDMAG=DDMAG+DDMAG
      IF(DDMAG.GE.1.0E38) DDMAG=1.0E38
      IF(DDMAX-DMAX)8,8,27
27    DDMAX=DMAX
      GO TO 8
13    IF(F-FA) 28,23,23
28    FC=FB
      DC=DB
29    FB=F
      DB=D
      GO TO 30
12    IF(F-FB) 28,28,31
31    FA=F
      DA=D
      GO TO 30
11    IF(F-FB)32,10,10
```

```
32    FA=FB
      DA=DB
      GO TO 29
71    DL=1.0
      DDMAX=5.0
      FA=FP
      DA=-1.0
      FB=FHOLD
      DB=0.0
      D=1.0
10    FC=F
      DC=D
30    A=(DB-DC)*(FA-FC)
      B=(DC-DA)*(FB-FC)
      IF((A+B)*(DA-DC))33,33,34
33    FA=FB
      DA=DB
      FB=FC
      DB=DC
      GO TO 26
34    D=0.5*(A*(DB+DC)+B*(DA+DC))/(A+B)
      DI=DB
      FI=FB
      IF(FB-FC)44,44,43
43    DI=DC
      FI=FC
44    GO TO (86,86,85),ITONE
85    ITONE=2
      GOTO 45
86    IF (ABS(D-DI)-DACC) 41,41,93
93    IF (ABS (D-DI)-0.03*ABS(D)) 41,41,45
45    IF ((DA-DC)*(DC-D)) 47,46,46
46    FA=FB
      DA=DB
      FB=FC
      DB=DC
      GO TO 25
47    IS=2
      IF((DB-D)*(D-DC))48,8,8
48    IS=3
      GO TO 8
41    F=FI
      D=DI-DL
      DD=SQRT((DC-DB)*(DC-DA)*(DA-DB)/(A+B))
      DO 49 I=1,N
      X(I)=X(I)+D*W(IDIRN)
      W(IDIRN)=DD*W(IDIRN)
      IDIRN=IDIRN+1
49    CONTINUE
      W(ILINE)=W(ILINE)/DD
      ILINE=ILINE+1
```

```
      IF(IPRINT-1)51,50,51
50    WRITE(IO,52)ITERC,F,(X(I),I=1,N)
52    FORMAT(/,3X,'ITERATION=',I5,2X,'FUNCTION VALUES=',E15.8/
     1 2(E16.8,2X))
      GO TO (51,53),IPRINT
51    GO TO (55,38),ITONE
55    IF(FPREV-F-SUM) 94,95,95
95    SUM=FPREV-F
      JIL=ILINE
94    IF(IDIRN-JJ) 7,7,84
84    GO TO (92,72),IND
92    FHOLD=F
      IS=6
      IXP=JJ
      DO 59 I=1,N
      IXP=IXP+1
      W(IXP)=X(I)-W(IXP)
59    CONTINUE
      DD=1.0
      GO TO 58
96    GO TO (112,87),IND
112   IF (FP-F) 37,37,91
91    D=2.*(FP+F-2.*FHOLD)/(FP-F)**2
      IF(D*(FP-FHOLD-SUM)**2-SUM) 87,37,37
87    J=JIL*N+1
      IF(J-JJ) 60,60,61
60    DO 62 I=J,JJ
      K=I-N
      W(K)=W(I)
62    CONTINUE
      DO 97 I=JIL,N
      W(I-1)=W(I)
97    CONTINUE
61    IDIRN=IDIRN-N
      ITONE=3
      K=IDIRN
      IXP=JJ
      AAA=0.0
      DO 65 I=1,N
      IXP=IXP+1
      W(K)=W(IXP)
      IF(AAA-ABS(W(K)/E(I))) 66,67,67
66    AAA=ABS(W(K)/E(I))
67    K=K+1
65    CONTINUE
      DDMAG=1.0
      W(N)=ESCALE/AAA
      ILINE=N
      GO TO 7
37    IXP=JJ
      AAA=0.0
```

```
      F=FHOLD
      DO 99 I=1,N
      IXP=IXP+1
      X(I)=X(I)-W(IXP)
      IF(AAA*ABS(E(I))-ABS(W(IXP))) 98,99,99
98    AAA=ABS(W(IXP)/E(I))
99    CONTINUE
      GO TO 72
38    AAA=AAA*(1.0+DI)
      GO TO (72,106),IND
72    IF(IPRINT-2) 53,50,50
53    GO TO (109,88),IND
109   IF (AAA-0.1) 20,20,76
76    IF(F-FP) 35,78,78
78    WRITE(IO,80)
80    FORMAT(5X,'ACCURACY LIMITED BY ERRORS IN F')
      GO TO 20
88    IDN=1
35    DDMAG=0.4*SQRT(FP-F)
      ISGRAD=1
108   ITERC=ITERC+1
      IF(ITERC-MAXIT) 5,5,81
81    NOLUCK=4
      IF(F-FKEEP) 20,20,110
110   F=FKEEP
      DO 111 I=1,N
      JJJ=JJJ+1
      X(I)=W(JJJ)
111   CONTINUE
      GO TO 20
101   JIL=1
      FP=FKEEP
      IF (F-FKEEP) 105,78,104
104   JIL=2
      FP=F
      F=FKEEP
105   IXP=JJ
      DO 113 I=1,N
      IXP=IXP+1
      K=IXP+N
      GO TO (114,115),JIL
114   W(IXP)=W(K)
      GO TO 113
115   W(IXP)=X(I)
      X(I)=W(K)
113   CONTINUE
      JIL=2
      GO TO 92
106   IF(AAA-0.1) 30,20,107
20    RETURN
107   INN=1
```

```
      GO TO 35
      END
```

```
      SUBROUTINE RESTNT(N,X,F,NDATA,Q,C)
      DIMENSION X(5),E(5),W(100)
      DIMENSION Q(15),C(15),T(15)
      X1=X(1)
      X2=X(2)
      X3=X(3)
      X4=X(4)
      X5=X(5)
      F=0.0
      DO 1000 I=1,NDATA
      T(I)=Q(I)-X1*C(I)-X2*C(I)**2-X3*C(I)**3
     1 -X4*C(I)**4
      F=F+T(I)*T(I)
1000  CONTINUE
      RETURN
      END
```

```
C      ***** SW11.FOR; DATE:OCT.18,1979 *****
C      ****** MAIN PROGRAM-------NEWTON,RAPHSON METHOD
C      ***** XOLD(I)'S ARE THE UNKNOWN VARIABLES
C      ***** A IS THE AUGMENT MATRIX OF THE NEWTON-RAPHSON METHOS
C      ***** ITMAX=MAXIMUN NUMBER OF THE ITERATION
C      ***** EPS1=CRITERIA OF CHOOSING THE PIVOTING VALUE
C      ***** EPS2=ACCURACY OF THE FINAL RESULTS,X(I)
C      ***** XINC(I)'S ARE THE INCERMENTS OF EACH
C      ***** ITERATION
C      ***** A1,B1,E1,A2,B2,E2=PARAMETERS OF THE ADS. ISOTHERMS
C      ***** NDATA=NUMBER OF THE DATA POINTS
       DIMENSION XOLD(21),XINC(21),A(21,21),TITLE(8)
       COMMON/LIST1/A1,B1,D1,E1,A2,B2,D2,E2
       COMMON/LIST2/C1,C2
       NI=1
       NO=4
       NDATA=4
       ICOUNT=1
C      *** READ AND PRINT INPUT DATA
10     READ(NI,100) ITMAX,IPRINT,N,EPS1,EPS2,T
100    FORMAT(3I,2E,F)
       READ(NI,110) (XOLD(I),I=1,N)
110    FORMAT(5F)
       READ(NI,120) (TITLE(I),I=1,8)
120    FORMAT(8A4)
       WRITE(NO,130) (TITLE(I),I=1,8),T
130    FORMAT(5X,'*** BI-SOLUTE SYSTEM DATA ENTRY ***'/
      1 5X,8A4/5X,'TEMP(K)=',F)
       WRITE(NO,200) ITMAX,IPRINT,N,EPS1,EPS2,(XOLD(I),I=1,N)
200    FORMAT(5X,'ITMAX=',I,5X,'IPRINT=',I,6X,'N=',I/5X,'EPS1=',
      1G,6X,'EPS2=',G/5X,'XOLD(1),XOLD(2)...'/5X,5(5X,F))
       READ(NI,205) A1,B1,D1,E1
       READ(NI,205) A2,B2,D2,E2
205    FORMAT(4G)
206    FORMAT(3G)
       WRITE(NO,207)A1,B1,D1,E1,A2,B2,D2,E2
20     READ(NI,206)C1,C2,Q
       WRITE(NO,209) C1,C2
       DO 90 ITER=1,ITMAX
       CALL CALCN(XOLD,A,21)
       DETER=SIMUL(N,A,XINC,EPS1,1,21)
       IF(DETER.NE.0.) GO TO   30
       WRITE(NO,201)
201    FORMAT(5X,'MATRIX IS ILL-CONDITIONED OR SINGULAR')
       STOP
30     ITCON=1
       DO 50 I=1,N
       IF(ABS(XINC(I)).GT.EPS2) ITCON=0
       XOLD(I)=XOLD(I)+XINC(I)
50     CONTINUE
       WRITE(NO,202) ITER,DETER,(XOLD(I),I=1,N)
```

```
      IF(ITCON.EQ.0) GO TO 90
      WRITE(NO,203) ITER,DETER,(XOLD(I),I=1,N)
      Q1=Q*XOLD(3)
      Q2=Q*(1.-XOLD(3))
      TYPE 210,Q1,Q2
210   FORMAT(5X,'Q1=',F,5X,'Q2=',F)
      IF(ICOUNT.EQ.NDATA) STOP
      GO TO 95
90    CONTINUE
      WRITE(NO,204)
      IF(ICOUNT.EQ.NDATA) STOP
95    ICOUNT=ICOUNT+1
      GO TO 20
202   FORMAT(5X,'ITER=',I,5X,'DETER=',G,/,
     1 5X,'XOLD(1),XOLD(2)..'/5X,5G)
203   FORMAT(5X,'SUCCESSFUL CONVERGENCE'/5X,'ITER=',I5X,
     1'DETER=',G/5X,'PI(1)=',G,5X,'PI(2)=',G,5X,'Z(1)=',F
     2 ,5X,'C1=',F,5X,'C2=',F)
204   FORMAT(5X,'NO CONVERGENCE')
207   FORMAT(5X,'PARAMETERS OF THE ADS. ISOTHERMS'/5X,
     1'A1=',E,5X,'B1=',E,5X,'D1=',E,5X,'E1=',E/5X,'A2='
     2,E,5X,'B2=',E,5X,'D2=',E,5X,'E2=',E)
208   FORMAT(5X,'SURFACE AREA(M2/G)=',G/5X,'TEPM(K)=',F)
209   FORMAT(5X,'C1=',G,5X,'C2=',G)
      END
```

```
C
C
C
C     ************************************************
C     CCC FUNCTION SIMUL IS REFERED TO CARNAHAN "APPLIED
C     CCC NUMERICAL METHODS" P 290  CCCCC
      FUNCTION SIMUL(N,A,X,EPS,INDIC,NRC)
      DIMENSION IROW(50),JCOL(50),JORD(50),Y(50),A(NRC,NRC),X(N)
      NO=4
      MAX=N
      IF(INDIC.GE.0) MAX=N+1
      IF(N.LE.50) GO TO 5
      WRITE(NO,200)
      SIMUL=0.0
200   FORMAT(5X,'N TOO BIG')
      RETURN
5     DETER=1.
      DO 18 K=1,N
      KM1=K-1
      PIVOT=0.
      DO 11 I=1,N
      DO 11 J=1,N
      IF(K.EQ.1) GO TO 9
      DO 8 ISCAN=1,KM1
      DO 8 JSCAN=1,KM1
      IF(I.EQ.IROW(ISCAN)) GO TO 11
      IF(J.EQ.JCOL(JSCAN)) GO TO 11
8     CONTINUE
9     IF(ABS(A(I,J)).LE.ABS(PIVOT)) GO TO 11
      PIVOT=A(I,J)
      IROW(K)=I
      JCOL(K)=J
11    CONTINUE
      IF(ABS(PIVOT).GT.EPS) GO TO 13
      SIMUL=0.
      RETURN
13    IROWK=IROW(K)
      JCOLK=JCOL(K)
      DETER=DETER*PIVOT
      DO 14 J=1,MAX
14    A(IROWK,J)=A(IROWK,J) /PIVOT
      A(IROWK,JCOLK)=1./PIVOT
      DO 18 I=1,N
      AIJCK=A(I,JCOLK)
      IF(I.EQ.IROWK) GO TO 18
      A(I,JCOLK)=-AIJCK/PIVOT
      DO 17 J=1,MAX
17    IF(J.NE.JCOLK) A(I,J)=A(I,J)-AIJCK*A(IROWK,J)
18    CONTINUE
      DO 20 I=1,N
      IROWI=IROW(I)
```

```
      JCOLI=JCOL(I)
      JORD(IROWI)=JCOLI
20    IF(INDIC.GE.0) X(JCOLI)=A(IROWI,MAX)
      INTCH=0
      NM1=N-1
      DO 22 I=1,NM1
      IP1=I+1
      DO 22 J=IP1,N
      IF(JORD(J).GE.JORD(I)) GO TO 22
      JTEMP=JORD(J)
      JORD(J)=JORD(I)
      JORD(I)=JTEMP
      INTCH=INTCH+1
22    CONTINUE
      IF(INTCH/2*2.NE.INTCH) DETER=-DETER
      IF(INDIC.LE.0) GO TO 26
      SIMUL=DETER
      RETURN
26    DO 28 J=1,N
      DO 27 I=1,N
      IROWI=IROW(I)
      JCOLI=JCOL(I)
27    Y(JCOLI)=A(IROWI,J)
      DO 29 I=1,N
28    A(I,J)=Y(I)
      DO 30 I=1,N
      DO 29 J=1,N
      IROWJ=IROW(J)
      JCOLJ=JCOL(J)
29    Y(IROWJ)=A(I,JCOLJ)
      DO 30 J=1,N
30    A(I,J)=Y(J)
      SIMUL=DETER
      RETURN
      END
```

```
C
C     ************************************************************
C     ***** SUBROUTINE CALCN IS THE AUGUMENT MATRIX
C     ***** PROVIDED BY THE USER *****
      SUBROUTINE CALCN(DXOLD,A,NRC)
      DIMENSION XOLD(20),DXOLD(NRC),A(NRC,NRC)
      COMMON/LIST1/A1,B1,D1,E1,A2,B2,D2,E2
      COMMON/LIST2/C1,C2
      R=8.317
      DO 1 I=1,5
      XOLD(I)=DXOLD(I)
      DO 1 J=1,6
      A(I,J)=0.0
1     CONTINUE
C     COMPUTE NON-ZERO ELEMENT OF A
      A(1,1)=1.0
      A(1,4)=-(A1+B1*2.*XOLD(4)+3.*D1*XOLD(4)**2+4.*E1
     1 *XOLD(4)**3)
      A(1,6)=-XOLD(1)+(A1*XOLD(4)+B1*XOLD(4)**2+D1*XOLD(4)**3
     1 +E1*XOLD(4)**4)
      A(2,2)=A(1,1)
      A(2,5)=-(A2+2.*B2*XOLD(5)+3.*D2*XOLD(5)**2+4.*E2
     1 *XOLD(5)**3)
      A(2,6)=-XOLD(2)+(A2*XOLD(5)+B2*XOLD(5)**2+D2
     1 *XOLD(5)**3+E2*XOLD(5)**4)
      A(3,3)=-XOLD(4)
      A(3,4)=-XOLD(3)
      A(3,6)=C1-XOLD(4)*XOLD(3)
      A(3,6)=-A(3,6)
      A(4,3)=XOLD(5)
      A(4,5)=-(1.0-XOLD(3))
      A(4,6)=C2-XOLD(5)*(1.-XOLD(3))
      A(4,6)=-A(4,6)
      A(5,1)=1.0
      A(5,2)=-1.
      A(5,6)=XOLD(1)-XOLD(2)
      A(5,6)=-A(5,6)
      RETURN
      END
```